Quality and Safety of Ultrasound Guided Lumbosacral Plexus Blockade Assessed by Ultrasound/MRI Fusion

PhD dissertation

Jennie Maria Christin Strid, MD

Health
Aarhus University
Department of Anaesthesiology and Intensive Care
Aarhus University Hospital

Supervisors

Thomas Fichtner Bendtsen, MD, PhD (main supervisor)
Department of Anaesthesiology and Intensive Care
Aarhus University Hospital
Denmark

Erik Morre Pedersen, MD, PhD, DMSc (co-supervisor)
Department of Radiology
Aarhus University Hospital
Denmark

Kjeld Søballe, Professor, MD, DMSc (co-supervisor)
Department of Orthopaedic Surgery
Aarhus University Hospital
Denmark

Chair

Bjarne Møller Madsen, MD, DMSc (chairman)
Department of Orthopaedic Surgery
Aarhus University Hospital
Denmark

Lukas Kirchmair, MD, PD Dr. (opponent)
Department of Anaesthesia and Intensive Care at the Community Hospital in Schwaz
Austria
Department of Anaesthesia and Intensive Care Medicine
Medical University of Innsbruck
Innsbruck
Austria

Caroline Ewertsen, MD, PhD (opponent)
Department of Radiology – Section of Ultrasound
Rigshospitalet
Copenhagen
Denmark

This PhD dissertation is based on the following original manuscripts

I. **Strid J.M.C.**, Sauter A.R., Ullensvang K., Andersen M.N., Daugaard M., Bendtsen M.A.F., Søballe K., Pedersen E.M., Børglum J., Bendtsen T.F. Shamrock vs. Lumbar Ultrasound Trident: Ultrasound Guided Lumbar Plexus Blockade in Volunteers - a Randomised Controlled Trial.

Accepted for publication with minor revision by British Journal of Anaesthesia

II. **Strid J.M.C**., Pedersen E.M., Al-Karradi S.N.H., Bendtsen M.A.F., Bjørn S., Dam M., Daugaard M., Hansen M.S., Linnet K.D., Børglum J., Søballe K., Bendtsen T.F. Real-time Ultrasound/MRI Fusion for Suprasacral Parallel Shift Approach to Lumbosacral Plexus Blockade and Injectate Spread - an Exploratory Randomised Controlled Trial.

Submitted to Anaesthesia

III. **Strid J.M.C.,** Pedersen E.M., Bendtsen M.A.F., Bjørn S., Dam M., Daugaard M., Hansen M.S., Vendelbo O., Børglum J., Søballe K., Bendtsen T.F. Real-time Ultrasound and MRI Fusion for Shamrock Lumbar Plexus Blockade and Analysis of Injectate Spread - an Exploratory Randomised Controlled Trial.

Planned submission to Anaesthesia

Table of Contents

Preface

This PhD dissertation and the included studies were completed during my employment as a PhD fellow at the Faculty of Health, Aarhus University, and at the Department of Anaesthesiology and Intensive Care, Aarhus University Hospital, in the period September 2013 to October 2016. The Department of Radiology, Aarhus University Hospital, was study venue for the trials.

Funding

The following institutions and foundations have kindly provided funding during the PhD study: A.P. Møller and Chastine Mc-Kinney Møller Foundation for General Purposes; Department of Anaesthesiology and Intensive Care, Aarhus University Hospital; Department of Radiology, Aarhus University Hospital; Department of Anaesthesiology, Oslo University Hospital Rikshospitalet; Kai Hovmand's Foundation; Helga and Peter Korning's Foundation; AU Going Abroad; the Oticon Foundation; King Christian X's Foundation; the Foundation of 1870; Family Hede Nielsen's Foundation; Orthopaedic Surgery Research Foundation; Danish Society of Radiology; Danish Society of Ultrasound Diagnostics; and International Society of Magnetic Resonance in Medicine.

Acknowledgements

I am grateful to Thomas F. Bendtsen for giving me the opportunity to explore fusion of ultrasound and MRI as well as regional anaesthesia and analgesia. Erik M. Pedersen and Kjeld Søballe, thank you for your patient co-supervision and introduction to your research environments. Through the collaborations with all three of you, I have met a wide spectrum of researchers, clinicians, and other professionals. For that I am thankful.

I would like to express my gratitude to Jens Børglum and Axel Sauter; not only for scientific support, advice, and opportunities, but also for your fabulous energy, humour, and laughs.

I am sincerely thankful to all volunteers for their participation and trust. I am deeply thankful to my colleagues and project staff for using their valuable time on my projects: Olga Vendelbo, Niels D. Nielsen, Siska Bjørn, Morten Daugaard, Mathias A. F. Bendtsen, Mette Dam, Martin S. Hansen, Gorm Nielsen, Morten N. Andersen, Sinan N. H. Al-Karradi, Kyrre Ullensvang, and Katrine D. Linnet. I could not have done it without you.

Niels Secher, Niels D. Nielsen, Siska Bjørn, and Frederik Boe: it has been a pleasure to share office and coffee as well as more or less scientific joys and sorrows with you. Niels and Siska: thank you for lending your bodies to my research. I would also like to thank: Charlotte Runge, Rasmus W. Hauritz, and Thomas Dahl in the RA-group; Mette Dam and Christian Kruse in the Roskilde group; Kim Sivesgaard and Kenneth S. Thorup in the MRI-group; and Asger Granfeldt, Anders Kjærgaard, Christine L. Hvas, Simon T. Vistisen, Christoffer Sølling, and Alexander d'Amore in the good old N-group. To all of you: I have truly enjoyed your company and our discussions during meetings and conferences as well as dinners. Heidi Poggianti, Karin Christensen, and Susanne Bruun: thank you for your work the behind the scenes. Especial thanks to Else Tønnesen for your trust and support since the beginning of my research career as a medical student. To my co-workers in Republikken: thank you for creative inspiration and company as well as for teaching me foosball.

I would also like to express my appreciation to my family and friends for your encouragement.

Last, but not least, my warmest and most sincere gratefulness to Morten Staberg. This work would not have been possible without your enduring ears and moral support. You are my rock (and) star that always makes me see the brightest side in the most frustrating situation.

Jennie M. C. Strid

Copenhagen, 2016

List of Abbreviations

Δ	Change
2D	Two-dimensional
3D	Three-dimensional
ASA	American Society of Anesthesiologists
BMI	Body mass index
CT	Computed tomography
DICOM	Digital imaging and communications in medicine
ED_{50}	Effective dose in 50% of the study population
EPI	Echo-planar imaging
GBP	Great British Pound
IPSC	Intra-psoas subcompartment
IQR	Interquartile range
L	Lumbar
LUT	Lumbar ultrasound trident
MAP	Mean arterial pressure
MRI	Magnetic resonance imaging
NRS	Numeric rating scale
P-lidocaine	Plasma concentration of lidocaine
PPC	Para-psoas compartment
RPSC	Retro-psoas subcompartment
S	Sacral
SD	Standard deviation
SSPS	Suprasacral parallel shift
T	Tesla
TE	Echo time

Th	Thoracic
TR	Repetition time
TSE	Turbo spin echo

Introduction

The majority of patients admitted for fracture and total replacement of the hip is 65 years or older.[1-3] The patients may be frail, obese, suffer from comorbidity, and have an increased risk of perioperative complications.[1 4]

Peripheral nerve blockade is based on injection of local anaesthetic around a nerve/nerves or a nerve plexus in the peripheral nervous system – either as a perineural injection or an injection into a fascial plane. Peripheral nerve/plexus blocks are associated with more stable haemodynamics and fewer complications compared with general and neuraxial anaesthesia.[5-10] A combination of nerve/plexus blockade and sedation is probably also associated with improved haemodynamics compared to standalone general anaesthesia. Moreover, peripheral nerve/plexus blocks provide adequate postoperative analgesia with a minimum requirement of opioids reducing the risk of opioid adverse effects.[7 11 12] Effective and safe peripheral nerve blockade in hip surgery patients are therefore suitable.

Ultrasound guided lumbosacral plexus block techniques for surgical anaesthesia and postoperative analgesia of the hip are limited by inadequate visualisation of particularly the target nerves and the topographical sonoanatomy.[13-23] Limited visualisation may limit the understanding of the spread of injectate and decrease the accuracy – and thereby the efficiency and safety – of the perineural injection. Fused real-time ultrasonography and magnetic resonance imaging (MRI) can be applied to improve ultrasound guided techniques by improving the visualisation of target nerves, sonoanatomy, and injectate spread.[24 25] Consequently, this improved understanding may increase the accuracy of perineural injection in ultrasound guided lumbosacral plexus blockade.[26] Hitherto, described ultrasound/MRI fusion of the lumbar spine for regional anaesthesia is limited to a fusion protocol in a phantom and in volunteers without application on needle guidance.[27]

We conducted three blinded randomised controlled trials with crossover design. We investigated block-procedure related outcomes, spread of injectate, effectiveness, safety, and cost-effectiveness of I) ultrasound guided Shamrock vs. Lumbar Ultrasound Trident techniques for lumbar plexus blockade, II) ultrasound/MRI fusion vs. ultrasound guided Suprasacral Parallel Shift techniques for lumbosacral plexus blockade, and III) ultrasound/MRI fusion vs. ultrasound guided Shamrock techniques for lumbar plexus blockade in healthy volunteers.

The originality of this dissertation is that we conducted the first randomised controlled trials of the ultrasound guided Shamrock technique and of the real-time ultrasound/MRI fusion application of the lumbar spine for needle guidance in regional anaesthesia. The dissertation contributes with new knowledge to the evidence-base of effectiveness, safety, ease-of-performance, procedure-associated outcomes, and injectate spread of the investigated techniques assessed with ultrasound/MRI fusion and MRI only in normal volunteers.

The following review presents the background of the research problem with a literature review, the research question, the aims and hypotheses, the methodological considerations, and the results. Finally, a discussion including the future aspects, the conclusions as well as a summary of the dissertation and the three studies are presented.

Background

Epidemiology of Hip Surgery Patients

The incidence rate of hip fracture worldwide is estimated to fourfold from 1.63 millions per year in 2000 to 3.94 millions per year in 2015 and 6.26 millions per year in 2050 due to demographic changes including an increasing population of elderly.[28 29] In the United States, the number of total hip replacements is expected to rise from 325,000 in 2005 to 669,000 in 2030 due to an increasing number of elderly and obese.[4 30 31] In Denmark, the prevalence of acute hospitalisation for hip fracture and elective surgery for hip replacement was 11.000 and 9.000, respectively, in 2015.[32]

The mean age of incident hip fracture patients in Denmark in 1998 to 2003 was 80 years – 90% were 65 years or older and 30% were 85 years or older.[1] Seventy percent were female.[1] Although there has been an increase in men aged 60 years or less undergoing primary total hip replacement at a British hospital,[33] the majority of total hip replacement patients worldwide are still female and 65 years or older.[2 3 33]

This is important because many elderly may present with comorbidities, e.g. diabetes, myocardial infarction, congestive heart failure, and chronic obstructive pulmonary disease.[1 12 29] Of the 11,985 patients hospitalised with an incident hip fracture in Denmark in 1998 to 2003, 53% suffered from comorbidity.[1] Some are "high-risk patients" with an increased risk of perioperative complications.[19]

The majority of hip fractures are treated with surgery.[10] Hip fractures account for the greater part of the direct medical costs for society compared with other fractures associated with osteoporosis.[34] In patients with arthritis of the hip, total hip replacement is successful in both clinical and cost-effective terms compared to other medical interventions.[31 35]

Anatomy of the Lumbosacral Plexus and Innervation of the Hip

The hip and lower extremity are innervated exclusively by the lumbosacral plexus (**Fig. 1**).[36 37] The lumbosacral plexus is the generic term for the lumbar plexus, the sacral plexus as well as the coccygeal and pudendal plexuses. Below is a general description of the anatomy that is most relevant for lumbosacral plexus innervation of the hip.[38]

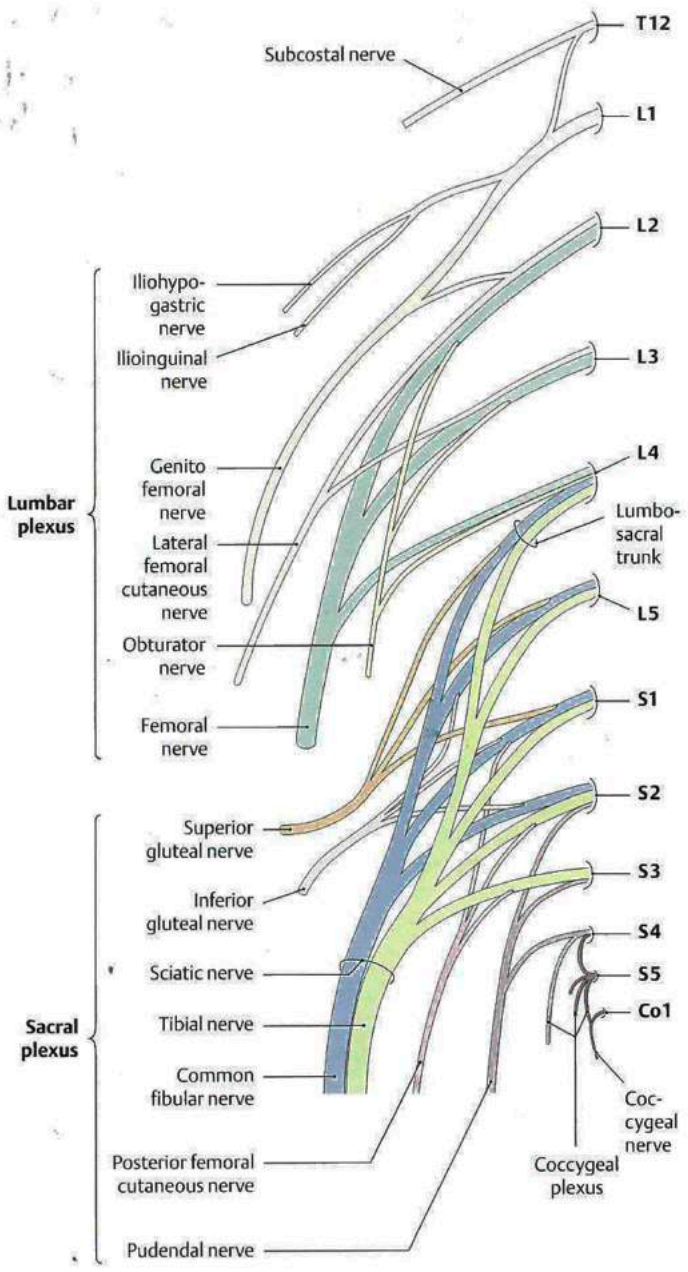

Fig. 1. Schematic overview over the lumbosacral plexus.[39]

The Lumbar Plexus

The lumbar plexus is derived from the anterior rami of the first three lumbar spinal nerves (L1 to L3), the major subset of the anterior ramus of the fourth lumbar spinal nerve (L4), and – in some humans – a branch from the anterior ramus of thoracic spinal nerve 12 (Th12) (**Figures 1 and 2)**.[36] [40] [41]

The femoral, obturator, and the lateral femoral cutaneous nerves are the three main terminal nerves of the lumbar plexus with relevance for hip surgical anaesthesia and post-operative analgesia.[36] The femoral nerve is formed by branches from the dorsal divisions of the anterior rami of spinal nerves L2, L3, and L4. The dorsal branches of the anterior rami of spinal nerves L2 and L3 also give rise to the lateral femoral cutaneous nerve. The obturator nerve arises by branches from the ventral divisions of the anterior rami of spinal nerves L2, L3 and L4. If present, an accessory obturator nerve arises from branches of the anterior rami of spinal nerves L3 and L4.[36] [40]

The lumbar plexus has a close relationship to the psoas major muscle. Therefore is the psoas major muscle often used as a proxy marker of the location of the plexus – in regional anaesthesia and in anatomical studies.[42] The psoas major muscle consists of a larger anterior and a smaller posterior lamina. The anterior lamina arises from the lateral margins of the vertebral bodies of Th12 to L4, the intervertebral discs between them, and from tendinous arches stretched over the sides of lumbar vertebrae L1 to L4. The posterior lamina arises from the anterior surface of the roots of the transverse processes of vertebrae L1 to L5. The spinal nerves L1 to L4 emerge from the intervertebral (neural) foramina. The anterior rami of spinal nerves L2 and L3 and part of the anterior ramus of L4 enter the fascial plane between the two lamina of the psoas major muscle anterior to the transverse processes. Here, in the "intra-psoas compartment" between the posterior one third and anterior two thirds of the psoas major muscle, the anterior rami of spinal nerves L2, L3, and partially L4 form the lumbar plexus.[40-43] The anterior ramus of spinal nerve L1 does not enter the fascial plane between the two lamina of the psoas major muscle. Thus, a lumbar plexus block with an injection into the fascial plane does not anaesthetise the lumbar plexus nerves from

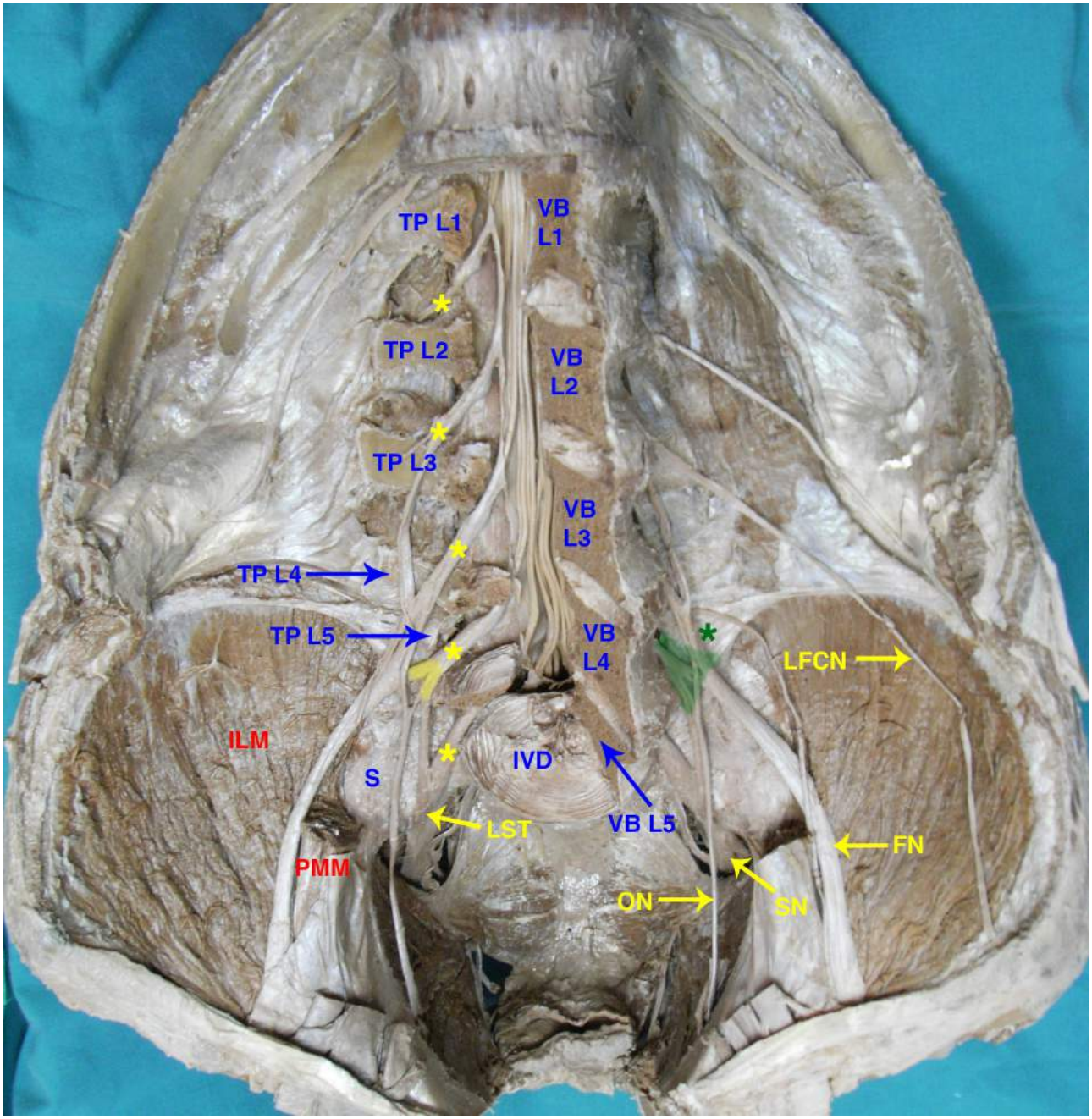

Fig. 2. Frontal overview of the lumbosacral plexus of a dissected cadaver. The preparation and the image are from professor emeritus Herbert Mauria, Division of Clinical and Functional Anatomy, Medical University of Innsbruck, Austria. Asterisks (yellow), ventral rami of spinal nerves L1 to L5; Area (green), simulation of cranial attachment of lumbosacral ligament; Area (yellow), furcal nerve; FN, femoral nerve; ILM, iliacus muscle; IVD, intervertebral disk; LFCN, lateral femoral cutaneous nerve; LST, lumbosacral trunk; ON, obturator nerve; PMM, psoas major muscle; S, sacral ala; SN, sciatic nerve; TP L1 to 5, transverse processes of vertebrae L1 to L5; VB L1 to L5, vertebral bodies of L1 to L5.

spinal nerve L1 – the iliohypogastric and ilioinguinal nerves. The lateral cutaneous branch of the iliohypogastric nerve innervates the skin of the lateral side of the hip region between the iliac crest and the greater trochanter. Rarely, the lumbar plexus is formed posterior to the psoas major muscle on the surface of the posterior abdominal wall.[43]

The femoral and lateral femoral cutaneous nerves lie closely together within the psoas major muscle and emerge from the postero-lateral margin of the muscle at the level of the transverse process of L5 and the cranial margin of the sacrum,[43] where the muscle begins to deviate antero-laterally (**Fig. 3**).[41] The femoral nerve runs in the groove between the psoas major and iliac muscles while the lateral femoral cutaneous nerve runs on the surface of the iliacus muscle. Both nerves lie between the muscle and the iliac fascia (i.e. the transversalis fascia).[44] The femoral nerve enters the thigh posterior to the inguinal ligament, where it is lateral to the femoral sheath. It ends in the femoral triangle, where it splits into numerous branches. It innervates the iliacus (in the abdomen), pectineus, quadriceps, and sartorius muscles as well as the antero-lateral hip joint capsule (**Fig. 4**) and the skin on the antero-medial thigh.[41 45 46]

The lateral femoral cutaneous nerve enters the femoral triangle medial to the anterior superior iliac spine and posterior to the lateral end of the inguinal ligament. It pierces or runs either superficial or deep to the sartorius muscle and pierces the fascia lata 5 to 10 cm caudal to the anterior superior iliac spine. The anterior branch of the lateral femoral cutaneous nerve innervates the skin and fascia of the antero-lateral surface of the thigh.[41] The posterior branch innervates the skin and fascia on the proximal lateral thigh in the region of the greater trochanter.

The obturator nerve emerges from the medial margin of the psoas major muscle at the level of vertebra L4. It descends anterior to the transverse process of L5 and the iliolumbar ligament, and then the ala sacrum, where it is located lateral to the lumbosacral trunk. The anterior and posterior branches of the obturator nerve innervate the external obturator, adductors (brevis, longus, and magnus), pectineus, and gracilis muscles as well as the antero-medial hip joint capsule (**Fig. 4**).[41 45]

[46] The cutaneous branch is frequently absent. Occasionally – when present – it innervates the distal two-thirds of the skin on the medial thigh.[38]

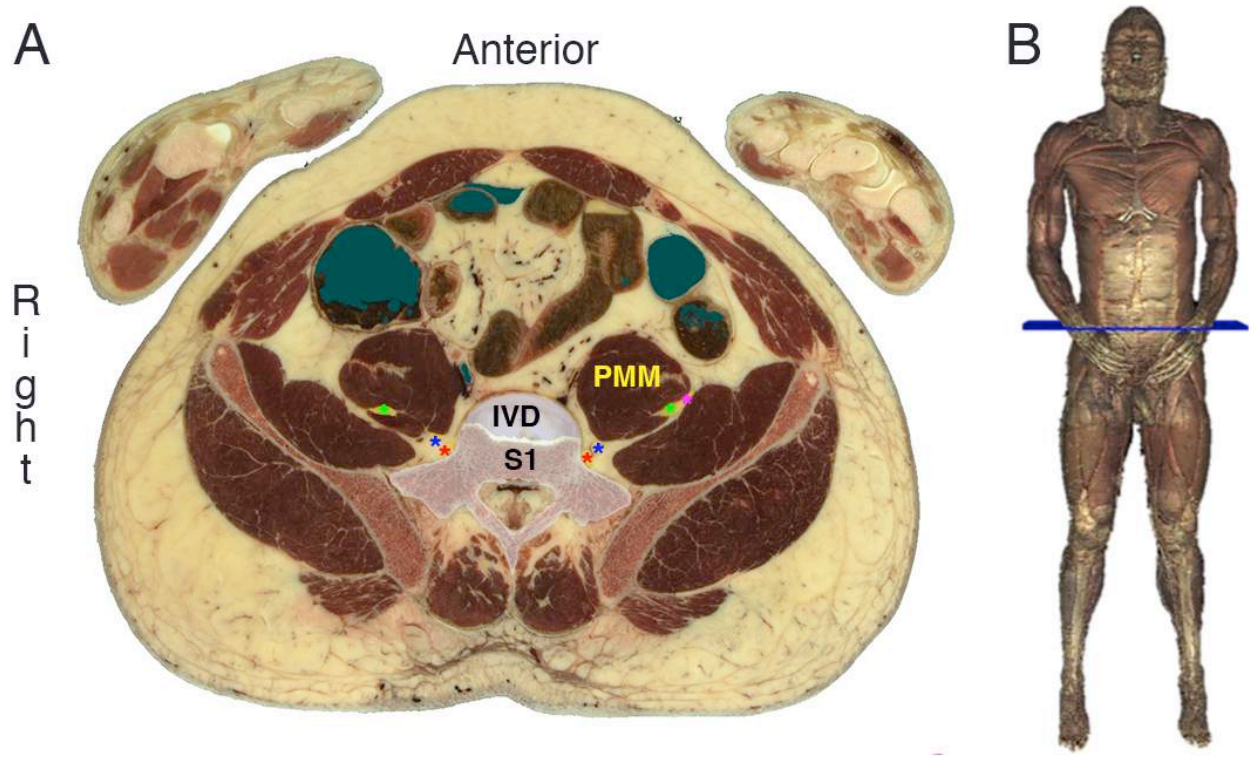

Fig. 3. A) Cross-sectional image of the lumbosacral region at level of the intervertebral disc L5/S1. Please note that the lateral femoral cutaneous nerve is displaced laterally compared to *in vivo*, where it is typically juxtapositioned to the femoral nerve at the lateral margin of the psoas major muscle. B) Overview where the blue plane represents the level of the axial plane displayed in A. Asterisks (blue), ventral ramus of spinal nerve L4; Asterisk (green), femoral nerve; Asterisk (magenta), lateral femoral cutaneous nerve; Asterisk (red), ventral ramus of spinal nerve L5; IVD, intervertebral disk of L5/S1; PMM, psoas major muscle; S1, vertebra of S1. Modified image from VH Dissector™ Pro v. 5.2.60 2003-2016 (Touch of Life Technologies Inc., Aurora, Colorado, USA).

The Sacral Plexus

The sacral plexus is composed of the lumbosacral trunk (from the anterior rami of spinal nerves L4 and L5) as well as the anterior rami of the first three sacral spinal nerves (S1 to S3) and a subset of the anterior ramus of the fourth sacral spinal nerve (S4) (**Fig. 1**).[41] The subset of the anterior ramus

of lumbar spinal nerve L4, which joins the anterior ramus of lumbar spinal nerve L5 to become the lumbosacral trunk, does not enter the intra-psoas compartment. At the level between the transverse process of L5 and the cranial margin of sacrum **(Fig. 3)**, the anterior rami of spinal nerves L4 and L5 are located together with the obturator nerve (not visualised on Fig. 3) postero-medial to the psoas muscle. The lumbosacral trunk is formed more caudal, medial to the psoas major muscle on the sacral ala, and descends and fuses with the anterior rami of spinal nerve S1.

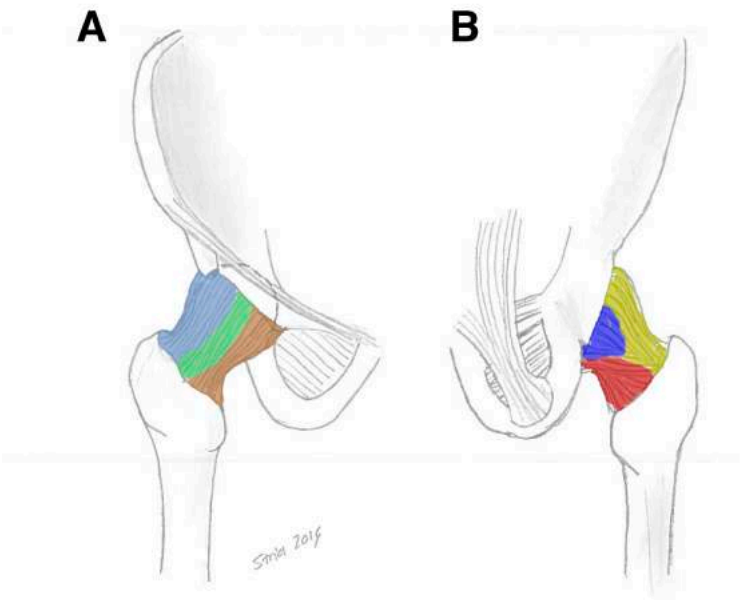

Fig. 4. Schematic illustration of the right hip capsule and its approximate innervation zones. A) Anterior view: the anterior and antero-lateral part (light blue) is primarily innervated by the femoral nerve; the anterior and antero-medial part (brown) is primarily innervated by the obturator nerve; and the mid anterior part is an overlap zone innervated by both the femoral and the obturator nerves. B) Posterior view: the postero-lateral part (yellow) is primarily innervated by the superior gluteal nerve; the postero-inferior part (red) is primarily innervated by the sciatic nerve via a branch to the quadratus femoris muscle; and the postero-superior part (blue) is primarily innervated directly by branches from the sciatic nerve.[46]

The lumbosacral and the sacral anterior rami of spinal nerves S1 to S3 (and partly S4) converge and form the triangular sacral plexus on the posterior pelvic wall and in the lesser sciatic foramen

between the piriformis muscle and the lesser pelvic fascia. The dorsal branches from spinal nerves L4 to S1 form the superior gluteal nerve. The superior gluteal nerve exits through the greater sciatic foramen superior to the piriformis muscle and innervates the gluteus medius and minimus muscles as well as the tensor fascia latae muscles and the postero-lateral hip joint capsule (**Fig. 4**).[46 47] The most cranial segments (L4 to S1) of the ventral branches from the sacral plexus that form the tibial nerve (L4 to S3) supply direct branches to the postero-superior part of the hip joint capsule.[45] Furthermore, a branch is formed to the quadratus femoris muscle. This branch also innervates the postero-inferior hip joint capsule with articular branches.[45] The tibial nerve from the sciatic nerve innervates – with a minor contribution from the common fibular nerve – the hamstrings and the gastrocnemius muscles.

Anaesthesia and Analgesia of the Hip

Anaesthesia

General and neuraxial anaesthesia are the most conventional techniques for surgical anaesthesia of the hip. General anaesthesia induces unconsciousness, amnesia, analgesia, loss of some autonomic reflexes, and sometimes muscle relaxation. This is achieved by either inhalation of anaesthetic gas, intravenous injection, or infusion of drugs – or by a combination. Neuraxial anaesthesia together with peripheral nerve and plexus blocks are generically termed regional anaesthesia. During sole regional anaesthesia, the patient remains conscious but is pain free in a specific anatomical region. This is achieved by perineural injection of local anaesthetic that penetrates the neuronal membrane and blocks the conduction of afferent signals to the brain. Hence, the dermatomes, myotomes, and sclerotomes that are innervated by the blocked nerve or nerves become anaesthetised and unresponsive to pain. With a neuraxial block, the local anaesthetic is injected into the central nervous system, either into the cerebrospinal fluid (intrathecal or spinal blockade) or into the epidural space (epidural blockade), and a bilateral anaesthesia at the lumbar and sacral levels is achieved. With a peripheral nerve/plexus block, the local anaesthetic is injected perineurally around selective terminal nerves or nerve plexuses and a selective unilateral anaesthesia can be achieved.

General and spinal anaesthesia are associated with a risk of complications,[7 10 48] *e.g.* aspiration, intraoperative awareness including long-term neuropsychological disorder, and pulmonary complications for general anaesthesia and infection, neural damage, epidural or intrathecal hematoma, and paraplegia for neuraxial blockades.[7] The worst-case scenario is fatal complications.[7 48] Although peripheral nerve/plexus blocks are associated with some complications similar to neuraxial anaesthesia, *e.g.* infections, neural damage, vascular puncture, and local anaesthetic systemic toxicity, complications are rare and peripheral nerve blocks for hip surgery are related to more stable haemodynamics and less complications compared to general and neuraxial anaesthesia – especially in elderly patients.[5 7-9 48-50] However, blockade of the lumbosacral plexus for hip surgery is based on a paravertebral injection of local anaesthetics, close to the neural foramina, and is therefore associated with a risk of epidural spread of local anaesthetic.[19 51-56]

Analgesia

Perioperatively, hip surgery patients suffer moderate to severe pain.[12 57] In addition to severe discomfort and dissatisfaction of the patient, insufficient pain treatment may result in prolonged in-hospital length of stay, impaired rehabilitation and recovery as well as increased risk of postoperative complications. Multimodal pain treatment based on non-opioid analgesics including non-steroid anti-inflammatory drugs has successfully decreased the use of opioids and resulted in increased patient satisfaction and early recovery.[12] However, patients treated with multimodal pain treatment often need considerable doses of opioids, *e.g.* morphine, in addition to the non-opioid analgesics. Opioids are associated with many adverse effects, *e.g.* nausea, vomiting, constipation, impaired motor function, depression of the central nervous system, and addiction. The use of opioids in old, frail, and/or high-risk hip surgery patients is therefore undesirable.[12 57] Peripheral nerve blocks provide efficient postoperative analgesia, which can minimise the use of opioids and thereby the risk of adverse effects.[11 54]

Lumbar and Lumbosacral Plexus Blocks and Ultrasound Guidance

Blockade of the lumbar plexus between the two lamina of the psoas major muscle, in the intra-psoas compartment, provides adequate postoperative analgesia of the hip and lower limb.[55 58 59] A lumbar plexus block also provides sufficient surgical anaesthesia for hip fracture surgery as well as total hip replacement if it is supplemented with sacral plexus and iliohypogastric nerve blocks.[51 55 60] Alternatively, a single-injection block that anaesthetises the caudal part of the lumbar plexus and the cranial part of the sacral plexus (hereafter referred to as a "lumbosacral plexus block") can be applied for surgical anaesthesia in hip fracture patients.[6 60]

Several lumbar plexus block techniques and one lumbosacral plexus block technique guided by anatomical landmarks, "loss-of-resistance", paresthesia, and/or electrical nerve stimulation have been presented.[51 60-63] These guidance techniques are referred to as "blind techniques" because they do not involve any visualisation of the target lumbar and sacral plexuses. On the contrary, ultrasound guidance has gained popularity within regional anaesthesia because of the real-time ultrasonographic visualisation of target nerves, anatomical landmarks, the block needle, and the perineural spread of local anaesthetics.[64]

Ultrasound Guided Lumbar Plexus Block Techniques

After the first description of the paravertebral ultrasonoanatomy in cadavers,[65] and studies of posterior ultrasound guided lumbar plexus block approaches in cadavers and paediatric patients,[13 20] multiple posterior ultrasound guided lumbar plexus block techniques have been presented.[14-18 21] The various techniques differ in positioning of the patient, level of injection, needle orientation in reference to the ultrasound probe, and location of the insertion point of the needle. However, they all apply a paravertebral location of the probe, close to the median plane and a needle insertion in-plane with an axial[13 14 16 18 21 43] or a sagittal[15 17] orientation of the ultrasound beam. Needle insertion between transverse processes of L4 and L5 is advocated in order to decrease the risk of renal puncture and hematoma.[66] Depending on the location of the needle insertion point and inclination of

the needle, the mean distance between the skin and the target lumbar plexus varies between 5.0 to 9.4 (standard deviation [SD] 2.1) cm in adults.[14 16 17 37] Due to the deep location of the target lumbar plexus and the paravertebral lumbar bony structures, the inherent limitations of ultrasonography (explained below) may result in insufficient visualisation of the target nerve plexus, the sonoanatomical landmarks, the block needle, the needle tip and trajectory, and the spread of local anaesthetic when a posterior paravertebral scanning technique is applied.[14-18 20 21] As a result, the accuracy of the injection of local anaesthetic may be decreased and thereby the efficiency of the blockade is impaired. In addition, insufficient visualisation may potentially reduce the safety due to an increased risk of vascular puncture, intravascular injection, nerve injury, muscular injury, renal injury and puncture, and epidural spread of local anaesthetic.

The Lumbar Ultrasound Trident (LUT) technique, using a paravertebral sagittal position of the probe and an out-of-plane needle insertion close to the probe, is the best-established ultrasound guided technique for lumbar plexus blockade.[15 19] However, in a case report of the LUT technique, the lumbar plexus was only visualised in 3/5 (60%) patients.[15] Moreover, the LUT technique was aborted in 1/20 (5%) volunteers due to bloody aspiration and 5/17 (29%) volunteers had epidural spread in a randomised controlled trial.[19]

The ultrasound guided Shamrock technique for lumbar plexus blockade is based on axial scanning from the flank of the patient and a posterior in-plane needle insertion.[59] This scanning position improves the visualisation of the lumbar paravertebral anatomy including the target lumbar plexus, the needle tip, and the local anaesthetic spread compared to the posterior paravertebral scanning techniques.[22 59] Furthermore, the axial orientation of the probe allows tissue compression, which decreases the distance from the probe to the target lumbar plexus.[67] The Shamrock technique and modifications hereof have been described in letters to the editor, investigated in a dose-finding study, and discussed in correspondences,[22 59 68-73] but – as most lumbar plexus block techniques[10-12 14-16 18] – not investigated in a randomised controlled trial.[13 14 16-18 20 21]

Lumbosacral Plexus Block Techniques

A paravertebral injection of local anaesthetic between the transverse process of L5 and the cranial margin of the sacral ala into the compartment posterior to the psoas major muscle may spread around the terminal nerves of the lumbar plexus – after they have emerged from the psoas major muscle – and to the cranial part of the sacral plexus (the lumbosacral trunk).[60] In a cadaver study, "reasonable" spread of injected dye to the lumbar plexus terminal nerves and the lumbosacral trunk was found after lumbosacral plexus block guided by anatomical landmarks and loss of resistance. However, 3/20 (15%) cadavers had only "very weak staining" of spinal nerve S1 and 2/20 (10%) had epidural spread.[60] Only one ultrasound guided lumbosacral plexus block technique – the Suprasacral Parallel Shift (SSPS) – has been described.[19] In a randomised controlled trial in healthy volunteers, the SSPS technique was equally effective for lumbar plexus blockade and more effective for blockade of the lumbosacral trunk compared with the LUT technique.[19] Two/18 (11%) volunteers had epidural spread when the SSPS technique was applied.[19]

Strengths and Limitations of Ultrasound Guidance

Compared to blind techniques guided by surface anatomical landmarks and/or electrical nerve stimulation, ultrasound is associated with avoidance of unpleasant muscle contractions during electric nerve stimulation, decreased risk of intraneural or intravascular injection of local anaesthetics (and hence the risk of local anaesthetic systemic toxicity), reduced block procedure time, reduced dose of local anaesthetic, faster onset time of blockade, and longer duration and improved effect of blockade.[49 64 74 75] Furthermore, ultrasound guidance (alone or in combination with electrical nerve stimulation) is associated with higher success of surgical anaesthesia compared with guidance by electrical nerve stimulation alone.[49] Ultrasound guidance has also shown to be more cost-effective than guidance with electrical nerve stimulation.[76] In practice though, blind techniques can be used to secure the correct position of the ultrasound probe (anatomical landmarks), indicate penetration of ligaments (loss of resistance), and alert to the risk of intraneural position of the needle tip (electrical nerve stimulation), which can be helpful particularly when ultrasonographic visualisation is limited.

Compared with other imaging modalities, ultrasound has several advantages as well.[77] Ultrasonography allows real-time visualisation of anatomy and pathology without potentially harmful ionizing radiation.[26 78] Ultrasound systems are portable point-of-care systems with low user and maintenance costs.[26 77] Ultrasound scanning has also proved to be a practical, fast, and successful examination.[77]

However, achievement of sufficient ultrasonographic visualisation may be impaired by the inherent limitations of ultrasonography.[64 77] First, high-resolution imaging requires sound waves of high frequency, but the high frequency decreases tissue transmission, resulting in low-resolution imaging at larger tissue depths. Second, sound waves cannot penetrate air or bony structures, resulting in dark or black acoustic shadows on the ultrasonographic image, which limit the visualisation of tissues or structures positioned in the acoustic shadow. Third, age-related anatomical changes and diseases, *e.g.* morphometric changes in the lumbar vertebrae and intervertebral discs,[79-81] osteoporosis, and decalcification, can cause decreased reflection of the bony landmarks and reduce the quality of the ultrasonographic image. Furthermore, as all practical procedures, the quality and time of the procedure are dependent of the skill of the operator.[64]

All these limitations are relevant for ultrasonographic visualisation of the lumbar and lumbosacral plexuses due to the deep target location and the demographics of the target patients. The limited visualisation may decrease the accuracy, and thereby the effectiveness and safety, of the blockade in these patients. Although ultrasonographic visualisation of the lumbar plexus is improved with the Shamrock technique, a recent dose-finding study reported poor visualisation of the lumbar plexus in 9/28 (32%) patients.[22] Although the ultrasound guided SSPS technique improved the success of lumbosacral blockade compared to the LUT technique, it may not block the lumbosacral trunk and thereby become insufficient for an incision in the hip capsule.[19] Furthermore, undesired epidural spread of local anaesthetic and bilateral anaesthesia may occur.[19]

Real-time Image Fusion of Ultrasound and MRI

Real-time image fusion of datasets acquired with multiple image modalities means that the image datasets are combined and displayed in overlay or side-by-side.[25] The rationale for medical image fusion is improved targeting of anatomical and/or pathological structures of interest in order to refine diagnostic accuracy, treatment, and monitoring of patients compared with the use of one image dataset only.[82, 83] By combining real-time ultrasonography with a high-resolution magnetic resonance imaging (MRI) dataset, the technical limitations of ultrasound can be overcome and the accuracy of the ultrasound guided procedure increased because of the additional visualisation with MRI.

In practice, an MRI dataset of the region of interest is recorded and uploaded to the advanced ultrasound system equipped with image fusion software. The ultrasound system is connected to a field generator that transmits an electromagnetic field. In this field, the system registers the position and orientation of a reference that is attached to the patient (patient tracker, **Fig. 5**). The system also registers the position and orientation of sensors that are attached to the ultrasound probe and the block needle (**Fig. 5**) in reference to the patient tracker. The MRI dataset is co-registered with the ultrasonographic reference space by match of a manually identified internal plane and point in that specific plane in both image datasets. Alternatively, the co-registration can be based on at least three manually identified – internal or external – points in any plane in both image datasets. After the co-registration, the MRI dataset is segmented and reformatted in real-time to best fit with the ultrasound matrix assuming exact three-dimensional (3D) congruence between the MRI and ultrasound datasets. Any tilt, rotation, and shift of the ultrasound probe – or the patient or parts of the patient in relation to the ultrasound probe – after the co-registration, results in a synchronic tilt, rotation, and shift applied as a real-time multiplanar reformatting of the 3D MR dataset in order to display the MR image in the same plane as the ultrasound image. Any misalignment of the fused image datasets can be adjusted at any time by means of tilt, rotation, and shift of the MRI dataset in relation to the ultrasonographic matrix.

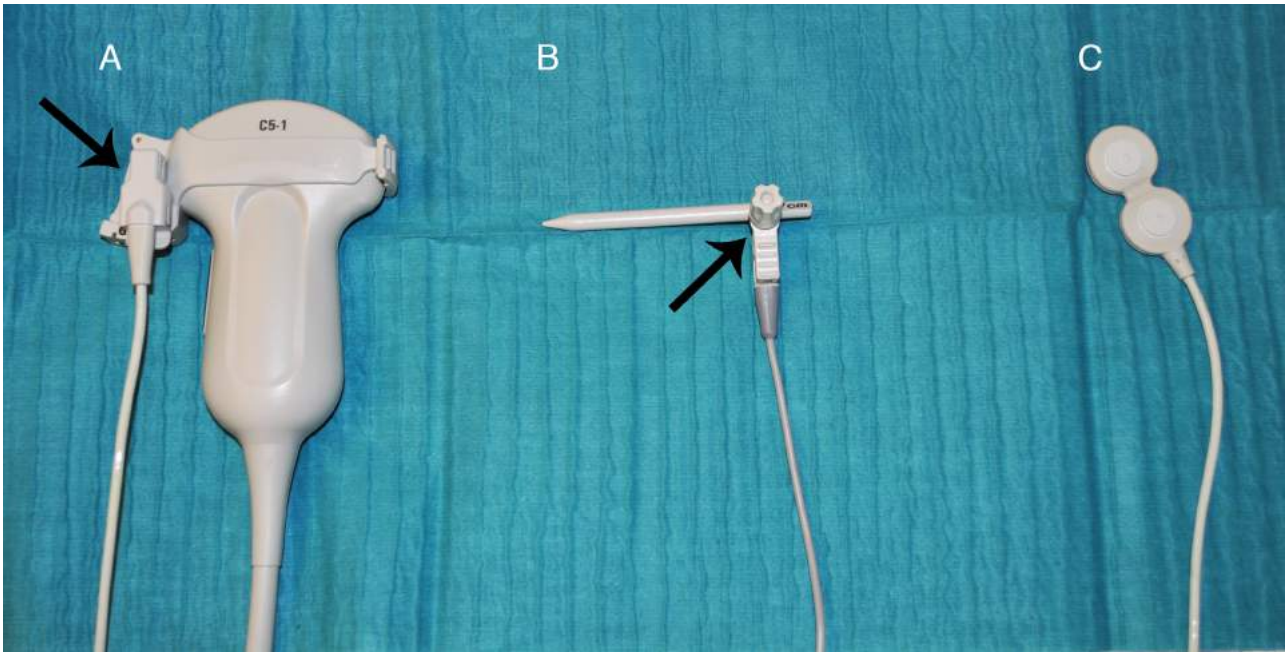

Fig 5. A) Ultrasound probe with mounted sensor (black arrow). B) Phantom needle with mounted sensor (black arrow). C) Patient tracker.

The image fusion software includes electronic needle tip tracking that displays the registered position of the block needle, its anticipated trajectory, and the presumed intersection between the needle tip and the ultrasound beam on the monitor. It is also possible to plan and assess the predicted needle trajectory (target planning). Target planning is carried out by marking the target and the anticipated entry point of the needle on the skin, which hereafter are displayed on both image modalities on the monitor.

The use of image fusion based on real-time ultrasound has gained popularity within multiple medical specialities, especially within interventional radiology.[25 82] The technique has been successfully applied on advanced image guided procedures, where high accuracy is desirable and blind techniques or ultrasound guidance alone are insufficient.[25 82] In interventional chronic pain management, applications of ultrasound/computed tomography (CT) or ultrasound/MRI fusion guided local anaesthetic injections have been reported for the hand, wrist, and sacroiliac joint and around the pudendal nerve in cadavers and in patients.[84-87] Ultrasound/CT fusion of cadavers has

also been described as a powerful educational tool to improve ultrasound guided periradicular and facet joint infiltrations of local anaesthetic.[26] Within regional anaesthesia, published material is limited to a brief description of approaches for ultrasound/CT fusion and ultrasound/MRI fusion of the lumbar spine in a phantom and in volunteers, respectively.[27] However, no injections were described and electronic needle guidance was not explored.[27] To the best of our knowledge, so far no reports have been published on ultrasound/MRI fusion guided injections of local anaesthetic in the lumbosacral region for surgical anaesthesia and/or postoperative analgesia.

Aims and Hypotheses

Study I

We aimed to compare block procedure time of ultrasound guided lumbar plexus blockade with the Shamrock technique vs. the LUT technique. Based on a pilot study, we hypothesised that the block procedure time would decrease from 280 s with the LUT technique to 140 s with the Shamrock technique.

Study II

We aimed to compare the proportion of study subjects with successful lumbosacral plexus blockade using the SSPS approach either with ultrasound/MRI fusion or ultrasound guidance. Based on a previous study and experimental training, we hypothesised that the proportion of study subjects with successful lumbosacral plexus blockade would increase from 75% with ultrasound to 100% with ultrasound/MRI fusion guidance.

In addition, we aimed to employ ultrasound/MRI fusion as well as the MRI sequences recorded after injection of local anaesthetics with added contrast to explore patterns of perineural and compartmentalised injectate spread.

Study III

We aimed to compare the proportion of study subjects with successful lumbar plexus blockade using the Shamrock approach either with ultrasound/MRI fusion or ultrasound guidance. Based on previous studies and experimental training, we hypothesised that the proportion of study subjects with successful lumbar plexus blockade would increase from 40% with ultrasound to 70% with ultrasound/MRI fusion guidance.

In addition, we aimed to employ ultrasound/MRI fusion as well as the MRI sequences recorded after injection of local anaesthetics with added contrast to explore patterns of perineural and compartmentalised injectate spread.

Methodological Considerations

Ethical Considerations

The ultrasound guided Shamrock technique has not been compared to the ultrasound guided LUT technique or investigated in a randomised controlled trial before. The ultrasound/MRI fusion protocols applied on the SSPS and Shamrock techniques were developed during the present PhD study. We therefore chose to assess the techniques in a standardised setting with healthy study subjects prior to any implementation in clinical studies with hip surgery patients. The Ethics Committee on Biomedical Research of the Central Denmark Region, the Danish Medicines Authority, and the Danish Data Protection Agency approved all trials. The Good Clinical Practice Unit of Aalborg and Aarhus University Hospitals monitored all trials. All trials were prospectively registered in EudraCT and ClinicalTrials.gov. All study subjects were included after informed oral and written consent. All trials were conducted according to the Declaration of Helsinki.[88]

Study Participants

We enrolled healthy (American Society of Anesthesiologists [ASA] physical status I[89]) study subjects 18 years or older. All study subjects were recruited through a Danish website for research volunteers.[90] The inclusion and exclusion criteria are specified in the supplemental Paper I to III.

Study Designs

All trials were blinded randomised controlled trials with crossover design. All trials were conducted at the Department of Radiology, Aarhus University Hospital. **Fig. 6** illustrates the general flow of the study subjects in all trials. However, the "MRI for fusion" was only conducted in studies II and III. The specific elements in **Fig. 6** and the endpoints are presented in detail in the supplemental Paper I to III and are considered below.

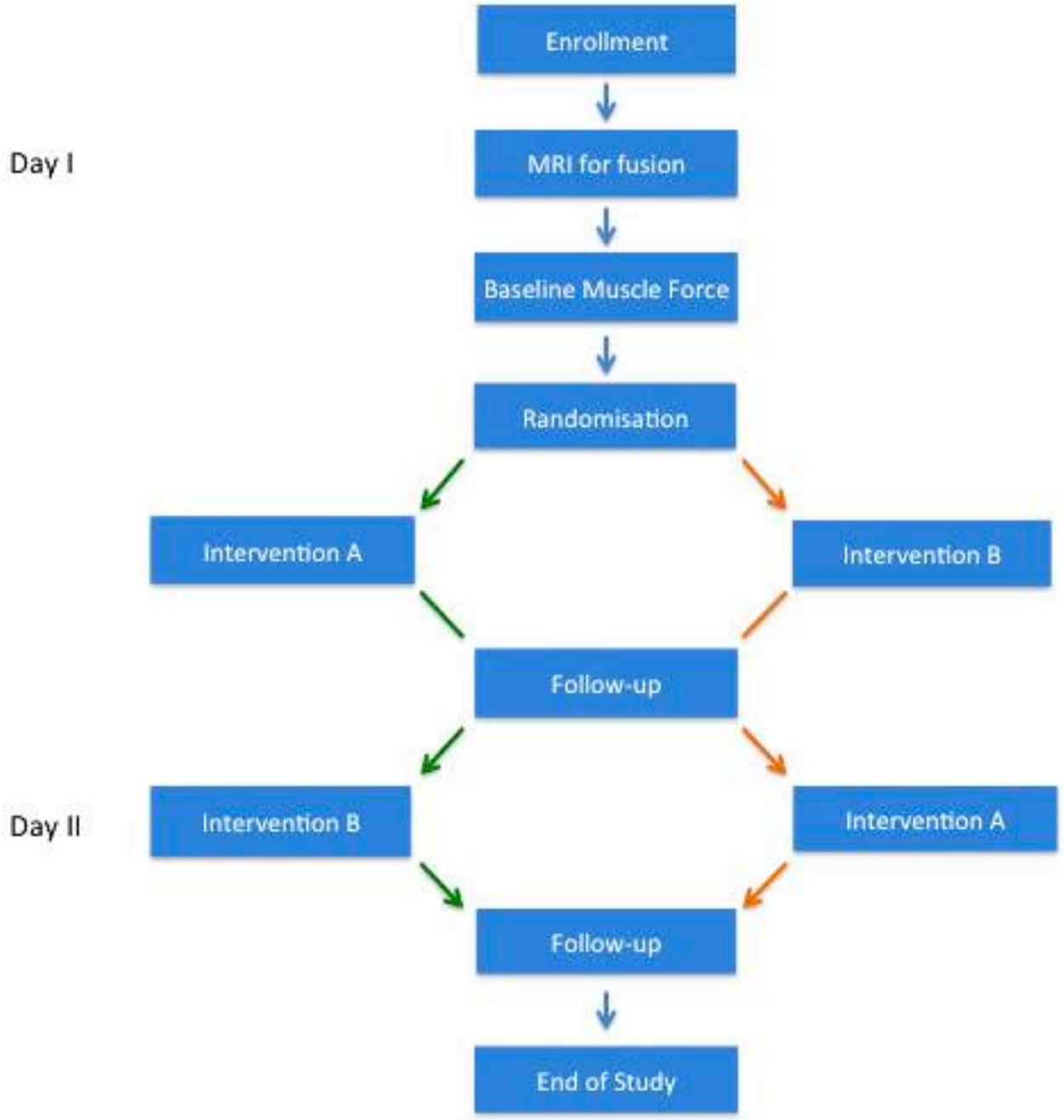

Fig 6. General study flow of the trials. Magnetic resonance imaging (MRI) for fusion was only conducted in studies II and III. The subjects were randomised to receive either intervention A on the first experimental day and intervention B on the second experimental day or *vice versa*; hence each subject followed either the green or the orange arrows.

MRI for Ultrasound/MRI Fusion (Studies II and III)

The purpose of the MRI dataset for fusion is to visualise the target nerves and the relevant sonoanatomy with a higher resolution compared to ultrasound. Supine is technically the most suitable body position and – for old and frail hip surgery patients – the most realistic choice of body position for recording MRI. However, the real-time ultrasound guided needle insertions in the SSPS and Shamrock techniques are performed in the lateral decubitus position. Change from supine to lateral decubitus positioning, movement, peristalsis, and respiration of the subject during the MRI recording and the real-time ultrasonography for fusion may affect the accuracy of the co-registered datasets,[25] and hence the accuracy of the ultrasound/MRI fusion guided block. Anyhow, the target lumbar plexus nerves are juxtapositioned to the rigid lumbosacral spine, and the iliopsoas muscle is not significantly displaced when position is changed from supine to lateral decubitus.[91] Furthermore, we have carried out a pilot study with study subjects 60 years or older, which showed only minor displacement of the ventral rami of spinal nerves L3 and L4 on MRI recorded in the lateral decubitus compared to the supine position (see Supplements). Consequently, we assessed that it was possible to adjust for the anticipated minor misalignments of the co-registered datasets (see below), and that residual inaccuracies would be within acceptable limits of measurement error of the procedure.

Based on the above, the subjects were placed in the supine position with a pillow supporting their knees to minimise lumbar lordosis before acquiring 3D T2-turbo spin echo (TSE) sequences with an isotropic resolution of 1.2x1.2x1.2 mm^3 (overlapping 2.3 mm slices with 1.2 mm spacing), echo time (TE) 60 ms, and repetition time (TR) 1,200 ms from vertebral body of L1 to S4 with a 1.5 tesla (T) Philips Ingenia MRI scanner (Koninklijke Philips Electronics N.V., Eindhoven, the Netherlands) (**Fig. 7**). We chose the 3D T2-TSE sequence for fusion because of the high-resolution isotropic nature and good soft tissue contrast for visualisation of the anatomy. The isotropic nature of this 3D sequence allows reconstruction in all planes with high resolution, which is optimal for real-time image fusion of ultrasound and MRI, where ultrasound defined arbitrary planes are reconstructed in real time. However, the 3D T2-TSE sequence was unsuitable for visualising neural

tissue (nerves and plexuses) inside the psoas major muscle, because it was not possible to separate the MR signal from the neural tissue from that of the muscular tissue. Consequently, both neural tissue and muscular tissue appears dark with the 3D T2-TSE sequence. Fat, however, appears bright with the 3D T2-TSE sequence and nerves were visible in fat tissue, *e.g*. inside the peri-psoas major compartments. The MR sequences were sampled in the coronal plane with a feet-head phase in order to minimise artefacts due to peristalsis and respiration. The 3D image datasets were reformatted to two-dimensional (2D) axial plane sequences, using a "digital imaging and communications in medicine" (DICOM) viewer (OsiriX v. 6.5.2. 64-bit; Pixmeo SARL, Bernex, Switzerland) prior to upload in the ultrasound system with image fusion software (PercuNav) (Epiq 7 1.4; Koninklijke Philips Electronics N.V., Eindhoven, the Netherlands). The reformatting was carried out because the Epiq 7 1.4 can only import datasets in the axial orientation for fusion.

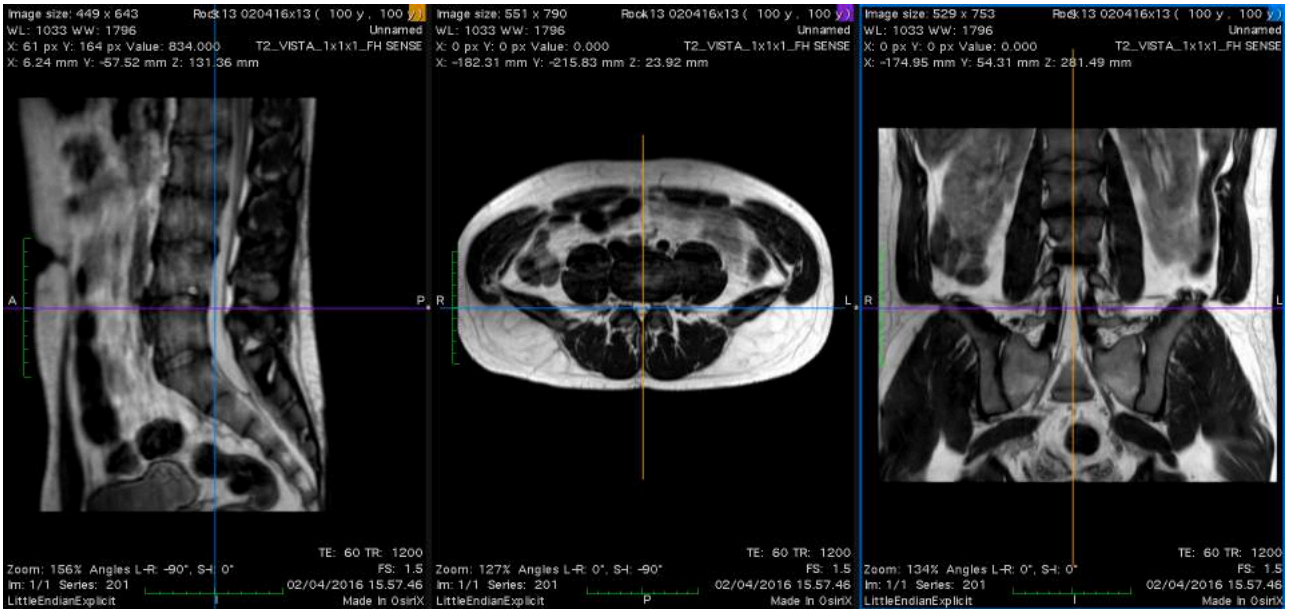

Fig 7. Three-dimensional isotropic T2-turbo spin echo sequence of one subject showing multiplanar reconstructions in all three standard planes (from the left: sagittal, axial, and coronal).

Interventions

All study subjects in each trial received two interventions in a randomised order with a one-week interim period (**Fig. 6**). All subjects had a peripheral intravenous access for safety (and for blood sampling in studies I and II) and were monitored with three-lead electrocardiography, non-invasive blood pressure measurement, and pulse oximetry. For all interventions, the subjects were placed in the lateral decubitus position with the side to be anaesthetised non-dependent and with slightly flexed hip and knee joints.

Study Medicine

All injections were composed of 20 ml 2% lidocaine with adrenaline 1:200,000 (Lidokain-adrenalin SAD; Amgros I/S, Copenhagen, Denmark)[92] added 1 ml of diluted 27.9% gadoterate meglumine (0.13 mL Dotarem®; Guerbet, Roissy CdG Cedex, France[93] in 0.87 ml 0.9% isotonic saline). Twenty ml 2% lidocaine-adrenaline corresponds approximately to the minimum effective anaesthetic volume to achieve lumbar plexus blockade with the Shamrock technique in 50% of patients (ED_{50}).[22] We chose to inject 20 ml lidocaine-adrenaline in order to standardise the comparisons and allow fast discharge of the subjects. The diluted MRI contrast agent (gadoterate meglumine) was added to the local anaesthetic prior to injection in order to allow assessment of spread of the injectate on MRI. A prospective laboratory study demonstrated that the local anaesthetic and the contrast agent as well as the local anaesthetic and contrast agent diluted in isotonic saline were physically compatible (see Supplements). Similar mixtures have been injected perineurally in other trials without reports of toxic reactions or harm.[19 94 95] Another gadolinium based contrast agent, gadopentetate dimeglumine, has been mixed with lidocaine and adrenaline without release of free gadolinium.[96] Considering the above and that only a very small volume of gadoterate meglumine (0.13 ml) was needed to visualise 20 ml lidocaine-adrenaline, it was assessed that the risk of toxic effects and of harm were negligible.

Operator and Equipment

Lumbar and lumbosacral plexus blocks are expert techniques that should only be performed by experienced regional anaesthetists. The ultrasound/MRI fusion protocol has been developed during the present PhD study. The anaesthesiologist (T.F.B.) – who conducted all interventions – has comprehensive clinical experience with lumbar and lumbosacral blocks guided by ultrasound and electrical nerve stimulation as well as experimental experience of SSPS and Shamrock blocks guided by ultrasound/MRI fusion and needle navigation. For all interventions, a curvilinear ultrasound probe was used to allow sonographic visualisation of the deeply located target plexuses and sonographic landmarks. In the ultrasound/MRI fusion studies, a sensor was mounted onto the probe to allow tracking of the position and orientation of the probe or strengthen blinding of the subjects.

Co-registration of Real-time Ultrasound and MRI (Studies II and III)

The subject was positioned supine and the patient tracker (Koninklijke Philips Electronics N.V., Eindhoven, the Netherlands) was fixed with adhesive transparent film to the subject's iliac crest on the side to be anaesthetised (**Fig. 8**).

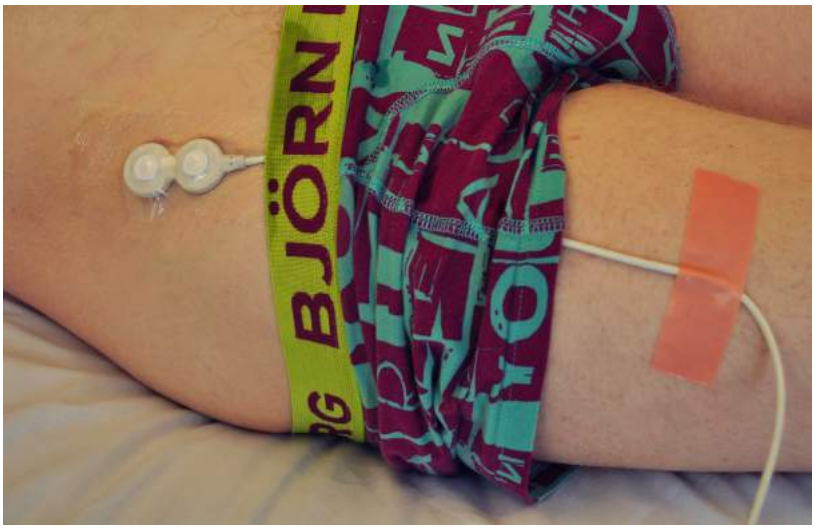

Fig. 8. Position of the patient tracker.

The position and orientation of the patient tracker serves as a reference for the sensors affixed to the ultrasound probe (and thereby for the MRI and ultrasound matrices) and the block needle. It is recommendable to attach the patient tracker to a rigid bony structure that assumedly does not deform with movement. We attached the patient tracker to the skin on the iliac crest on the side of the intervention, because the patient tracker needs to be within the electromagnetic field of the transmitter. Care has to be taken that the patient tracker does not overlap the anticipated needle insertion point or placement of the probe on the skin.

The field generator (Koninklijke Philips Electronics N.V., Eindhoven, the Netherlands) was positioned so that the dome-shaped electromagnetic field covered the abdomen, the lumbosacral region, and the flanks (**Fig. 9A**).

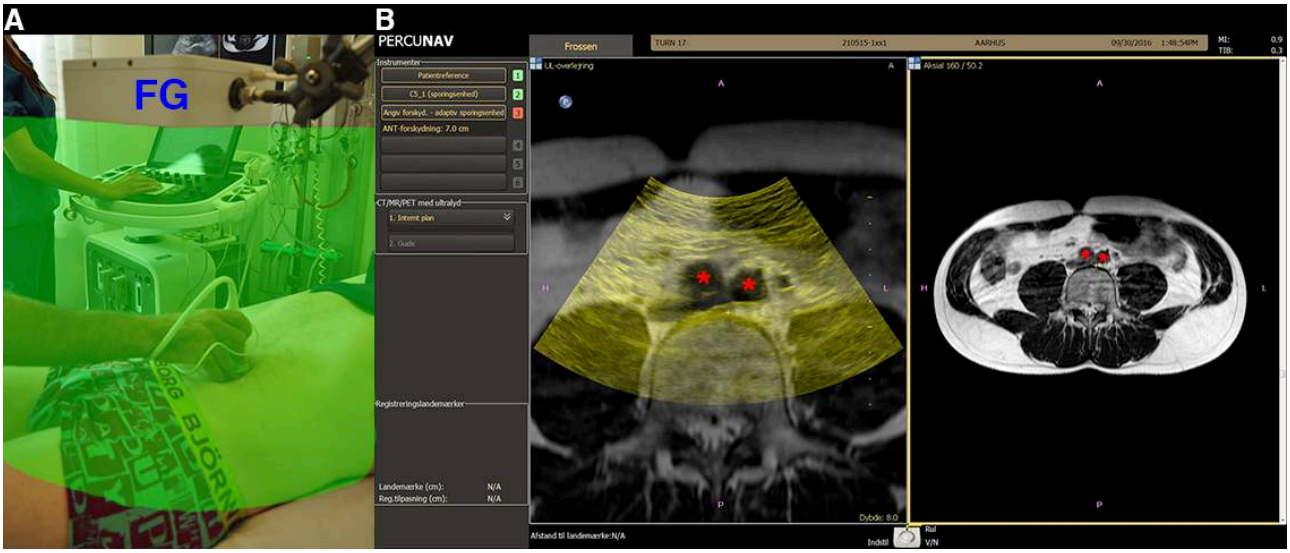

Fig. 9. Co-registration of real-time ultrasound and magnetic resonance imaging (MRI) datasets using an axial internal plane. A) The field generator (FG) is positioned so that the dome-shaped electromagnetic field (green) covers the region of interest. The ultrasound probe with the mounted sensor is axially oriented approximately at the level of the umbilicus. B) Screen-shot of the monitor displaying the internal plane-match of the axial plane intersecting the jointing of the common iliac arteries (red asterisks) on both image modalities. On the left-hand side of the monitor, the ultrasonogram is visualised as a transparent yellow overlay superimposed onto the MR image. The MR image is shown alone on the right-hand side of the monitor.

The probe with the mounted sensor was placed in the axial plane approximately at the level of the umbilicus (**Fig. 9A**). The axial plane that intersected with the jointing of the bifurcation of aorta and a corresponding point were identified and marked on both the MR and the real-time ultrasonographic image (**Fig. 9B**). A plane match was executed to obtain the best match between the MRI and the ultrasonographic image, which would allow linked scrolling with real-time 2D segmenting and reformatting of the MRI dataset. The alignment of the fused image modalities was reviewed using the anterior border of the vertebral body, the abdominal aorta, the inferior vena cava, and the common iliac arteries (**Fig. 10**).

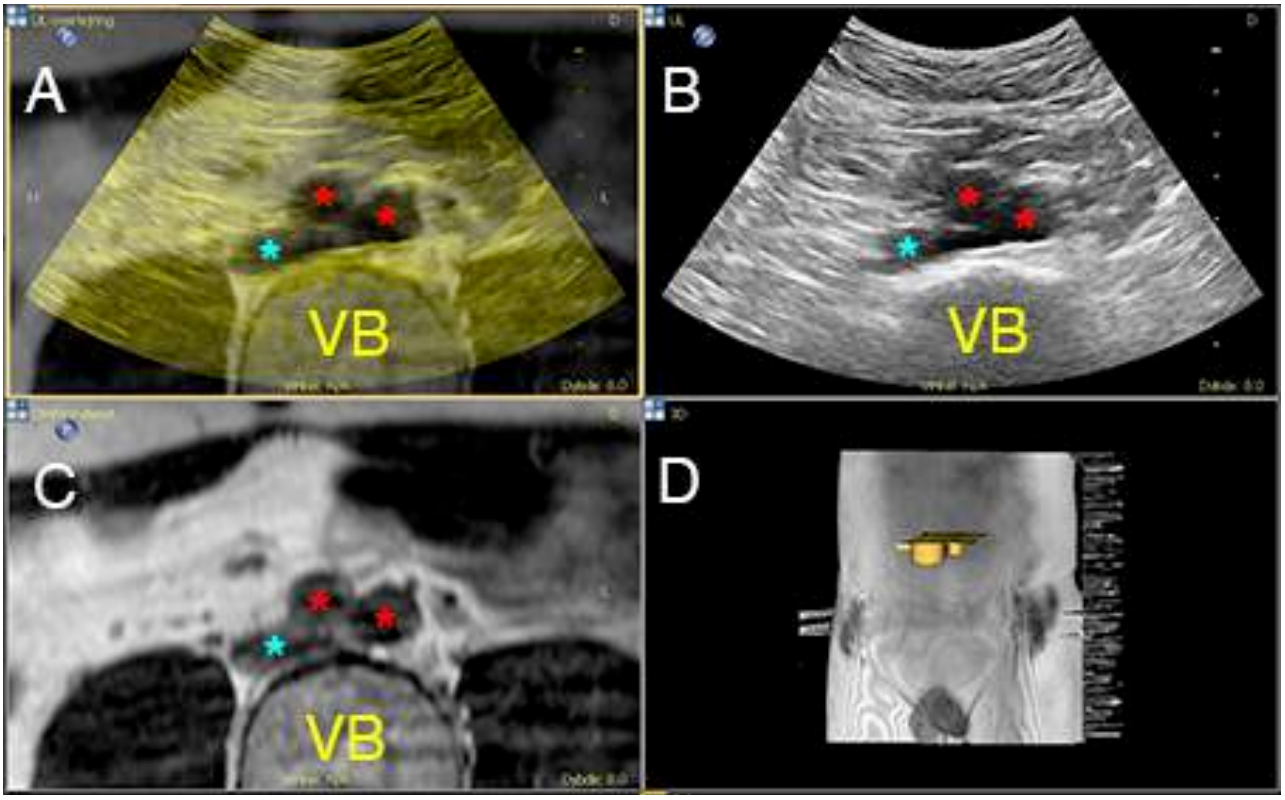

Fig. 10. Screen-shot of the monitor displaying the real-time sonogram and the previously sampled magnetic resonance (MR) image, which are co-registered and visualised as overlay (A) and as separate images (B and C). Image D visualises the three-dimensional position and orientation of the ultrasound probe and beam in relation to the MRI dataset. The common iliac arteries (red asterisks), the inferior vena cava (turquoise asterisks), and the anterior border of the vertebral body (VB) are employed for alignment of the ultrasound and MR images.

We chose to conduct an internal plane match instead of a point match because of the difficulty of identifying at least three identical points in the lumbar region that are visible with both MRI and with real-time ultrasound imaging. The plane match was carried out in the supine position using the jointing of the common iliac arteries as landmark in order to obtain the same axial level with both image modalities. The subject was turned to the lateral decubitus position in order to allow posterior needle insertion. Similar to the Shamrock technique, the probe was placed with axial orientation in the mid-axillary line in the flank of the subject. In order to compensate for any inaccuracies of the co-registration due to the positions change, the paravertebral sonoanatomy and the MRI dataset were aligned using the borders of the vertebral body, transverse process, and the neural foramen of L4, and the positions of the psoas major, the quadratus lumborum, and the erector spinae muscles. Any misalignment was adjusted with the system built-in means of rotating and aligning the MR image in relation to the ultrasonographic image.

Ultrasound/MRI Fusion and Ultrasound Guided Lumbar and Lumbosacral Plexus Blocks

We chose to compare the Shamrock technique with the LUT technique, because the LUT technique is probably the best-established technique of the posterior paravertebral approaches to lumbar plexus blockade. We chose to investigate real-time ultrasound/MRI fusion applied on the SSPS technique for lumbosacral plexus blockade and on the Shamrock technique for lumbar plexus blockade, because these deep blocks with inherent limitations of ultrasonography are important for hip surgery anaesthesia and analgesia.[19 22]

The ultrasound guided Shamrock, LUT, and SSPS techniques have been described in-depth previously.[6 15 19 22 59] The ultrasound guided Shamrock and LUT technique are described briefly in the supplemental Paper I. The ultrasound/MRI fusion guidance applied on the SSPS and Shamrock techniques is described in the supplemental Paper II and III. **Figures 11 to 15** illustrate the position of the probe and landmark sonograms of the techniques. All injections were carried out with the subject in the lateral decubitus position with the side to be anaesthetised non-dependent.

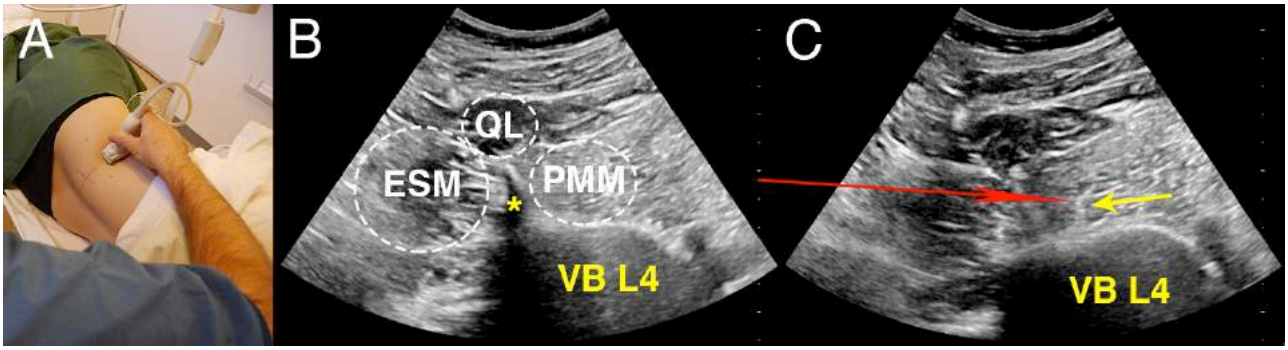

Fig. 11. The Shamrock technique guided by ultrasound used in studies I and III. A) The probe was axially orientated in the axillary midline in the flank of the subject. B) The probe was slid posteriorly and the Shamrock landmark sonogram – the erector spinae (ESM), quadratus lumborum (QL), and psoas major (PMM) muscles representing the three leaves, and the transverse process (yellow asterisk) of vertebra L4 (VB L4) representing the stem of a three-leaved cloves – was visualised. C) The tail of the probe was tilted cranially to improve any visualisation of the anterior rami of spinal nerve L4 (yellow arrow) to the lumbar plexus. Hereafter, the needle (red arrow) was inserted in-plane, approximately 3 to 4 cm lateral to the lumbar median, until the needle tip was visualised within the mass of psoas major muscle, at the margin of the target lumbar plexus, if possible.

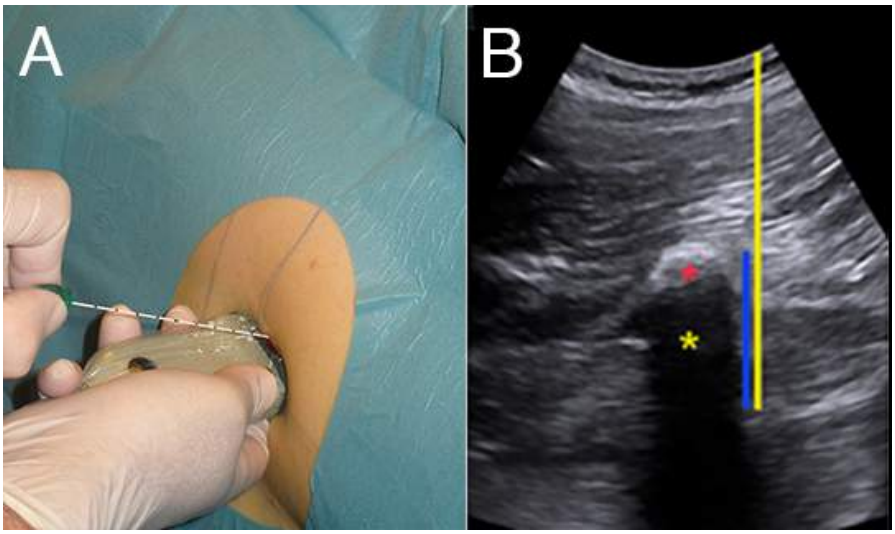

Fig. 12. The Lumbar Ultrasound Trident technique guided by ultrasound used in study I. The probe was placed in the sagittal orientation across the caudal margin of the transverse process of L5 and the cranial margin of the sacral ala. The probe was slid cranially while counting the transverse process of L4, L3, and L2. If possible, the lumbar plexus was visualised within the psoas major muscle anterior to the transverse processes. A) The block needle was inserted with a steep out-of-plane technique. B) The needle (represented

by the yellow line) was advanced until the needle tip was approximately 20 mm (represented by the blue line) anterior to the posterior margin of transverse process of L3 or L4 (red asterisk). The transverse process generates an acoustic shadow coined the “trident sign” (yellow asterisk). The image is modified from Bendtsen et al. [19]

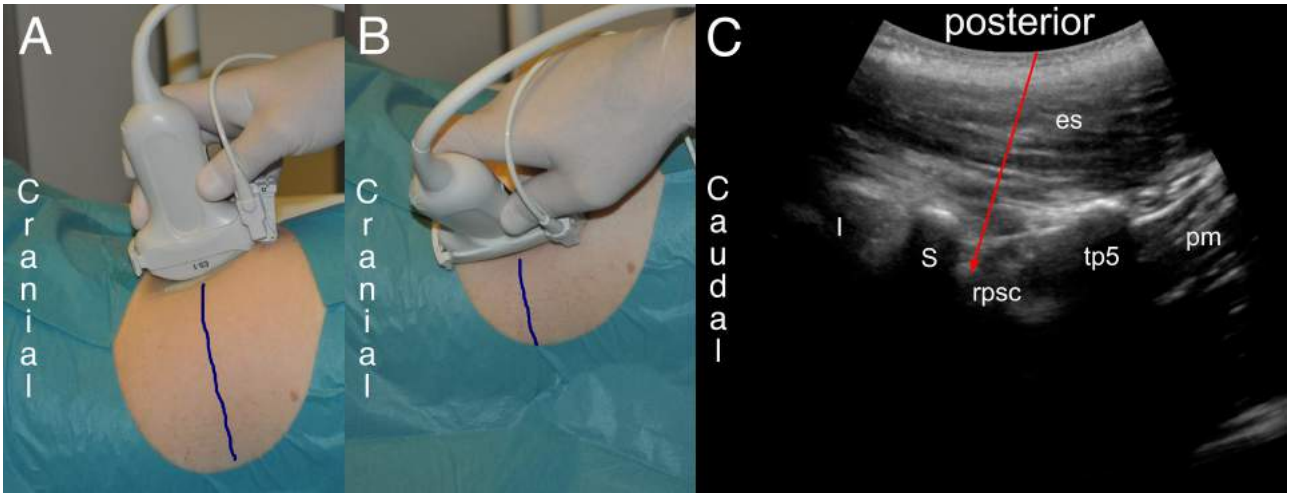

Fig. 13. The Suprasacral Parallel Shift technique guided by ultrasound used in study II. A and B) The probe was placed across the iliac crest (blue line) on the side to be anaesthetised. The probe is shifted parallel and medial until the interspace (osteofibrotic) between the caudal margin of the transverse process of L5 (tp5) and the cranial margin of the sacral ala (S) was visualised. Here, the probe was rotated to the sagittal plane. C) The osteofibrotic tunnel was centred in the ultrasonographic image. In this position, the block needle (red arrow) was inserted with a steep out-of-plane technique. The needle tip was advanced until it penetrated the lumbosacral ligament, confirmed with “loss-of-resistance” and ultrasonographic visualisation – if possible, and was in the retro-psoas subcompartment (rpsc). Es, erector spinae muscle; i, iliac bone; pm, psoas major.

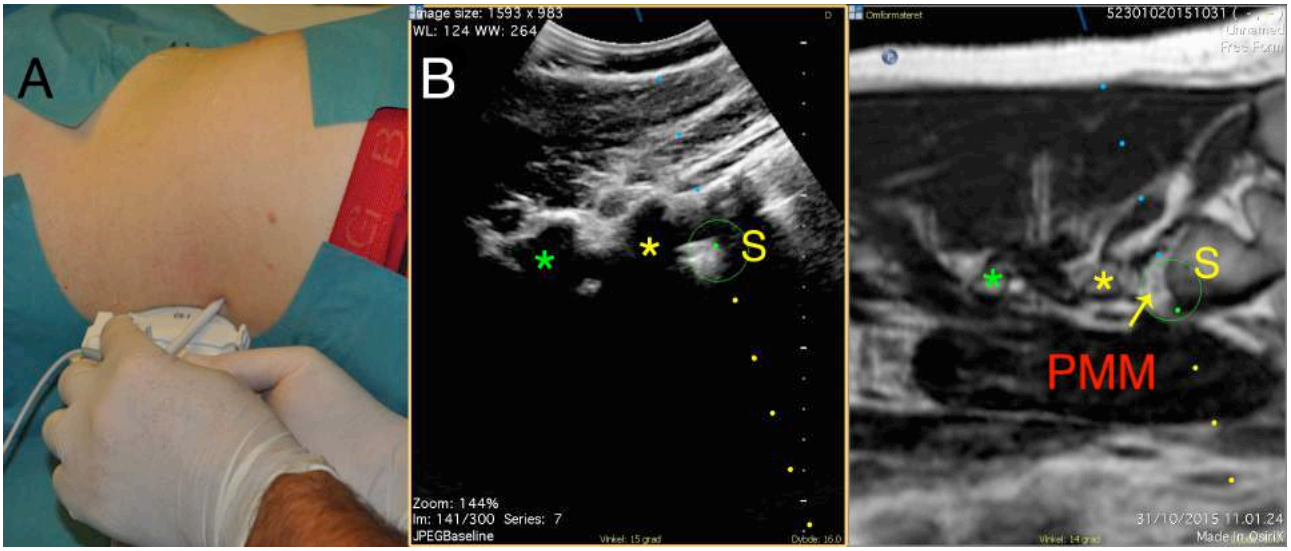

Fig. 14. The Suprasacral Parallel Shift technique guided by ultrasound/magnetic resonance imaging (MRI) used in study II. A) The probe was placed in the sagittal orientation across the transverse process of vertebra L5 and the cranial margin of the sacral ala. The needle with mounted sensor is held in an out-of-plane orientation. B) Fused real-time ultrasound (left) and MRI (right) displayed side-by side. The needle is projected as the blue line in the top of the images. The green circle marks the assumed intersection between the needle tip and the image plane, coinciding with the target plexus nerves (yellow arrow) between the transverse process of L5 (yellow asterisk) and the cranial margin of the sacral ala (S). The green dots mark the needle trajectory in-plane. The blue and yellow dots mark the needle trajectory out-of-plane. Asterisk (green); transverse process of vertebra L4; PMM, psoas major muscle.

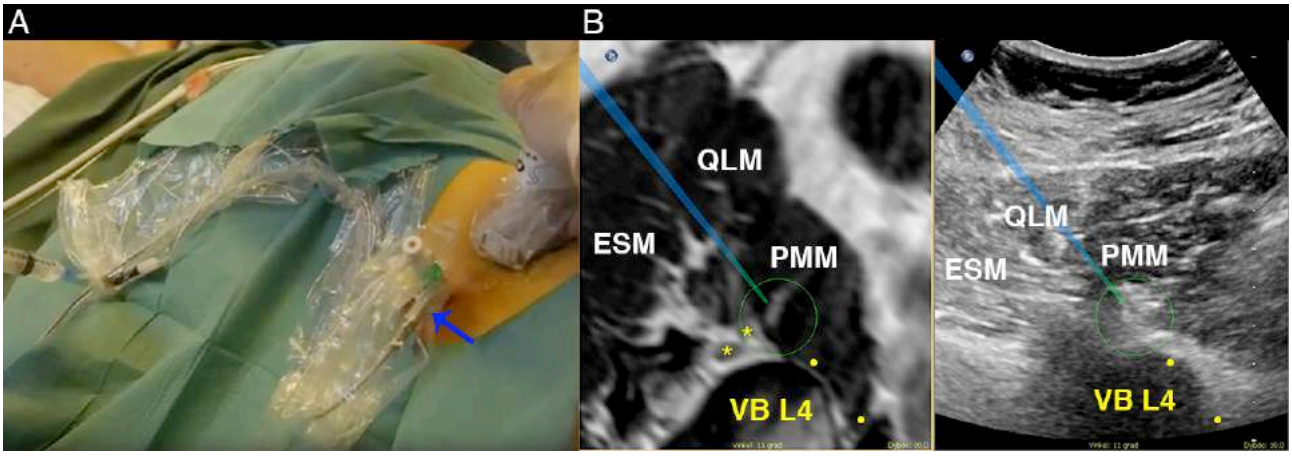

Fig. 15. The Shamrock technique guided by ultrasound/magnetic resonance imaging (MRI) used in study III. A) The probe is placed in the axial orientation in the flank of the patient. The block needle with the mounted

sensor (blue arrow) is inserted in-plane. B) Fused real-time ultrasound and MRI displayed side-by side: ultrasound to the left and MRI to the right. The block needle is projected as the blue/green line, where the green needle tip is in-plane with the image plane. The needle tip and the large green circle, which marks the intersection between the needle tip and the image plane, is in the intra-psoas compartment between the anterior and posterior lamina of the psoas major muscle (PMM). Asterisk (yellow); the anterior rami of spinal nerve L4 and the branch to the femoral nerve; ESM, erector spinae muscle, QLM, quadratus lumborum muscle; VB L4, vertebral body of L4.

Endpoints

In all three studies (I to III), we assessed procedure related outcomes, patterns of perineural spread of the injectate on MRI, epidural spread, sensorimotor effects, and cost-effectiveness. In studies I and II, we also assessed the time-dependent plasma concentration of lidocaine (p-lidocaine).

Procedure-related Outcomes

In order to compare time consumption, precision, and safety of the interventions, we recorded the following procedure related outcomes:

- preparation time (studies II and III)
- procedure time
- the minimal electrical nerve stimulation required to trigger a motor or paraesthesia response prior to injection
- the frequency of type of motor/paraesthesia response – if any
- the number of needle insertions
- the horizontal distance from the needle skin insertion point to the lumbar median
- the distance from the needle skin insertion point to the needle tip immediately prior to injection
- the discomfort of the procedure assessed by the subject on a numeric rating scale (NRS) 0 to 10 immediately after completed intervention

- the change in mean arterial pressure (ΔMAP) from immediately before start of pre-scanning (and co-registration) to five minutes after completed intervention
- the frequency of direct ultrasonographic visualisation of the lumbar plexus (study III)

Injectate Spread Analysed on MRI

Assessment of injectate spread on MRI is an objective proxy measure of the accuracy and effectiveness of the injection. We scanned 3D T1-weighted mDixon sequences that can be reconstructed to generate both in-phase, out-of-phase, water-only (fat-suppressed), and fat-only (water-suppressed) images from the same scan.[97] The 3D T1-weighted mDixon sequence is suitable for analysis of gadolinium-enhanced injectate spread. On these images the MRI contrast agent (Dotarem®) provides a strong signal – although water is suppressed – and is visualised as very bright areas due to the effect of the contrast agent on the T1 relaxation. We assumed that the gadolinium contrast agent was fully dissolved in the local anaesthetic, and hence that the visual spread of the contrast agent corresponded to the spread of the local anaesthetic. In order to improve visual differentiation of nerves and muscle, an additional standard single shot echo-planar imaging (EPI) diffusion weighted sequence with b-values of 0 and 500 was sampled, as this sequence provides different contrast for neural and muscular tissue and therefore allows identification of the nerves when they are located inside the psoas major muscle.[98] The MR sequences were analysed in a DICOM viewer (OsiriX v. 6.5.2. 64-bit) in order to estimate the perineural spread of the injectate and compartmentalised injection spread.

Sensorimotor Blockade

Standard clinical criteria for an effective and successful blockade, i.e. no requirement for rescue blocks, conversion to general or spinal anaesthesia, or analgesics, are inapplicable in healthy study subjects. Dermatomal mapping for sensory testing of the lower limb can be used, but is relatively unreliable due to considerable anatomical variation, overlapping of contiguous segmental and terminal nerve territories as well as missing innervation in some cutaneous areas.[99] We therefore chose to use motor blockade based on tests of baseline and post-block muscle force with a hand-

held dynamometer (Commander Muscle Testing; JTECH Medical, Midvale, USA) as a proxy marker of sensory blockade of the femoral, obturator, and superior gluteal (lumbosacral trunk) nerves as well as – in study I – the sciatic nerve. In order to take account of multiple nerve innervation of the hip adductors, motor blockade was defined as ≥ 50% decrease in post-block muscle force compared to baseline in study I. However, to the best of our knowledge, no consensus exists on the association between decreased muscle force in healthy subjects and an effective sensory blockade in clinical patients. We therefore defined motor blockade as a decrease in post-block muscle force compared to baseline in studies II and III. As a supplement and in order to evaluate epidural spread, we mapped sensory blockade of the subjects' sensations for cold, warmth, touch, and pain in the appropriate dermatomes. The method for testing motor force and sensory mapping is described in the supplemental Paper I to III.

Pharmacokinetics of Lidocaine

Bio banks were established and blood was sampled during 90 minutes after the completed interventions in studies I and II. The p-lidocaine was analysed with liquid chromatography tandem mass spectrometry.[100]

Cost-effectiveness

As a measurement of cost-effectiveness or "price per patient",[76] unit costs were collected and converted into Great British Pound (GBP). The cost for the use of the Philips Ingenia 1.5T MRI scanner was expressed in time units due to the complexity of calculating and generalising the cost expressed in monetary units.

Randomisation and Blinding

All studies were blinded randomised controlled trials. The procedure of randomisation in each study is described in the supplemental Papers I to III. All observers and analysts of data were blinded to the allotted sequence of intervention. T.F.B. performed blinded analyses of injectate spread on the

anonymised MRI sequences in a random order using the DICOM viewer OsiriX v. 6.5.2. 64-bit. We sought to blind all study subjects by identical trial setup and not reveal randomisation prior to finalisation of all data analyses. A strict protocol was designed for the operating anaesthesiologist who could not be blinded. A non-blinded assistant double-controlled the allotted sequence of intervention in order to control the protocol compliance of the operating anaesthesiologist.

Results

All results are reported in detail in the supplemental Paper I to III. The key findings are summarised below.

Study I: Ultrasound Guided Shamrock vs. LUT

The ultrasound guided Shamrock technique had a shorter block procedure time compared with the ultrasound guided LUT technique (238 [SD 74] vs. 334 [SD 156] s; p = 0.009).

The Shamrock technique required fewer needle insertions for correct placement of the block needle tip (2 [interquartile range (IQR) 1 to 3] vs. 6 [2 to 12] insertions; p =0.003) and was also assessed as a more comfortable procedure (3 [IQR 2 to 4]) vs. 4 [IQR 3 to 6] NRS units; p = 0.03) compared to the LUT technique.

There was no difference in the proportion of subjects with blockade of the femoral, obturator, and lateral femoral cutaneous nerves. For both techniques, the analyses of sensory blockade and perineural spread on MRI showed a similar primary effect on and perineural spread to the anterior rami of spinal nerves L2 to L4 and the terminal femoral, obturator, and lateral femoral cutaneous nerves. There was no difference in ΔMAP, proportion of subjects with epidural spread, or lidocaine pharmacokinetics (**Fig. 16**) between the techniques. The mean marginal cost was Δ£2.0 per lumbar plexus block in favour of the Shamrock technique.

No serious adverse reactions or harm occurred.

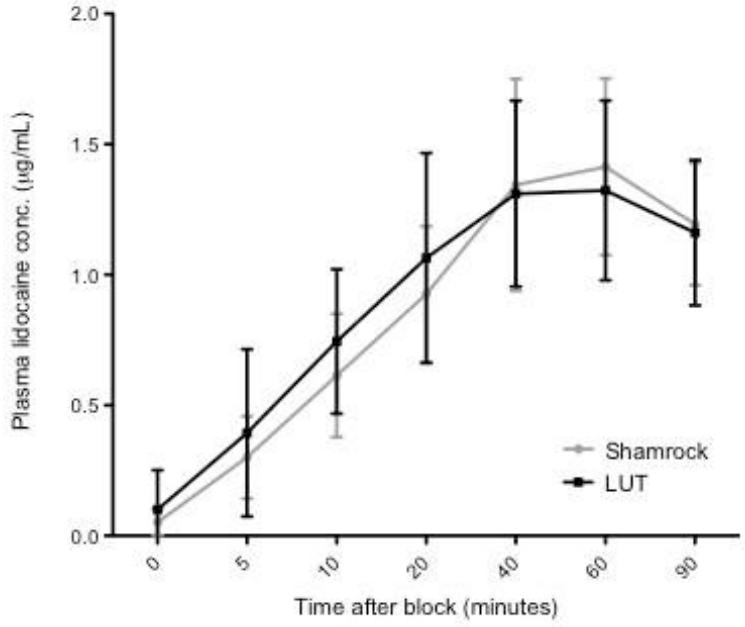

Fig. 16. Plasma concentration of lidocaine 0 to 90 minutes after ultrasound guided injection with the Shamrock vs. Lumbar ultrasound Trident (LUT) techniques. Values are presented as mean (standard deviation).

Study II: Ultrasound/MRI Fusion vs. Ultrasound Guided SSPS

There was no difference in the proportion of subjects with blockade of the femoral and obturator nerves and the lumbosacral trunk between the ultrasound/MRI fusion vs. the ultrasound guided SSPS techniques (23/26 [88%] vs. 23/26 [88%] subjects; p = 1.00).

The ultrasound/MRI fusion guided SSPS required longer time for preparation and performance of the block compared with the ultrasound guided technique (preparation time: ultrasound/MRI, 686 [IQR 552 to 1,023] s; ultrasound, 196 [IQR 167 to 228] s; p < 0.001, and performance time: ultrasound/MRI, 333 [IQR 254 to 439] s; ultrasound, 216 [IQR 176 to 294] s; p = 0.001).

The analyses of sensory blockade and perineural spread on MRI showed a similar primary effect on and perineural spread to the anterior rami of spinal nerves L2 to S1 and the terminal femoral, obturator, and lateral femoral cutaneous nerves and the lumbosacral trunk. There was no difference

in ΔMAP, proportion of subjects with epidural spread, or lidocaine pharmacokinetics (**Fig. 17**) between the two techniques. The mean marginal cost was Δ£22.91 and 6 min and 34 s in the 1.5T MRI scanner per lumbosacral plexus block in favour of the ultrasound guided SSPS technique.

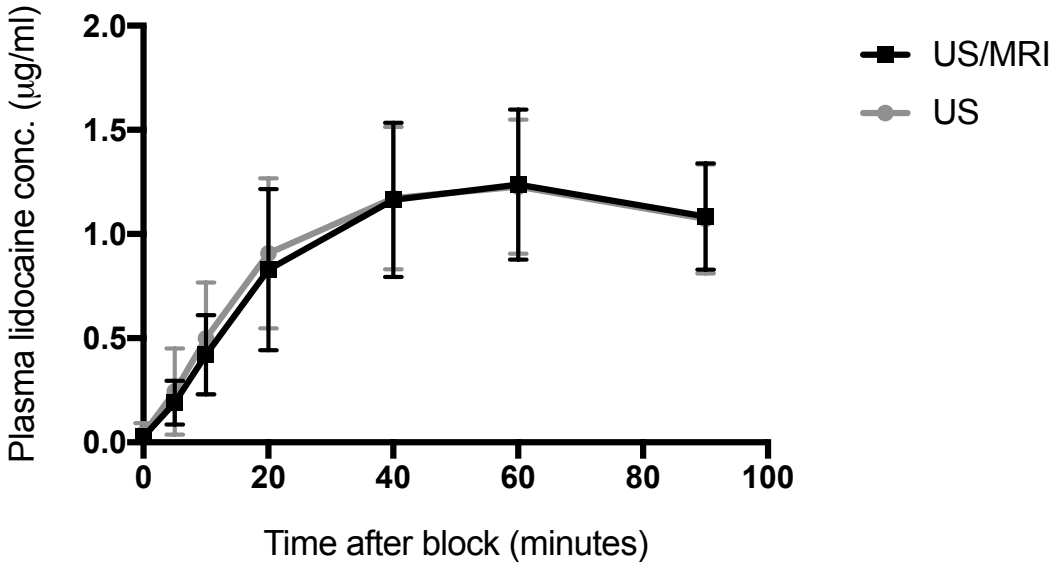

Fig. 17. Plasma concentration of lidocaine 0 to 90 minutes after ultrasound/magnetic resonance imaging (US/MRI) fusion guided vs. US guided injection with the Suprasacral parallel shift technique. Estimates are presented as mean (standard deviation).

During the MRI analysis of spread of lidocaine-adrenaline added contrast, we identified three characteristic patterns of spread. These were medial (inside the so-called *para-psoas compartment* [PPC], **Fig. 18**), posterior (inside the so-called *retro-psoas subcompartment* [RPSC], **Fig, 19**), and lateral (inside the *retroperitoneal compartment*, **Fig. 20**) to the psoas major muscle, respectively.

No serious adverse reactions occurred. Few adverse events and reactions occurred – these are described in the supplemental Paper II.

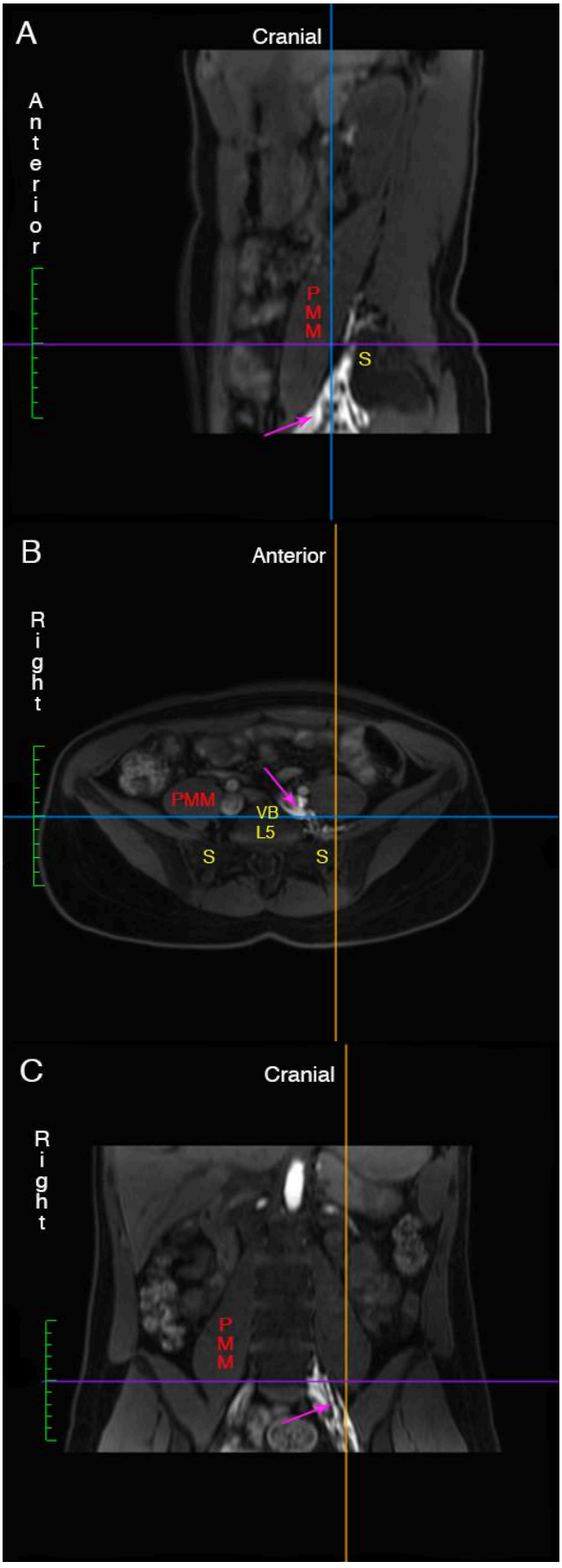

Fig. 18. Magnetic resonance imaging of the spread of injectate (magenta arrow) primarily inside the compartment medial to the psoas major muscle, *i.e.* in the para-psoas compartment, in one volunteer. A) Sagittal plane. B) Axial plane. C) Coronal plane. Line (blue), projection of the coronal plane; Line (orange), projection of the sagittal plane; Line (purple), projection of the axial plane; PMM, psoas major muscle; S, sacral ala; VB L5, vertebral body of L5

.

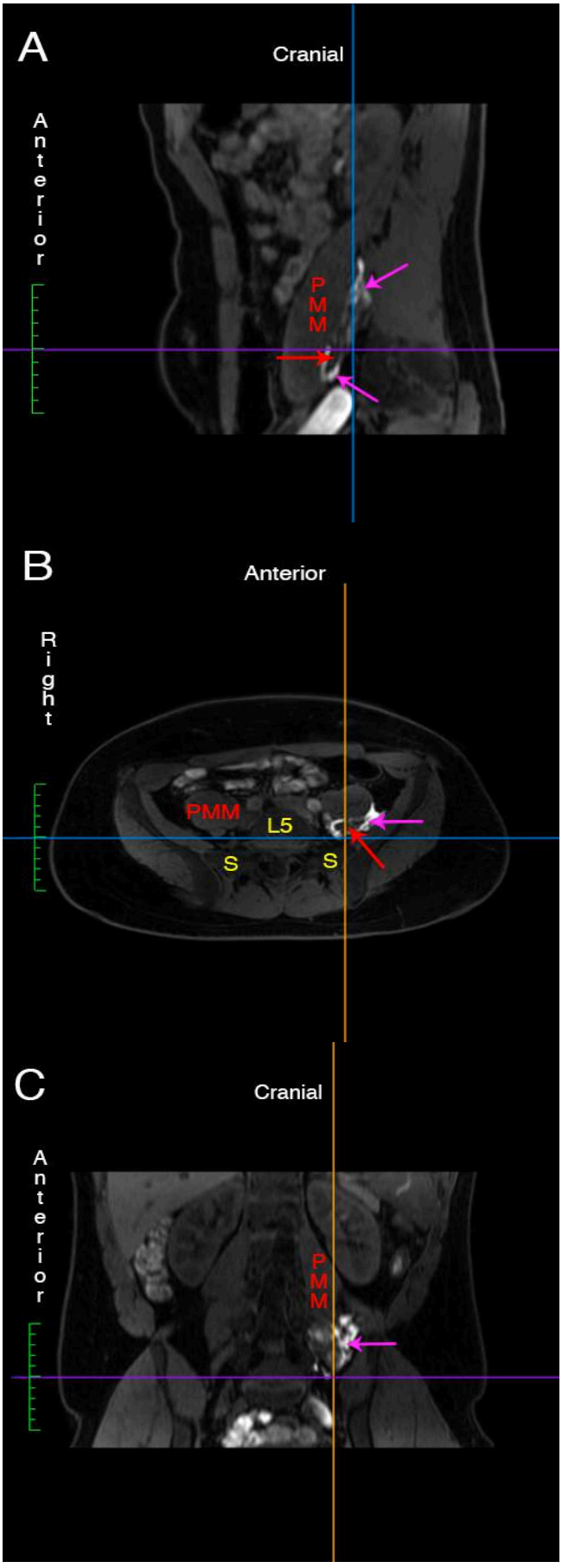

Fig. 19. Magnetic resonance imaging of the spread of injectate (magenta arrow) in the compartment posterior to the psoas major muscle, *i.e.* in the retro-psoas subcompartment, in one volunteer. Minor seeping into the compartment between the anterior and posterior lamina of the psoas major muscle is seen. A) Sagittal plane. B) Axial plane. C) Coronal plane. Arrow (red), posterior lamina of psoas major muscle; L5, vertebral body of L5; Line (blue), projection of the coronal plane; Line (orange), projection of the sagittal plane; Line (purple), projection of the axial plane; PMM, psoas major muscle; S, sacral ala.

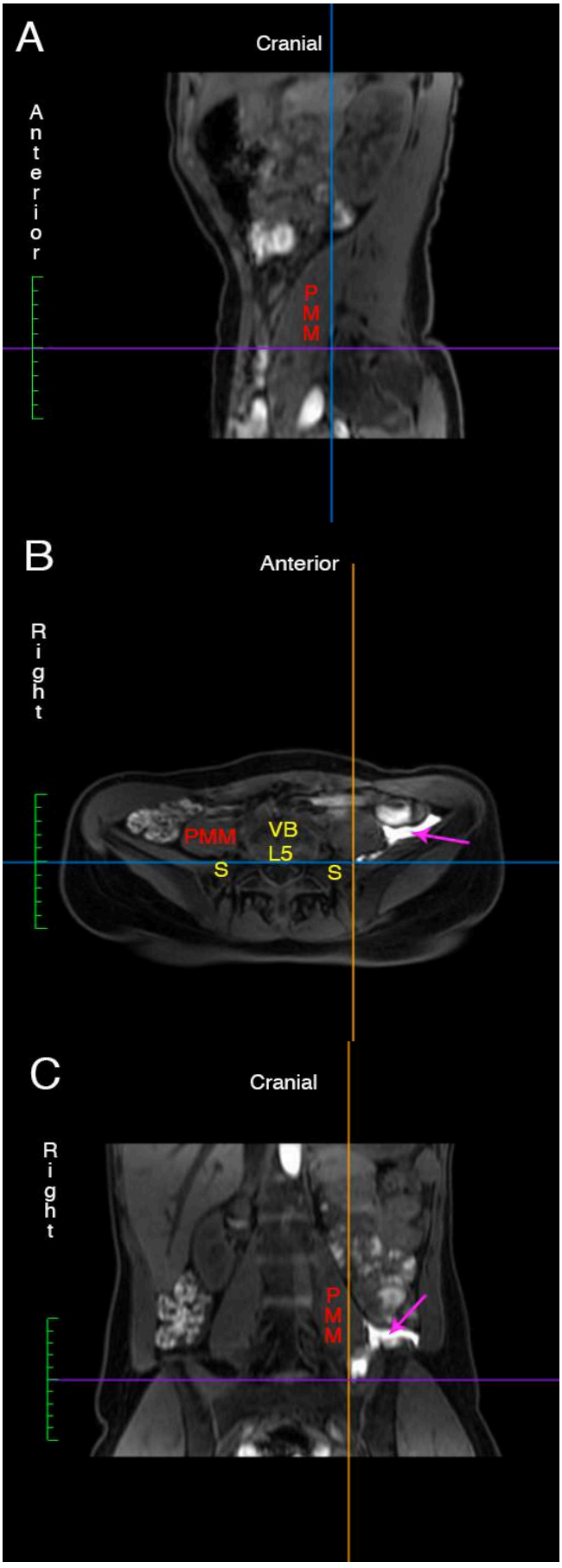

Fig. 20. Magnetic resonance imaging of the spread of injectate (magenta arrow) primarily in the compartment lateral to the psoas major muscle, *i.e.* in the retroperitoneal compartment, in one volunteer. A) Sagittal plane. B) Axial plane. C) Coronal plane. Line (blue), projection of the coronal plane; Line (orange), projection of the sagittal plane; Line (purple), projection of the axial plane; PMM, psoas major muscle; S, sacral ala; VB L5, vertebral body of L5.

Study III: Ultrasound/MRI Fusion vs. Ultrasound Guided Shamrock

There was no difference in the proportion of subjects with blockade of the femoral, obturator, and lateral femoral cutaneous nerves with the ultrasound/MRI fusion vs. the ultrasound guided Shamrock techniques (16/22 [73%] vs. 18 [82%] subjects; $p = 0.69$).

The ultrasound/MRI fusion guided technique required longer block preparation time compared with the ultrasound guided technique (ultrasound/MRI, 868 [IQR 661 to 947] s; ultrasound, 471 (IQR 369 to 631) s; $p < 0.001$). The sensory mapping corresponded to the analysis of perineural spread of injectate, which was similar for both techniques, showed primarily spread to the anterior rami of spinal nerves L2 and L3 and the terminal femoral, obturator, and lateral femoral cutaneous nerves. There was no difference in ΔMAP or proportion of subjects with epidural spread between the techniques. The mean marginal cost was Δ£17.64 and 6 min and 34 s in the 1.5T MRI scanner per lumbar plexus block in favour of the ultrasound guided Shamrock technique.

The MRI analysis of injectate spread demonstrated a consistent spread of the injectate within the intra-psoas subcompartment (IPSC) between the anterior and posterior lamina of the psoas major muscle (**Fig. 21)**. In the cranio-medial direction, the injectate did consistently spread to the neural foramina of L2 and L3. In the caudal direction, the injectate deviated with the psoas major muscle antero-laterally. We did not observe spread of the injectate posterior to the psoas major muscle inside the RPSC. No or minor spread was observed into the PPC medial to the iliopsoas compartment and caudal to the transverse process of vertebra L5.

No serious adverse reactions occurred. Few adverse events and reactions occurred – these are described in the supplemental Paper III.

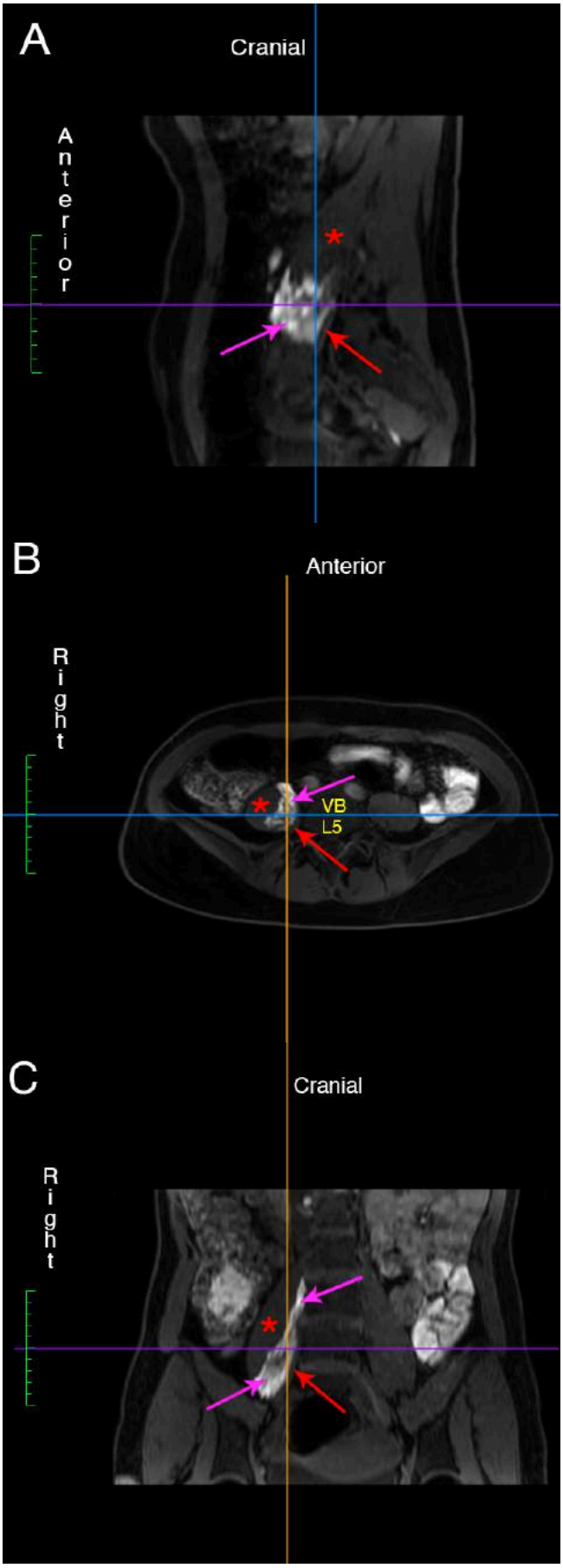

Fig. 21. Magnetic resonance imaging of the spread of injectate (magenta arrow) in the compartment between the anterior and posterior lamina of the psoas major muscle, *i.e.* in the intra-psoas compartment, in one volunteer. A) Sagittal plane. B) Axial plane. C) Coronal plane. Arrow (red), posterior lamina of the psoas major muscle; Asterisk (red), anterior lamina of the psoas major muscle; Line (blue), projection of the coronal plane; Line (orange), projection of the sagittal plane; Line (purple), projection of the axial plane; VB L5, vertebral body of L5.

Discussion

The three studies are discussed in detail in the supplemental Paper I to III. Below is a general discussion of the study design, the study subjects, and the ultrasound guided and ultrasound/MRI fusion guided techniques for lumbar and lumbosacral plexus blocks. The discussion focuses on quality and safety, the benefits and limitations of MRI in regional anaesthesia, compartmental spread, and future aspects.

Study Design and Subjects: Randomised Controlled Trials with Healthy Volunteers

Several techniques for ultrasound guided lumbar plexus block and one technique for ultrasound guided lumbosacral plexus block have been described previously.[13-22 59 101] However, to the best of our knowledge, only two of these techniques have been compared in a randomised controlled trial.[19] Thus the evidence-base of assessment of the effectiveness, safety, and ease-of-performance of the described techniques is very limited. Randomised controlled trials on healthy volunteers allow a relatively fast recruitment process and an exhaustive, in-depth study design and data sampling. Furthermore, investigation of new techniques like real-time ultrasound/MRI fusion guidance in regional anaesthesia in healthy volunteers allows validation prior to any implementation in clinical trials and clinical practice. Similarly, other novel ultrasound guided techniques for lumbar plexus blockade have initially been validated in cadavers and in healthy volunteers.[20 21 65] Our studies contribute with new knowledge about effectiveness, safety, ease-of-performance, block related outcomes, cost-effectiveness, and injectate spread of the investigated techniques based on assessment of ultrasound/MRI fusion in normal volunteers. The new insight may assist regional anaesthetists in the choice of block technique and improve the anatomical understanding of injectate spread. However, as discussed in the supplemental Paper I to III, the results of our studies should be considered as measures of comparisons of the techniques and an initial assessment of the fusion protocol developed during this PhD study – not as results directly applicable in a clinical setting with old, frail, comorbid and/or obese patients for hip surgery.

Ultrasound Guided Techniques for Lumbar Plexus Blockade: Shamrock vs. LUT

Quality and Efficiency

We found that the ultrasound guided Shamrock technique was faster to perform and it required fewer needle insertions compared to the ultrasound guided LUT technique in healthy normal weight volunteers. The procedure time and the number of needle insertions can be considered proxy markers for the difficulty of achieving sufficient visualisation of the target nerves. Our study therefore supports previous literature, claiming that the ultrasound guided Shamrock technique is more easy-to-perform and improves visualisation of the paravertebral lumbar sonoanatomy – including the target lumbar plexus and ultrasonographical landmarks – as well as the block needle tip, the needle trajectory, and the perineural spread of injectate compared to a posterior paravertebral scanning technique.[22 59 68 69] Scanning from the flank allows some tissue compression, reducing the distance from the ultrasound probe to the target. Scanning from the flank while the needle is inserted some distance away from the probe in the posterior paravertebral lumbar region also allows avoidance of a needle skin insertion that may interrupt the contact between the skin and the probe.[74] However, in overweight patients, in whom fat deposits tend to be located at the flanks rather than at the paravertebral lumbar region, a posterior paravertebral scanning technique may be advantageous. It may also be a challenge to localize the best needle skin insertion point and angulation of the needle with the ultrasound probe placed in the flank and the needle in the paravertebral region.

The subjects' assessment of comfort was better for the Shamrock technique compared to the LUT technique, which may be explained by the lower number of needle insertions required for the Shamrock technique.

Sensorimotor effect was used as a surrogate marker for efficiency of the blockade. Because sensorimotor mapping in normal volunteers may be unreliable, we included analysis of perineural injectate spread on MRI as an objective measure of the efficiency. The sensorimotor mapping and

the analysis of injectate spread of both techniques demonstrated a consistent effect on the anterior rami of spinal nerve L2 to L4 and on the terminal nerves of the lumbar plexus – the femoral, obturator, and lateral femoral cutaneous nerves. Consequently, there was no evidence for any difference in block success; the proportion of subjects with motor blockade of the femoral and obturator nerves as well as sensory blockade of the lateral femoral cutaneous nerve was similar. Because the target of injection was the same, this result was – to some extent – expected. The Shamrock has primarily been described in letters to the editor and in case reports.[59 68 69 102] Anyhow, our results are in keeping with the results of a dose-finding study of Shamrock lumbar plexus blockade in patients undergoing lower limb surgery.[22] The LUT technique has been described in a case series and investigated in a randomised controlled trial with healthy volunteers.[15 19] Nevertheless, the LUT lumbar plexus blockade was combined with a sacral plexus blockade in the case series and a different definition of "block success" was used in the randomised controlled trial.[15] Consequently, the results are not directly comparable with our results, though the results on sensory blockade of the anterior rami of spinal nerves L3 to S1 and of the lateral femoral cutaneous nerve were similar with ours for the LUT technique.[19]

Finally, the cost-effectiveness was in favour of the Shamrock technique, which was explained by the shorter procedure time for this technique.

Safety

Change in MAP, incidence of epidural spread, and lidocaine pharmacokinetics were used as proxy markers of the safety of the techniques. There was no evidence of any differences in ΔMAP or incidence of epidural spread between the techniques; however, the study was not powered to detect such differences. The incidence of epidural spread in our study was low compared to the dose-finding study of the Shamrock technique and the randomised controlled trial of the LUT technique.[19, 22] However, in the dose-finding study of the Shamrock technique up to 52.2 ml of 0.5% ropivacaine was injected. In the present study, 20 ml of local anaesthetic was injected in all study subjects. Injections of a more clinical relevant volume, larger than 20 ml, may have resulted

in a higher proportion of subjects with epidural spread – as well a greater difference in ΔMAP and higher p-lidocaine – in the present study. Continuing, also the lidocaine pharmacokinetics of the Shamrock and LUT techniques were similar between the techniques and did not exceed toxic levels.[92] Similar to previous studies on plasma concentration of local anaesthetics in regional anaesthesia, the maximum concentration of lidocaine peaked approximately one hour after injection.[19 103] This result implies that if any local anaesthetic systemic toxicity is suspected, a patient should be observed for at least one hour. Finally, we did not observe any serious adverse effects or harm during or after the trial.

Ultrasound/MRI Fusion Guidance of SSPS and Shamrock Techniques

Quality, Efficiency, and Safety

We applied real-time ultrasound/MRI fusion to improve visualisation and needle navigation of the SSPS and Shamrock techniques in order to assess the potential benefit of ultrasound/MRI fusion on effectiveness and safety compared to ultrasound guidance alone. However, in studies II and III, we did not observe such potential differences. We found that the ultrasound/MRI fusion and the ultrasound guided techniques were equally effective and safe in healthy, normal-weight, young volunteers. Kwok and Karmakar have briefly described an application of fused real-time ultrasound and CT as well as MRI of the lumbar spine in a phantom and in healthy volunteers.[27] The authors did not use fusion for needle guidance nor did they investigate fusion with needle navigation. Therefore our studies are not directly comparable with the observational study by Kwok and Karmakar.[27] Klauser et al and Zacchino et al assessed accuracy and efficiency of fusion of real-time ultrasound and CT or MRI for guidance of sacroiliac joint injections in cadavers and in patients after failed conventional therapy.[85 86] They found that real-time image fusion is accurate and efficient in chronic pain treatment.[85 86]

Common for the techniques by Kwok and Karmakar, Klauser et al as well as Zacchino et al is that the real-time fusion and – for Klauser et al and Zacchino et al – needle guidance was performed in

the same body position as the CT or MRI recording.[27 85 86] Moreover, Klauser et al and Zacchino et al co-registered their datasets based on match of points on bony structures, e.g. on the lumbosacral spine, the pelvis, and the femoral heads, and achieved a registration error < 3 mm.[85 86] We sampled the MRI datasets in the supine position while the real-time fusion needle guidance was performed in the lateral decubitus position. The shift in position may have decreased the congruence and dimensional stability of the 3D topography of MRI and real-time ultrasound, and hence the accuracy of the ultrasound/MRI fusion guided procedures compared to Kwok and Karmakar, Klauser et al as well as Zacchino et al. The use of two different body positions for co-registration and alignment is also more time-consuming compared to one single position. Although our observation of prolonged preparation time and – for the ultrasound/MRI fusion guided SSPS technique – performance time is in keeping with previous studies on image fusion guided techniques.[24] Co-registration based on plane match is associated with a higher registration error compared to point match, according to the producer of the ultrasound system with fusion software. With point match, the MRI is segmented and reformatted based on three registration points and an increased number of points proportionally decreases the registration error. With plane match, it is critically important that the ultrasound image plane corresponds as exactly as possible to the internal MRI plane, because a minor shift, rotation, and/or angulation of the probe – in any axis – in relation to the internal MRI plane results in a misalignment that increases with increased distance from the matched plane. However, the plane match involved fewer steps and was faster and more practical compared to point registration in our hands.

The number of needle insertions and procedural comfort were similar for the ultrasound/MRI fusion and ultrasound guided techniques. In study I, the performance time together with the number of needle insertions and procedural comfort were used as a surrogate marker for ease of visualisation of the target lumbar plexus. Applying the same parameters to assess ease of visualisation of the target lumbar plexus in the fusion-studies (studies II and III using the SSPS and Shamrock technique, respectively), real-time ultrasound/MRI fusion guidance was equal to ultrasound guidance alone. In study III, the target lumbar plexus was visualised in an equal proportion of

subjects with the ultrasound/MRI fusion and ultrasound guided Shamrock techniques. The overall results of the fusion-studies may be explained by the demographics of the subjects. We investigated the ultrasound/MRI fusion guidance in normal young volunteers in whom sufficient ultrasonographic visualisation was probably achieved with a higher frequency compared to clinical patients.

In neither of the fusion-studies was there any difference in the proportion of subjects with a successful blockade in the ultrasound/MRI fusion group compared to the ultrasound group. There was concordance between the sensorimotor assessment and the analysis of perineural spread of the injectate on MRI in both studies. The proportion of successful lumbar plexus blockade with the Shamrock technique was higher in study III compared to study I. This difference can be explained by the different definition of a "successful" blockade in study I compared to studies III (and II). Any definition of successful blockade in healthy volunteers is an arbitrary measure that can only be used as a measure of comparison between the alternative techniques, and should not be considered as an external valid measure of successful blockade in a clinical setting. The estimates of successful blockade in the fusion-studies (studies II and III) should be interpreted with caution because they are based on proxy motor estimators of successful sensory blockade of the femoral and obturator nerves. The estimates are potentially biased by triple innervation of the hip adductor muscles. The analyses of compartmentalised injectate spread are discussed below.

There was no evidence of any difference in the safety surrogate markers between the ultrasound/MRI fusion and ultrasound guided techniques. I.e. the estimates of number of needle insertions, ΔMAP, incidence of epidural spread, and – in study II – pharmacokinetics of lidocaine were similar for the compared groups. The results were similar compared to a previous study concerning the SSPS technique in healthy volunteers.[19] In addition, the results of ΔMAP and epidural spread of the ultrasound/MRI fusion guided and ultrasound guided Shamrock techniques in Study III were similar to the results of the ultrasound guided Shamrock technique in Study I.

However, none of the studies were powered to detect such assumed differences. No serious adverse events occurred; neither in study II nor in study III.

Finally, the cost-effectiveness analyses favoured ultrasound guidance compared to ultrasound/MRI fusion guidance. These differences were explained by the time spent on preparing and performing the MRI scan for fusion by the radiographer, and by the ancillary time spent by the anaesthesiologist and the assistant on co-registering and aligning the real-time ultrasound and MRI datasets for fusion and on needle navigation.

MRI in Regional Anaesthesia: Potential Benefits and Limitations

Image Fusion

Image fusion has several limitations: 1) the high-end ultrasound systems with image fusion software are expensive compared to low- or midrange ultrasound systems usually employed by anaesthesiologists; 2) a MRI dataset has to be recorded in advance; 3) the MRI dataset has a size limit and it is required to have a format that is compatible with the fusion software; 4) the MRI dataset has to be transferred to the ultrasound system; 5) the fusion technique requires expertise and – for use in regional anaesthesia – inter-disciplinary cooperation between radiologists and anaesthesiologists; 6) the fusion procedure is time-consuming compared to ultrasound guidance alone; and 7) the image fusion systems and software are in the process of being fully developed.[82]

Our present protocoled application of high-resolution 3D MRI for fusion with real-time ultrasound has contributed to the understanding of the complex anatomy and ultrasonoanatomy relevant for lumbar and lumbosacral region. This is in keeping with Galiano et al, who found a form of video-based fusion of real-time ultrasound and CT in cadavers to be a useful educational tool to improve identification of ultrasonographical landmarks and alignment of the block needle in relation to the ultrasound beam for lumbar and cervical facet joints injections.[26] Although Karmakar et al did not apply MRI for fusion, the authors compared the ultrasonoanatomy of the lumbar region with axial

MRI and images from the Visible Human Project cadaver dataset for validation of an ultrasound guided lumbar plexus blockade prior to investigation in a clinical study.[104] In study II, the ultrasound/MRI fusion based observations of compartmentalised spread of local anaesthetic generated the insight to the proposal of a new lumbosacral block technique with an anterior approach.

Perineural and Compartmental Injectate Spread

We employed MRI to visualise the perineural and compartmental anatomical spread of a contrast agent added to the local anaesthetic.[19 105] This is a powerful supplement in the assessment of a regional anaesthetic technique in healthy volunteers, because – as discussed in the supplemental Paper I to III and above – the sensorimotor assessment of a "successful blockade" may be unreliable as well as arbitrary. The assessment of injectate spread on MRI does not only allow evaluation of perineural injectate spread, but also allows evaluation of compartmental patterns of injectate spread. Bendtsen *et al* and Mannion *et al* have investigated the injectate spread in volunteers with MRI after single-shot lumbosacral plexus blocks and continuous psoas compartment blocks (lumbar plexus blocks), respectively.[19 105] Our observations of perineural spread (anterior rami of spinal nerves L2 to L5, the femoral and obturator nerves, and the lumbosacral trunk) using the SSPS technique in study II are comparable to the observations made by Bendtsen et al.[19] In addition, we estimated perineural spread to the anterior ramus of spinal nerve S1 and to the lateral femoral cutaneous nerve.

Moreover, we employed MRI after local anaesthetic/contrast injection to explore patterns of compartmentalised spread of injectate. We observed consistent patterns of spread into three compartments. First, into the *para-psoas compartment (PPC)*, which is located medial to the iliopsoas compartment.[106] The PPC contains the anterior rami of spinal nerves L4 and L5, the lumbosacral trunk, and the terminal part of the obturator nerve. Second, into the *retro-psoas subcompartment (RPSC)*, which is an iliopsoas subcompartment posterior to the psoas major muscle caudal to the transverse process of vertebra L5 and anterior to the iliacus muscle. The RPSC

contains the femoral and lateral cutaneous nerves after they emerge from the psoas major muscle. Third, into the retroperitoneal compartment, which is lateral to the psoas major muscle and the iliopsoas compartment. The retroperitoneal compartment contains no nerves. Chayen et al originally described the RPSC.[62] Because it is a subcompartment of the iliopsoas compartment, we suggest coining it the "retro-psoas subcompartment". Our observations imply that local anaesthetic has to be injected into the PPC as well as into the RPSC in order to produce a sufficient spread the injectate to all target lumbosacral plexus nerves for surgical anaesthesia of the hip. Based on these observations, we presented a plausible ultrasound/MRI fusion guided anterior approach for lumbosacral plexus blockade.

In study III, we observed consistent injectate spread inside the *intra-psoas compartment*, surrounding the anterior rami of spinal nerves L2 and L3 and the lumbar plexus between the anterior and posterior lamina of the psoas major muscle. Mannion *et al* observed perineural spread around all anterior rami of the spinal nerves L1 to L4 in addition to spread into the space between the psoas major and quadratus lumborum muscles, which are in contrast to our observations.[105] We concluded that the Shamrock technique primarily blocks the anterior rami of spinal nerves L2 and L3, the lumbar plexus, and only the femoral nerve subset of the anterior ramus of spinal nerve L4.

Limitations

The limitations of the studies are discussed in the supplemental Paper I to II. The studies are based on samples of healthy, normal-weight, and young volunteers, which limits the external validity. The lumbar paravertebral anatomy and pharmacokinetics change with age.[79-81 107] The typical hip surgery patient is older than 65 years and may be frail, comorbid, and obese. Moreover, we employed a relatively low local anaesthetic volume of 20 ml 2% lidocaine-adrenaline, which corresponds approximately to the ED_{50} of 0.5% ropivacaine required for successful lumbar blockade in patients undergoing lower limb surgery.[22] Injection of a more clinical relevant volume, greater than 20 ml of local anaesthetic, would result in a higher plasma concentration of lidocaine. Further, we cannot exclude that an injection of a greater volume than 20 ml would result in different

values of ΔMAP and epidural spread as well as different patterns of compartmentalised spread. However, the aim of our trials was to investigate the effectiveness and safety of ultrasound/MRI fusion and ultrasound guidance using Shamrock and SSPS approaches in healthy volunteers – not to obtain clinical applicable results. It should be noted that procedure time and success rate of a new technique is proportional to experience. Before the full potential and benefit of ultrasound/MRI fusion can be assessed, more research is needed. Finally, blinding of the operator was impossible. We endeavoured to reduce the effect of this potential source of bias by adhering to a strict double-controlled protocol.

Future Aspects

Based on the findings of compartmentalised injectate spread using the SSPS technique in study II, we have suggested an anterior ultrasound/MRI fusion guided approach in the supine position for injection of local anaesthetics into the retro-psoas subcompartment as well as into the para-psoas compartment. This approach would probably be time-efficient and produce effective blockade of all the terminal nerves from the lumbosacral plexus that are relevant for hip joint innervation. Further research is, however, needed to validate this technique.

Our present real-time ultrasound/MRI fusion protocol is not matured for use in clinical research or practice. Short procedure time and high success rate follow a learning curve. Target planning can be used to simplify the guidance of the needle and to increase safety of the needle insertion. Multiple MRI datasets can be imported for fusion with real-time ultrasound. It would be possible to import both a 3D T2-TSE MRI sequence for optimal imaging of the lumbar paravertebral anatomy, as well as a diffusion weighted MRI sequence for optimal visualisation of the target lumbar plexus and terminal nerves. Co-registration can be carried out using point registration of external landmarks (MRI compatible fiducials) as an alternative to plane registration. Further, the hardware and software for real-time ultrasound and MRI fusion are rapidly evolving. Automatic co-registration based on image recognition of the hepatic blood vessels in both image datasets is a time-efficient alternative to manual co-registration (**Fig. 22**). Additional research is needed before the final value

of ultrasound/MRI fusion in regional anaesthesia for hip surgery and postoperative analgesia can be assessed.

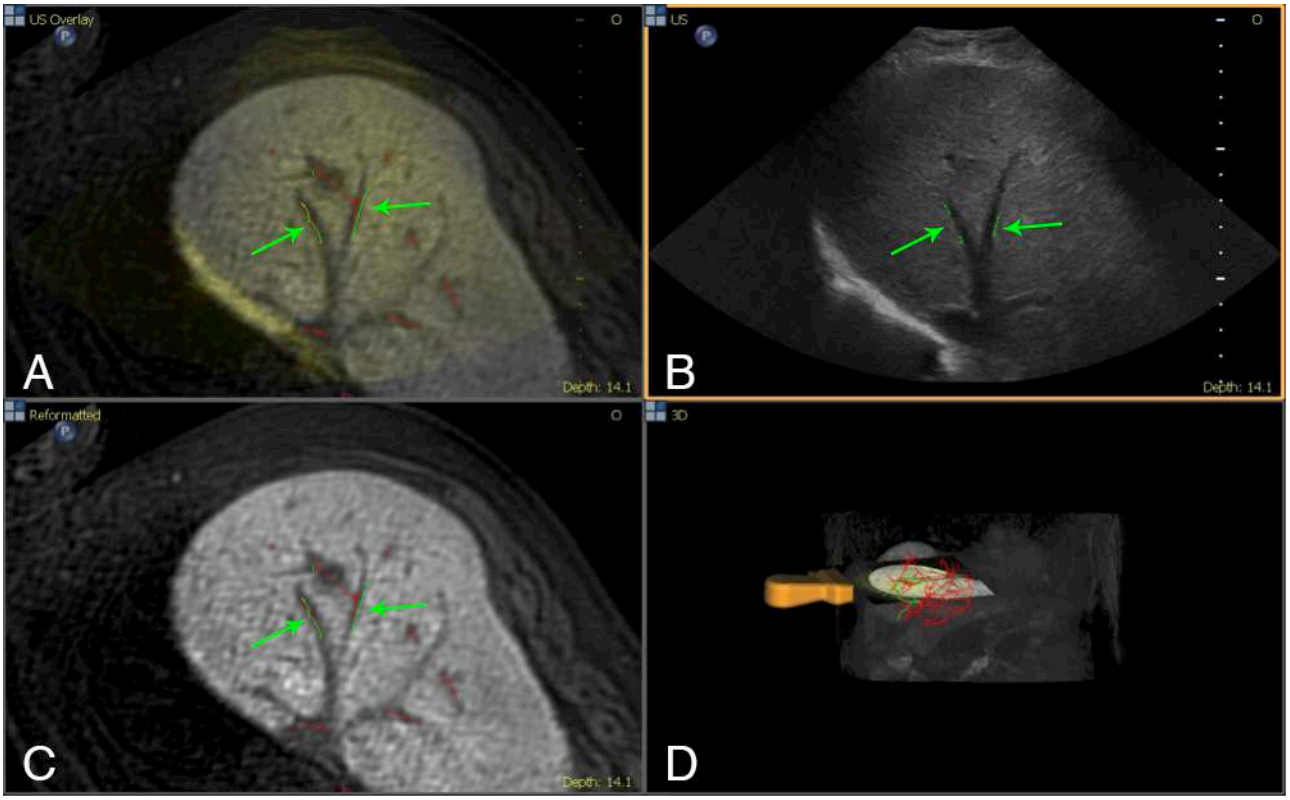

Fig. 22. Automatic co-registration based on MR and ultrasound image recognition of the hepatic blood vessels. The red lines mark the hepatic blood vessels that are automatically identified in the MRI dataset only. The green lines mark the hepatic blood vessels that are automatically identified in a recorded ultrasound sweep of the liver as well as in the MRI dataset. The latter vessels are used for the automatic co-registration. A) Overlay of ultrasound and MRI. B) Ultrasonography alone. C) MRI alone. D) Reformatted 3D image of the MRI dataset illustrating the position and orientation of the ultrasound probe and image plane. Image provided with permission to print from Philips Ultrasound, Bothell, Washington, USA.

Conclusions

Study I

The ultrasound guided Shamrock technique for lumbar plexus blockade was faster to perform, required fewer needle insertions, and was a more comfortable procedure for the study subjects compared to the ultrasound guided Lumbar Ultrasound Trident technique. The shorter performance time and fewer needle insertions required for the Shamrock compared to the Lumbar Ultrasound Trident technique were probably due to the improved ultrasonographical visualisation of the lumbar plexus, ultrasonographic landmarks, needle tip and trajectory, and the perineural spread of the injectate.

Study II

The ultrasound/MRI fusion guided Suprasacral Parallel Shift (SSPS) technique had similar success of lumbosacral plexus blockade, but prolonged preparation and performance times, compared to the ultrasound guided SSPS technique. The similar block success was probably explained by a high frequency of easy and good quality ultrasonographic visualisation of the anatomical landmarks and target lumbosacral plexus in the normal, healthy, and young study subjects. The prolonged preparation and performance times of the ultrasound/MRI fusion guided technique were explained by the additional time spent on co-registration and alignment of real-time ultrasound and MRI and the time spent on use of needle navigation.

In addition, three consistent patterns of compartmentalised injectate spread were observed. First, into the so-called para-psoas compartment (PPC), which is medial to the iliopsoas compartment, caudal to the transverse process of vertebra L5, and anterior to the sacral ala. The PCC contains the anterior rami of spinal nerves L4 and L5, the lumbosacral trunk, and the obturator nerve after emergence form the psoas major muscle. Second, into the so-called retro-psoas subcompartment (RPSC), which is posterior to the psoas major muscle caudal to the transverse process of vertebra

L5. The RPSC contains the femoral and lateral femoral cutaneous nerves after they emerge from the psoas major muscle. Third, into the so-called retroperitoneal compartment lateral to the iliopsoas compartment. The retroperitoneal compartment contains no major terminal nerves from the lumbar plexus. Based on our observations of the compartmentalised spread, we suggest an anterior approach to the lumbosacral plexus blockade using real-time ultrasound/MR image fusion guidance, which would allow injection into the PPC and the RPSC with the patient supine. However, further research is required to validate the efficacy, safety, and ease-of-performance of this technique.

Study III

The ultrasound/MRI fusion and ultrasound guided Shamrock techniques for lumbar plexus blockade were equally successful. The fusion technique required prolonged preparation time compared to the ultrasound guidance. The similar block success rate was probably explained by the high frequency of easy and good ultrasonographic visualisation of the target lumbar plexus nerves in the normal, healthy, and young volunteers. The prolonged preparation time of the ultrasound/MRI fusion guided technique was explained by the additional time spent on co-registration and alignment of real-time ultrasound and MRI.

In addition, we observed a consistent pattern of injectate spread into the so-called intra-psoas subcompartment (IPSC). The IPSC contains the anterior rami of spinal nerves L2 and L3, the branch of anterior ramus of spinal nerve L4 to the femoral nerve, and the femoral and lateral femoral cutaneous nerves. It was not possible to assess whether the obturator nerve subset of anterior ramus of spinal nerve L4 entered the IPSC, and joined the L2 and L3 contribution to the obturator nerve, before it descended into the PPC alongside the lumbosacral trunk. No or minor injectate was observed inside the PPC or inside the PPC caudal to the transverse process of L5. The Shamrock approach provides lumbar plexus blockade primarily of the anterior rami of spinal nerves L2 and L3, the intra-psoas part of the lumbar plexus, the femoral and lateral cutaneus nerves as well as the L2/L3 subset of the obturator nerve.

Summary

Summary in English

Ultrasound guided lumbosacral plexus blockade for anaesthesia and postoperative analgesia in hip surgery may be limited by insufficient ultrasonographical visualisation of the target lumbosacral plexuses and the topographic anatomy. Limited visualisation may reduce the accuracy of perineural injection – and thereby the effectiveness and safety of the lumbosacral plexus blockade. Real-time ultrasound may be fused with magnetic resonance imaging (MRI) in order to increase the accuracy of image guided procedures, but ultrasound/MRI fusion guidance is practically non-existent in regional anaesthesia research and clinical practice.

The aims of the this PhD dissertation and the three randomised controlled trials with healthy volunteers were to investigate quality (block procedure related outcomes, spread of the injectate, sensorimotor effectiveness, and cost effectiveness) and safety (number of needle insertions, change in mean arterial pressure, epidural spread of the injectate, and lidocaine pharmacokinetics) of:

I. ultrasound guided Shamrock vs. Lumbar Ultrasound Trident (LUT) technique for lumbar plexus blockade
II. real-time ultrasound/MRI fusion vs. ultrasound guided Suprasacral Parallel Shift (SSPS) technique for lumbosacral plexus blockade
III. real-time ultrasound/MRI fusion vs. ultrasound guided Shamrock techniques for lumbar plexus blockade.

The ultrasound guided Shamrock technique was faster, more comfortable, required fewer needle insertions, and was equally effective and safe compared to the ultrasound guided LUT technique. The ultrasound/MRI fusion guided techniques were equally effective and safe compared to the US guided techniques, but required longer preparation and – for the SSPS technique – performance

time. Distinct patterns of compartmentalised injectate spread were observed on MRI after the SSPS and Shamrock techniques, respectively. The patterns of spread indicated that consistent anaesthesia of all lumbosacral nerves relevant for hip joint anaesthesia would require injection of local anaesthetic into the para-psoas compartment as wells as into the retro-psoas subcompartment. We present a new anterior ultrasound/MRI fusion guided approach for lumbosacral plexus block.

In conclusion, the Shamrock approach provides good visualisation of the lumbar paravertebral sonoanatomy and is faster-to-perform and equally effective and safe compare to the LUT technique in healthy volunteers. We used ultrasound/MRI fusion and MRI to validate established ultrasound guided lumbar and lumbosacral block techniques and to suggest a new anterior approach for lumbosacral plexus blockade.

Resumé på dansk

Ultralydvejledt plexus lumbalis og plexus lumbosacralis blokade med henblik på hoftekirurgisk anæstesi og postoperativ analgesi kan have begrænset effekt på grund af insufficient ultrasonografisk visualisering af målnerverne og de omkringliggende anatomiske strukturer. Insufficient visualisering kan mindske præcisionen af den perineurale injektion – og dermed effektivitet of sikkerhed af lumbosacral plexusblokade. Fusion i realtid af ultralyd og magnetisk resonans (MR) billeddannelse kan øge præcisionen af billedvejledte procedurer, men ultralyd/MR fusion til regional bedøvelse er praktisk talt uudforsket.

Formålene med denne ph.d. afhandling og de tre randomiserede, kontrollerede undersøgelser med raske forsøgspersoner var at undersøge kvalitet (procedure-relaterede parametre, spredningsmønstre af injektatet, sensomotorisk effektivitet) og sikkerhed (antal af nålefremføringer, ændring i middel arterielt blodtryk, epidural spredning af injektatet og farmakokinetik af lidokain) af:

I. ultralydvejledt Shamrock vs. Lumbar Ultrasound Trident (LUT) teknik til plexus lumbalis blokade

II. ultralyd/MR fusion vs. ultralyd ved Suprasacral Parallel Shift (SSPS) teknik plexus lumbosacralis blokade

III. ultralyd/MR fusion vs. ultralyd ved Shamrock teknik til plexus lumbalis blokade

Ultralydvejledt Shamrock teknik var hurtigere, mere behagelig for forsøgspersonerne, krævede færre nåleindstik og var lige så effektiv og sikker som ultralydvejledt LUT teknik. De ultralyd/MR fusionsvejledte teknikker var lige så effektive og sikre som de ultralydvejledte teknikker, men krævede længere forberedelsestid og – for SSPS – tillige gennemførelsestid. Vi observerede karakteristiske spredningsmønstre for injiceret lokalanalgetikum med kontrast på MR for både SSPS og Shamrock teknikkerne. Spredningsmønstrene indikerede at konsistent analgesi af alle lumbosacrale terminale nerver med relevans for anæstesi og analgesi af hofteleddet ville kræve injektion af lokalanalgetikum i para-psoas compartment og i retro-psoas subcompartment. Vi præsenterer et nyt anteriort ultralyd/MR billedfusionsvejledt blok til lumbosacral plexusblokade.

Konklusion: Shamrock-teknikken giver god ultrasonografisk visualisering af den lumbale paravertebrale sonoanatomi og er hurtigere at udføre og lige så effektiv og sikker som LUT teknikken til plexus lumbalis blokade i raske forsøgspersoner. Vi anvendte ultralyd/MR fusion i realtid til at validere etablerede teknikker til ultralydvejledt blokade af plexus lumbalis og plexus lumbosacralis. Vi foreslår en ny teknik til anterior lumbosacral plexusblokade.

Table of References

1. de Luise C, Brimacombe M, Pedersen L, Sørensen HT. Comorbidity and mortality following hip fracture: a population-based cohort study. *Aging Clin Exp Res* 2008; **20**: 412-8.

2. Centers for disease control and prevention/National Center for Health Statistics National Hospital Discharge Survey, 2010. Number of all-listed procedures for discharges from short-stay hospitals, by procedure category and age: United States, 2010. Available from http://www.cdc.gov/nchs/data/nhds/4procedures/2010pro4_numberprocedureage.pdf (accessed 24 October 2016).

3. Mäkelä KT, Matilainen M, Pulkkinen P*, et al*. Countrywise results of total hip replacement. An analysis of 438,733 hips based on the Nordic Arthroplasty Register Association database. *Acta Orthop* 2014; **85**: 107-16.

4. Cram P, Lu X, Callaghan JJ, Vaughan-Sarrazin MS, Cai X, Li Y. Long-term trends in hip arthroplasty use and volume. *J Arthroplasty* 2012; **27**: 278-85.

5. de Visme V, Picart F, Le Jouan R, Legrand A, Savry C, Morin V. Combined lumbar and sacral plexus block compared with plain bupivacaine spinal anesthesia for hip fractures in the elderly. *Reg Anesth Pain Med* 2000; **25**: 158-62.

6. Bendtsen TF, Søballe K, Petersen EM*, et al*. Ultrasound Guided Single Injection Lumbosacral Plexus Blockade For Hip Surgery Anaesthesia. *Br J Anaesth* E-letter published on April 15, 2013. Available from http://bja.oxfordjournals.org/forum/topic/brjana_el%3B9982 (accessed 24 October 2016).

7. Gottschalk A, Van Aken H, Zenz M, Standl T. Is anesthesia dangerous? *Dtsch Arztebl Int* 2011; **108**: 469-74.

8. Memtsoudis SG, Rasul R, Suzuki S*, et al*. Does the impact of the type of anesthesia on outcomes differ by patient age and comorbidity burden? *Reg Anesth Pain Med* 2014; **39**: 112-9.

9. Whiting PS, Molina CS, Greenberg SE, Thakore RV, Obremskey WT, Sethi MK. Regional anaesthesia for hip fracture surgery is associated with significantly more peri-operative complications compared with general anaesthesia. *Int Orthop* 2015; **39**: 1321-7.

10. Guay J, Parker MJ, Gajendragadkar PR, Kopp S. Anaesthesia for hip fracture surgery in adults. *Cochrane Database Syst Rev* 2016; **2**: CD000521.

11. Chelly JE, Casati A, Al-Samsam T, Coupe K, Criswell A, Tucker J. Continuous lumbar plexus block for acute postoperative pain management after open reduction and internal fixation of acetabular fractures. *J Orthop Trauma* 2003; **17**: 362-37.

12. Bono JV, Robbins CE, Mehio AK, Aghazadeh M, Talmo CT. Pharmacologic pain management before and after total joint replacement of the hip and knee. *Clin Geriatr Med* 2012; **28**: 459-70.

13. Kirchmair L, Enna B, Mitterschiffthaler G*, et al*. Lumbar plexus in children. A sonographic study and its relevance to pediatric regional anesthesia. *Anesthesiology* 2004; **101**: 445-50.

14. Morimoto M, Kim JT, Popovic J, Jain S, Bekker A. Ultrasound-guided lumbar plexus block for open reduction and internal fixation of hip fracture. *Pain Pract* 2006; **6**: 124-6.

15. Karmakar MK, Ho AM, Li X, Kwok WH, Tsang K, Ngan Kee WD. Ultrasound-guided lumbar plexus block through the acoustic window of the lumbar ultrasound trident. *Br J Anaesth* 2008; **100**: 533-537.

16. Doi K, Sakura S, Hara K. A modified posterior approach to lumbar plexus block using a transverse ultrasound image and an approach from the lateral border of the transducer. *Anaesth Intensive Care* 2010; **38**: 213-4.

17. Ilfeld BM, Loland VJ, Mariano ER. Prepuncture ultrasound imaging to predict transverse process and lumbar plexus depth for psoas compartment block and perineural catheter insertion: a prospective, observational study. *Anesth Analg* 2010; **110**: 1725-8.

18. Madison SJ, Ilfeld BM, Loland VJ, Mariano ER. Posterior lumbar plexus perineural catheter insertion by ultrasound guidance alone. *Acta Anaesthesiol Scand* 2011; **55**: 1031-2.

19. Bendtsen TF, Pedersen EM, Haroutounian S*, et al*. The suprasacral parallel shift vs lumbar plexus blockade with ultrasound guidance in healthy volunteers--a randomised controlled trial. *Anaesthesia* 2014; **69**: 1227-40.

20. Kirchmair L, Entner T, Kapral S, Mitterschiffthaler G. Ultrasound guidance for the psoas compartment block: an imaging study. *Anesth Analg* 2002; **94**: 706-10; table of contents.

21. Karmakar MK, Li JW, Kwok WH, Hadzic A. Ultrasound-guided lumbar plexus block using a transverse scan through the lumbar intertransverse space: a prospective case series. *Reg Anesth Pain Med* 2015; **40**: 75-81.

22. Sauter AR, Ullensvang K, Niemi G*, et al*. The Shamrock lumbar plexus block: A dose-finding study. *Eur J Anaesthesiol* 2015; **32**: 764-70.

23. Cappelleri G, Ghisi D, Ceravola E*, et al*. A randomised controlled comparison between stimulating and standard catheters for lumbar plexus block. *Anaesthesia* 2015; **70**: 948-55.

24. Zacchino M, Calliada F. Ultrasound image fusion: a new strategy to reduce x-ray exposure during image guided pain therapies. In: Nenoi M, ed. *Current topics in ionizing radiation research.* Rijeka: InTech, 2012; 395-406

25. Ewertsen C, Săftoiu A, Gruionu LG, Karstrup S, Nielsen MB. Real-time image fusion involving diagnostic ultrasound. *AJR Am J Roentgenol* 2013; **200**: W249-55.

26. Galiano K, Obwegeser AA, Bale R*, et al*. Ultrasound-guided and CT-navigation-assisted periradicular and facet joint injections in the lumbar and cervical spine: a new teaching tool to recognize the sonoanatomic pattern. *Reg Anesth Pain Med* 2007; **32**: 254-7.

27. Kwok WH, Karmakar MK. Fusion imaging: Ultrasound and CT or ultrasound and MRI image fusion for spinal sonography - preliminary experience. In: Karmakar MK, ed. *Musculoskeletal ultrasound for regional anaesthesia and pain medicine*. Hong Kong: Department of Anaesthesia and Intensive Care, The Chinese University of Hong Kong, 2016; 503-508

28. Cooper C, Campion G, Melton LJ 3rd. Hip fractures in the elderly: a world-wide projection. *Osteoporos Int* 1992; **2**: 285-9.

29. Brauer CA, Coca-Perraillon M, Cutler DM, Rosen AB. Incidence and mortality of hip fractures in the United States. *JAMA* 2009; **302**: 1573-9.

30. Kurtz S, Ong K, Lau E, Mowat F, Halpern M. Projections of primary and revision hip and knee arthroplasty in the United States from 2005 to 2030. *J Bone Joint Surg Am* 2007; **89**: 780-5.

31. Iorio R, Robb WJ, Healy WL*, et al*. Orthopaedic surgeon workforce and volume assessment for total hip and knee replacement in the United States: preparing for an epidemic. *J Bone Joint Surg Am* 2008; **90**: 1598-605.

32. Danish Health Authority. *[Specialty guidance for orthopedic surgery]*. 4-1012-14/29, Copenhagen S, Denmark, 2016.

33. Chidambaram R, Cobb AG. Change in the age distribution of patients undergoing primary hip and knee replacements over 13 years – an increase in the number of younger men having hip surgery. *Orthopaedic Proceedings* 2009; **91-B**: 152.

34. Johnell O, Kanis JA. An estimate of the worldwide prevalence, mortality and disability associated with hip fracture. *Osteoporos Int* 2004; **15**: 897-902.

35. Jenkins PJ, Clement ND, Hamilton DF, Gaston P, Patton JT, Howie CR. Predicting the cost-effectiveness of total hip and knee replacement: A health economic analysis. *Bone Joint J* 2013; **95-B**: 115-21.

36. Sim IW, Webb T. Anatomy and anaesthesia of the lumbar somatic plexus. *Anaesth Intensive Care* 2004; **32**: 178-87.

37. Di Benedetto P, Pinto G, Arcioni R*, et al*. Anatomy and imaging of lumbar plexus. *Minerva Anestesiol* 2005; **71**: 549-54.

38. Romanes GJ. *Cunningham's textbook of anatomy.* 12th ed. Cary: Oxford University Press, 1981.

39. Schuenke M, Schulte E, Schumacher U. *Thieme atlas of anatomy.* New York: Thieme, 2006.

40. Gebarski KS, Gebarski SS, Glazer GM, Samuels BI, Francis IR. The lumbosacral plexus: anatomic-radiologic-pathologic correlation using CT. *Radiographics* 1986; **6**: 401-25.

41. Dietemann JL, Sick H, Wolfram-Gabel R, Cruz da Silva R, Koritke JG, Wackenheim A. Anatomy and computed tomography of the normal lumbosacral plexus. *Neuroradiology* 1987; **29**: 58-68.

42. Lu S, Chang S, Zhang YZ, Ding ZH, Xu XM, Xu YQ. Clinical anatomy and 3D virtual reconstruction of the lumbar plexus with respect to lumbar surgery. *BMC Musculoskelet Disord* 2011; **12**: 76.

43. Kirchmair L, Lirk P, Colvin J, Mitterschiffthaler G, Moriggl B. Lumbar plexus and psoas major muscle: not always as expected. *Reg Anesth Pain Med* 2008; **33**: 109-14.

44. Gallaudet BB. A description of the planes of fascia of the human body, with special reference to the fascia of the abdomen, pelvis and perineum. *Am J Surg* 1931; **17**: 458-9.

45. Birnbaum K, Prescher A, Hessler S, Heller KD. The sensory innervation of the hip joint--an anatomical study. *Surg Radiol Anat* 1997; **19**: 371-5.

46. Simons MJ, Amin NH, Cushner FD, Scuderi GR. Characterization of the Neural Anatomy in the Hip Joint to Optimize Periarticular Regional Anesthesia in Total Hip Arthroplasty. *J Surg Orthop Adv* 2015; **24**: 221-4.

47. Apaydin N, Kendir S, Loukas M, Tubbs RS, Bozkurt M. Surgical anatomy of the superior gluteal nerve and landmarks for its localization during minimally invasive approaches to the hip. *Clin Anat* 2013; **26**: 614-20.

48. Lienhart A, Auroy Y, Pequignot F*, et al*. Survey of anesthesia-related mortality in France. *Anesthesiology* 2006; **105**: 1087-97.

49. Bendtsen TF, Haskins S, Kølsen Petersen JA, Børglum J. Do ultrasound-guided regional blocks signify a new paradigm in high-risk patients? *Best Pract Res Clin Anaesthesiol* 2016; **30**: 191-200.

50. Jeng CL, Torrillo TM, Rosenblatt MA. Complications of peripheral nerve blocks. *Br J Anaesth* 2010; **105**: i97-107.

51. Parkinson SK, Mueller JB, Little WL, Bailey SL. Extent of blockade with various approaches to the lumbar plexus. *Anesth Analg* 1989; **68**: 243-8.

52. Gentili M, Aveline C, Bonnet F. Total spinal anesthesia after posterior lumbar plexus block. *Ann Fr Anesth Reanim* 1998; **17**: 740-2.

53. Vaghadia H, Kapnoudhis P, Jenkins LC, Taylor D. Continuous lumbosacral block using a Tuohy needle and catheter technique. *Can J Anaesth* 1992; **39**: 75-8.

54. Stevens RD, Van Gessel E, Flory N, Fournier R, Gamulin Z. Lumbar plexus block reduces pain and blood loss associated with total hip arthroplasty. *Anesthesiology* 2000; **93**: 115-21.

55. Capdevila X, Macaire P, Dadure C*, et al*. Continuous psoas compartment block for postoperative analgesia after total hip arthroplasty: new landmarks, technical guidelines, and clinical evaluation. *Anesth Analg* 2002; **94**: 1606-13, table of contents.

56. Gadsden JC, Lindenmuth DM, Hadzic A, Xu D, Somasundarum L, Flisinski KA. Lumbar plexus block using high-pressure injection leads to contralateral and epidural spread. *Anesthesiology* 2008; **109**: 683-8.

57. Davis MP, Srivastava M. Demographics, assessment and management of pain in the elderly. *Drugs Aging* 2003; **20**: 23-57.

58. Dadure C, Raux O, Gaudard P*, et al*. Continuous psoas compartment blocks after major orthopedic surgery in children: a prospective computed tomographic scan and clinical studies. *Anesth Analg* 2004; **98**: 623-8, table of contents.

59. Sauter A, Ullensvang K, Bendtsen T, Børglum J. The "Shamrock Method" - a new and promising Technique for Ultrasound Guided Lumbar Plexus Blocks. *Br J Anaesth* E-letter published on February 16, 2013. Available from http://bja.oxfordjournals.org/forum/topic/brjana_el%3B9814 (accessed 24 October 2016).

60. Huntoon MA, Yeasting A. Analysis of Contrast Spread of a Modified Posterior Approach to Lumbosacral Plexus Blockade in a Cadaver Model. *Reg Anesth Pain Med* 1998; **23**: 16.

61. Winnie AP, Ramamurhty S, Durrani Z, Radonjic R. Plexus blocks for lower extremity surgery. *Anesth Rev* 1974; **1**: 11-16.

62. Chayen D, Nathan H, Chayen M. The psoas compartment block. *Anesthesiology* 1976; **45**: 95-99.

63. Hanna MH, Peat SJ, D'Costa F. Lumbar plexus block: an anatomical study. *Anaesthesia* 1993; **48**: 675-8.

64. Marhofer P, Greher M, Kapral S. Ultrasound guidance in regional anaesthesia. *Br J Anaesth* 2005; **94**: 7-17.

65. Kirchmair L, Entner T, Wissel J, Moriggl B, Kapral S, Mitterschiffthaler G. A study of the paravertebral anatomy for ultrasound-guided posterior lumbar plexus block. *Anesth Analg* 2001; **93**: 477-81, 4th contents page.

66. Aida S, Takahashi H, Shimoji K. Renal subcapsular hematoma after lumbar plexus block. *Anesthesiology* 1996; **84**: 452-5.

67. Strid JM, Børglum J, Bendtsen TF, Sauter AR. Lumbar Plexus Block Part II. The Shamrock Technique. In: Karmakar MK, ed. *Musculoskeletal Ultrasound for Regional Anaesthesia and Pain Medicine*. Hong Kong, PA: Department of Anaesthesia and Intensive Care, The Chinese University of Hong Kong, 2016

68. Aksu,C, Gürkan,Y. Shamrock method may prevent kidney injury. *Br J Anaesth* E-letter published on December 19, 2013. Available from http://bja.oxfordjournals.org/forum/topic/brjana_el%3B9814 (accessed 24 October 2016).

69. Lin JA, Lu HT, Chen TL. Ultrasound standard for lumbar plexus block. *Br J Anaesth* 2014; **113**: 188-9.

70. Lin JA, Lu HT. Solution to the challenging part of the Shamrock method during lumbar plexus block. *Br J Anaesth* 2014; **113**: 516-517.

71. Lin JA, Lee YJ, Lu HT. Finding the bulging edge: a modified shamrock lumbar plexus block in average-weight patients. *Br J Anaesth* 2014; **113**: 718-20.

72. Lin JA. Importance of half-the-air pressure test in Shamrock lumbar plexus block. *Eur J Anaesthesiol* 2016; **33**: 784.

73. Mænchen N, Dam M, Sauter AR*, et al*. Reply to: importance of half-the-air pressure test in Shamrock lumbar plexus block. *Eur J Anaesthesiol* 2016; **33**: 784-5.

74. Gray AT. Ultrasound-guided regional anesthesia: current state of the art. *Anesthesiology* 2006; **104**: 368-73, discussion 5A.

75. Walker KJ, McGrattan K, Aas-Eng K, Smith AF. Ultrasound guidance for peripheral nerve blockade. *Cochrane Database Syst Rev* 2009; **(4):** CD006459.

76. Ehlers L, Jensen JM, Bendtsen TF. Cost-effectiveness of ultrasound vs nerve stimulation guidance for continuous sciatic nerve block. *Br J Anaesth* 2012; **109**: 804-8.

77. NPS MedicineWise. Comparing different types of imaging. Available from: http://www.nps.org.au/medical-tests/medical-imaging/for-individuals/imaging-compared (accessed 24 October 2016).

78. Hangiandreou NJ. State-of-the-art ultrasound imaging technology. *J Am Coll Radiol* 2004; **1**: 691-3.

79. Amonoo-Kuofi HS. Changes in the lumbosacral angle, sacral inclination and the curvature of the lumbar spine during aging. *Acta Anat* 1992; **145**: 373-7.

80. Shao Z, Rompe G, Schiltenwolf M. Radiographic changes in the lumbar intervertebral discs and lumbar vertebrae with age. *Spine* 2002; **27**: 263-8.

81. Sevinc O, Barut C, Is M, Eryoruk N, Safak AA. Influence of age and sex on lumbar vertebral morphometry determined using sagittal magnetic resonance imaging. *Ann Anat* 2008; **190**: 277-83.

82. Pattichis CS, Pattichis MS, Micheli-Tzanakou E. Medical imaging fusion applications: an overview. *Conference Record of the Eleventh Annual Asilomar Conference on Signals, Systems, and Computers*. Pacific Grove: 1977; 1263-7.

83. Omar Z, Stathaki T. Image fusion: An overview. *IJSSST* 2014; **13**: 306-10.

84. Iagnocco A, Perella C, D'Agostino MA, Sabatini E, Valesini G, Conaghan PG. Magnetic resonance and ultrasonography real-time fusion imaging of the hand and wrist in osteoarthritis and rheumatoid arthritis. *Rheumatology* 2011; **50**: 1409-13.

85. Klauser AS, De Zordo T, Feuchtner GM*, et al*. Fusion of real-time US with CT images to guide sacroiliac joint injection in vitro and in vivo. *Radiology* 2010; **256**: 547-53.

86. Zacchino M, Almolla J, Canepari E, Merico V, Calliada F. Use of ultrasound-magnetic resonance image fusion to guide sacroiliac joint injections: a preliminary assessment. *J Ultrasound* 2013; **16**: 111-8.

87. Zacchino M, Allegri M, Canepari M*, et al*. Feasibility of pudendal nerve anesthetic block using fusion imaging technique in chronic pelvic pain. *European Journal of Pain Supplements* 2010; **4**: 329-33.

88. World Medical Association. *World Medical Association Declaration of Helsinki - Ethical Principles for Medical Research Involving Human Subjects*. Seul, 2008.

89. American Society of Anesthesiologists. ASA Physical Status Classification System. Available from https://www.asahq.org/resources/clinical-information/asa-physical-status-classification-system (accessed 24 October 2016).

90. Forsøgsperson.dk. [Researchvolunteer.dk]. Available from https://www.asahq.org/resources/clinical-information/asa-physical-status-classification-system (accessed 24 October 2016).

91. Deukmedjian AR, Le TV, Dakwar E, Martinez CR, Uribe JS. Movement of abdominal structures on magnetic resonance imaging during positioning changes related to lateral lumbar spine surgery: a morphometric study: Clinical article. *J Neurosurg Spine* 2012; **16**: 615-23.

92. Danish Health and Medicines Authority. *[Summary of product characteristics for lidocaine-adrenaline SAD, injection, solution]*. Copenhagen, 2015.

93. Danish Health and Medicines Authority. *[Summary of product characteristics for Dotarem, injection solution in pre-filled syringe, for intravenuously use, single-dose container, Guerbet]*. Copenhagen, 2015.

94. Almeida DR, Belliveau MJ, Enright T, Islam O, El-Defrawy SR, Gale J. Anatomic distribution of gadolinium contrast medium by high-resolution magnetic resonance imaging after peribulbar and retrobulbar injections. *Arch Ophthalmol* 2012; **130**: 743-8.

95. Hauritz RW, Pedersen EM, Linde FS*, et al*. Displacement of popliteal sciatic nerve catheters after major foot and ankle surgery: a randomized controlled double-blinded magnetic resonance imaging study. *Br J Anaesth* 2016; **117**: 220-7.

96. Brown RR, Clarke DW, Daffner RH. Is a mixture of gadolinium and iodinated contrast material safe during MR arthrography? *AJR Am J Roentgenol* 2000; **175**: 1087-90.

97. Russell JM, Kransdorf MJ, Bancroft LW, Peterson JJ, Berquist TH, Bridges MD. Magnetic resonance imaging of the sacral plexus and piriformis muscles. *Skeletal Radiol* 2008; **37**: 709-13.

98. Takahara T, Hendrikse J, Kwee TC*, et al*. Diffusion-weighted MR neurography of the sacral plexus with unidirectional motion probing gradients. *Eur Radiol* 2010; **20**: 1221-6.

99. Downs MB, Laporte C. Conflicting dermatome maps: educational and clinical implications. *J Orthop Sports Phys Ther* 2011; **41**: 427-34.

100. Sørensen LK, Hasselstrøm JB. A high-throughput multi-class liquid chromatography tandem mass spectrometry method for quantitative determination of licit and illicit drugs in whole blood. *Anal Methods* 2013; **5**: 3185-93.

101. Bendtsen TF, Lönnqvist PA, Jepsen KV, Petersen M, Knudsen L, Børglum J. Preliminary results of a new ultrasound-guided approach to block the sacral plexus: the parasacral parallel shift. *Br J Anaesth* 2011; **107**: 278-80.

102. Gürkan Y, Aksu C, Kus A, Toker K, Solak M. One operator's experience of ultrasound guided lumbar plexus block for paediatric hip surgery. *J Clin Monit Comput* Advanced access published on March 31, 2016; doi: 10.1007/s10877-016-9869-x.

103. Børglum J, Jensen K, Christensen AF*, et al*. Distribution patterns, dermatomal anesthesia, and ropivacaine serum concentrations after bilateral dual transversus abdominis plane block. *Reg Anesth Pain Med* 2012; **37**: 294-301.

104. Karmakar MK, Li JW, Kwok WH, Soh E, Hadzic A. Sonoanatomy relevant for lumbar plexus block in volunteers correlated with cross-sectional anatomic and magnetic resonance images. *Reg Anesth Pain Med* 2013; **38**: 391-7.

105. Mannion S, Barrett J, Kelly D, Murphy DB, Shorten GD. A description of the spread of injectate after psoas compartment block using magnetic resonance imaging. *Reg Anesth Pain Med* 2005; **30**: 567-71.

106. Van Dyke JA, Holley HC, Anderson SD. Review of iliopsoas anatomy and pathology. *Radiographics* 1987; **7**: 53-84.

107. Sadean MR, Glass PS. Pharmacokinetics in the elderly. *Best Pract Res Clin Anaesthesiol* 2003; **17**: 191-205.

Supplements

I. **Study I**

II. **Study II**

III. **Study III**

IV. **Methodological study I**

V. **Methodological study II**

Study I

Shamrock vs. Lumbar Ultrasound Trident: Ultrasound Guided Lumbar Plexus Blockade in Volunteers - a Randomised Controlled Trial

J. M. C. Strid[1], A. R. Sauter[2,3], K. Ullensvang[4], M. N. Andersen[5], M. Daugaard[1], M. A. F. Bendtsen[6], K. Søballe[7], E. M. Pedersen[8], J. Børglum[9], and T. F. Bendtsen[1]

[1]Department of Anaesthesiology and Intensive Care, Aarhus University Hospital, Nørrebrogade 44, DK-8000 Aarhus C, Denmark

[2]Department of Research and Development, Division of Emergencies and Critical Care, Oslo University Hospital, Kirkeveien 166, N-0450 Oslo, Norway

[3]Department of Anaesthesiology and Pain Medicine, Inselspital, Bern University Hospital, University of Bern, Freiburgstrasse 8, CH-3010 Bern, Switzerland

[4]Department of Anaesthesiology, Oslo University Hospital Rikshospitalet, Sognsvannsveien 20, N-0372 Oslo, Norway

[5]Department of Biomedicine, Faculty of Health, Aarhus University, Vennelyst Blvd. 4, DK-8000 Aarhus C, Denmark

[6]Medical Science, Faculty of Health, Aarhus University, Nordre Ringgade 1, DK-8000 Aarhus C, Denmark

[7]Department of Orthopaedic Surgery, Aarhus University Hospital, Tage-Hansens Gade 2, DK-8000 Aarhus C, Denmark

[8]Department of Radiology, Aarhus University Hospital, Nørrebrogade 44, DK-8000 Aarhus C, Denmark

[9]Department of Anaesthesiology and Intensive Care Medicine, Zealand University Hospital, University of Copenhagen, Sygehusvej 10, DK-4000 Roskilde, Denmark

Corresponding author: Thomas F. Bendtsen, research anaesthetist, associate professor, M.D., Ph.D., Department of Anaesthesiology, Aarhus University Hospital, Nørrebrogade 44, DK-8000 Aarhus, Denmark. Phone +4551542997, Email: tfb@dadlnet.dk

Running title: Shamrock vs. LUT – US guided lumbar plexus blocks

Abstract

Background The currently best-established ultrasound guided lumbar plexus block (LPB) techniques employ paravertebral location of the probe, e.g. the Lumbar Ultrasound Trident (LUT). However, paravertebral ultrasound scanning can provide inadequate sonographic visualisation of the lumbar plexus in some patients. The ultrasound guided Shamrock LPB technique allows real time sonographic visualisation of the lumbar plexus, various anatomical landmarks, advancement of the needle, and spread of local anaesthetic injectate in most patients. We aimed to compare block procedure outcomes, effectiveness, and safety of Shamrock vs. LUT.

Methods Twenty healthy men underwent ultrasound guided Shamrock and LUT LPBs (20 ml 2% lidocaine-adrenaline added 1 ml diluted contrast) in a blinded randomised crossover study. Primary outcome was block procedure time. Secondary outcomes were procedural discomfort, number of needle insertions, injectate spread assessed with MRI, sensorimotor effects, and lidocaine pharmacokinetics.

Results Shamrock LPB procedure was faster than LUT (238 [SD 74] s vs. 334 [SD 156] s; *P*=0.009), more comfortable (Numeric rating scale 0 to 10: 3 [interquartile range (IQR) 2 to 4] vs. 4 [IQR 3 to 6]; *P*=0.03), and required fewer needle insertions (2 [IQR 1 to 3) vs. 6 [IQR 2 to 12]; *P*=0.003). Perineural injectate spread visualised with MRI was similar between the groups and consistent with motor and sensory mapping. Zero/20 (0%) and 1/19 (5%) subjects had epidural spread after Shamrock and LUT (*P*=1.00), respectively. The lidocaine pharmacokinetics were similar between the groups.

Conclusions Shamrock was faster and more comfortable compared to LUT. The techniques were equally effective.

Keywords

lumbosacral plexus; nerve block; ultrasonography

Clinical trial registration

NCT02255591

Peripheral regional anaesthesia for hip surgery is related to improved haemodynamic stability and fewer complications compared with general or spinal anaesthesia.[1-5] Peripheral regional anaesthesia also provides effective perioperative analgesia with minimal use of opioids.[3 6 7]

Complete anaesthesia of the three main lumbar plexus nerves that innervate the hip region – the femoral, obturator, and lateral femoral cutaneous nerves – can be achieved with a single lumbar plexus block (LPB).[8 9] Combined with an iliohypogastric nerve block and a sacral plexus block, LPB provides effective anaesthesia for hip surgery.[10 11]

Previously described ultrasound guided LPB techniques recommended a paravertebral position of the ultrasound probe with axial or sagittal orientation.[12-20] The well-established Lumbar Ultrasound Trident (LUT) technique, described in 2008, employs a sagittally oriented probe in the paravertebral lumbar region.[15 21] However, this often provides inadequate sonographic visualisation of the target lumbar plexus, topography, needle, needle tip, and perineural spread of local anaesthetic.[15 21] Furthermore, LUT may be associated with a relatively high incidence of epidural spread of local anaesthetics (5/17 [29%] subjects) and may thereby impair hemodynamic stability.[21] An effective and safe LPB technique is desirable because patients admitted for hip surgery are typically elderly and may suffer severe cardiovascular comorbidity.[22-24]

The ultrasound guided Shamrock technique, first described in 2013, employs an axially oriented probe placed in the posterior axillary line in the flank of the patient.[10 25] This provides fast, easy, and sufficient real-time sonographic visualisation of the target lumbar plexus, surrounding anatomical structures, needle, needle tip, and perineural local anaesthetic spread. Theoretically, the improved visualisation will increase the precision, hence the efficiency and the safety of the block.

The aim of this prospective randomised controlled crossover trial in volunteers was to evaluate whether the Shamrock technique would reduce procedural time, defined as the time from placement of the probe on the skin until withdrawal of the block needle, compared to LUT. Secondary outcomes were procedure-related estimates, injectate spread, sensorimotor function, and lidocaine pharmacokinetics.

Methods

Ethics

This blinded randomised controlled crossover study was approved by the Regional Ethics Committee (MJ: 1-10-72-138-14), the Danish Health and Medicines Authority (2013-005346-10), and the Danish Data Protection Agency (1-16-02-423-14), and was monitored by the Good Clinical Practice (GCP) Unit at Aalborg and Aarhus University Hospitals. Written informed consent was obtained from all volunteers. The study was prospectively registered in ClinicalTrials.gov (NCT02255591) and complied with the Declaration of Helsinki II.

Study subjects

We recruited male subjects aged ≥18 yr with ASA I status via a Danish website for research volunteers during February 9-24, 2015. Exclusion criteria were inability to cooperate or communicate in Danish, daily consumption of analgesics, allergy to local anaesthetics or contrast agents, abuse of medicine or alcohol, infection or prior surgery in the lumbar paravertebral region or the flank, contraindications to magnetic resonance imaging (MRI), and legal incompetence.
The trial was conducted during two 2-day sessions one week apart in February and March 2015 at the Department of Radiology, Aarhus University Hospital, Denmark.

Block procedures

During the study, all subjects received two ultrasound guided LPBs – one with the Shamrock[10 25] and one with the LUT[15 21] technique – on the contralateral side one week apart. Each LPB was a single injection of 20 ml 2% lidocaine-adrenaline with addition of 1 ml contrast – i.e. 0.13 ml MRI contrast agent (27.9% gadoterate meglumine [Dotarem®; Guerbet, Roissy CdG Cedex, France]) diluted in 0.87 ml 0.9% isotonic saline.
Peripheral IV access was established prior to each block. The subjects were monitored with 3-lead electrocardiography, non-invasive blood pressure, and pulse oximetry. The subjects were placed in the lateral decubitus position with the side to be anaesthetised facing upwards.
One anaesthesiologist (T.F.B.) with extensive experience of ultrasound and electrical

nerve stimulation guided lumbar plexus blocks for LUT as well as Shamrock techniques performed all blocks using a Sonosite X-porte ultrasound system (Sonosite, Bothell, Washington, USA) and a 5-2 MHz curved array transducer (C60xp; Sonosite, Bothell, Washington, USA). A pre-scan including marking of the anticipated needle insertion point was performed. The skin was swapped with chlorhexidine in isopropyl alcohol and a sterile fenestrated sheet. The probe was draped with a sterile cover. The skin and subcutaneous tissue were infiltrated with 2 ml 2% lidocaine before insertion of the 22 Gauge, 100 mm nerve block needle (Stimuplex Ultra, B. Braun, Melsungen, Germany).

Shamrock: The curvilinear probe was aligned axially in the flank of the subject immediately cephalad to the iliac crest. The probe was shifted posteriorly until the transverse process of vertebra L4 and the quadratus lumborum, erector spinae, and psoas major muscles were identified as a shamrock or three-leaved clover.[10 25] The tail of the probe was tilted cephalad, targeting the hyperechoic lumbar plexus between the thin posterior and the thick anterior lamina of the psoas major muscle. The needle was inserted in-plane, 3 to 4 cm lateral to the sagittal lumbar midline, and advanced in a postero-anterior direction between the L4 and L5 transverse processes until the needle tip was visible at the lateral margin of the lumbar plexus.

LUT: The probe was oriented paramedian, visualising the upper margin of the sacral ala and the L5 transverse process. By shifting the probe first cephalad and then medial, the L3 transverse process and the L3 superior articular facet of the L2/L3 zygapophyseal joint were identified. The L2, L3, and L4 transverse processes were visualised as the “trident sign”.[15 21] With the psoas major muscle anterior to the transverse processes, the lumbar plexus was identified within the major psoas muscle whenever possible. The block needle was inserted with a steep out-of-plane approach and advanced until the needle tip was located approximately 20 mm[26] anterior to the posterior border of the L3 and L4 transverse processes immediately lateral to the zygapophyseal joint.

During both procedures, an electrical nerve stimulator (0.1 ms, 2 Hz, 0.2 mA) was connected to the block needle as a safety device in order to alert about intraneural needle tip location. The endpoint of injection was an adequate visualisation of the needle tip adjacent to the target lumbar plexus or an appropriate motor response to electrical nerve stimulation with 0.3 to 0.5 mA either from the quadriceps femoris or the thigh adductors

whenever the lumbar plexus was not ultrasonographically visible. Local anaesthetic with added MRI contrast agent was injected in refracted doses with intermittent aspiration. Both techniques have been described in detail previously.[10 15 21 25]

Time zero (T_0) min was defined as the time when the block needle was withdrawn after completed injection. The follow-up continued until T_{90}. Each subject was observed until the sensorimotor blockade had worn off.

Outcomes and assessment

The primary outcome was block procedure time (s) defined as the time from placement of the probe on the skin after sterile preparations until withdrawal of the block needle.

The secondary outcomes were: (a) number of block needle insertions estimated as the number of retractions of the block needle followed by advancement regardless of the number of skin penetrations; (b) horisontal distance (cm) from median to needle skin insertion point; (c) distance (cm) from needle skin insertion point to needle tip at the endpoint of injection gauged by reading the markings on the needle shaft; (d) minimum electrical nerve stimulation level (mA) required to trigger a motor response immediately prior to injection; (e) type of response to electrical nerve stimulation (“Quadriceps femoris”, “Sartorius”, “Other motor”, "Paraesthesia” or "No response"); (f) maximum procedural discomfort assessed by the subject on a NRS (0=no discomfort, 10=worst possible discomfort) at T_0; (g) change in mean arterial blood pressure (Δ MAP) from baseline to T_5; (h) perineural spread of lidocaine; (i) epidural spread of lidocaine; (j) motor blockade; (k) sensory blockade; (l) block success rate; (m) peak plasma concentration of lidocaine (C_{max} of p-lidocaine); (n) time to C_{max} (T_{omc}); (o) p-lidocaine concentration-time area under the curve; and (p) cost-effectiveness.

Spread of the injectate was evaluated on axial 3D T1-weighted MRI sequences (mDixon all generating in-phase, out-of-phase, water, and fat images and diffusion weighted images) sampled with a 3T Philips Achieva 3.0T dstream scanner (Koninklijke Philips Electronics, Eindhoven, the Netherlands) at T_{15}. Perineural spread was assessed as "present" or "absent" direct visual contact between the injectate and the anterior rami of the spinal nerves L1 to S1, the femoral, obturator, and lateral femoral cutaneous nerves, and the lumbosacral trunk, respectively. Epidural spread was defined as “present” when

circumferential (360°) epidural distribution of the injectate was observed on any level together with absent sensation for cold in at least one pair of bilateral dermatomes during the sensory mapping at T_{45}.

Motor blockade of the femoral, obturator, superior gluteal, and tibial (sciatic) nerves were defined as a ≥50% reduction in muscle strength (mmHg) at T_{30} compared to baseline. Muscle strength was assessed in the supine position as active strength against resistance with a handheld dynamometer (Commander Muscle Testing; JTECH Medical, Midvale, USA) during knee extension (with 90° flexion of the hip and knee joints), hip adduction (with extended and 45° abducted lower limb), hip abduction (with extended lower limb), and knee flexion (with extended knee and passive elevation of the lower limb), respectively.[25] An observer instructed the subject to exert pressure with maximum strength against the stationary held dynamometer. The maximum value of three tests with intermittent 20 s intervals was recorded for each type of movement.

Sensory blockade of warmth, cold, touch, and pain in the dermatomes Th8 to S3 and in the skin area innervated by the lateral femoral cutaneous nerve were tested bilaterally at T_{45}. Somatosensation was assessed either as "present" or "absent", where absence was considered a successful sensory blockade. Warmth, cold, touch, and pain were tested with standardised stimuli: 40° and 25° thermo test (Rolltemp II; Somedic, Hörby, Sweden), brush (SENSELab^{TM} Brush-05; Somedic AB, Hörby, Sweden), and punctuate needle stimulator (PinPrick 512 mN; MRC Systems GmbH, Heidelberg, Germany), respectively. Block success was defined as motor blockade of the femoral and obturator nerves and sensory blockade (pain and/or cold) of the lateral femoral cutaneous nerve.

Blood samples for the pharmacokinetic analysis of p-lidocaine were collected via the IV access at $T_{0, 5, 10, 20, 40, 60, \text{and } 90}$ and centrifuged at 1,800 G for 9 minutes. The plasma was transferred to 1.5 ml cryotubes and stored at -80 °C until analysis. P-lidocaine concentration was measured using liquid chromatography tandem mass spectrometry.[21 27]

Cost-effectiveness was estimated as the difference in mean marginal cost for the techniques.[28] For medical staff, average annual wages including pensions, holiday pay, and employer fees for 1,924 paid hours were collected in Danish Kroner (DKK) in July 2016 and converted into British Pound (100 GBP=874 DKK).

Randomisation and Blinding

Three study-independent assistants performed computerised randomisation assigning the sequences of intervention (Shamrock and LUT) and left and right side to 20 anonymous identification numbers. Twenty sheets pre-printed with the randomly allocated sequences were put in 20 identical opaque sealed envelopes marked with the identification numbers. Immediately prior to each procedure, T.F.B. who performed the blocks and A.R.S. who double-controlled the randomised procedure opened the envelope, checked the allocated intervention and side without revealing it to others, returned the sheet to the envelope, and resealed it. The procedure was repeated on the second experimental day.
Independent observers who were blinded to the allocation and did not attend the block procedure sampled all data. The MRI data were anonymised and analysed by an anaesthesiologist (T.F.B) with extensive knowledge of the lumbar paravertebral anatomy.

Statistical analysis

The primary outcome was block procedure time in seconds. Based on a pilot study, we hypothesised that the Shamrock technique would reduce block procedure time from 280 s to 140 s compared with LUT. Detection of a 50% reduction in a crossover trial and 80% power (1-β) and α=0.05 would require a sample size of 17 subjects in a two-sided crossover analysis (Stata IC 10.1; StataCorp LP, College Station, USA). Twenty subjects were enrolled to avoid decreased power due to dropouts.
All statistical analyses were conducted with Stata IC 14.1 (StataCorp LP, College Station, USA). Normality of distribution was assessed visually with normal Q-Q plot. Differences between paired continuous variables with normal distribution were analysed with the one-sample Student t-test. Differences between paired continuous variables with non-normal distribution and between paired ordinal variables were analysed with the Wilcoxon matched-pairs signed rank test. Differences between paired categorical variables were analysed with McNemar's test. The level of significance was 0.05. Data are presented as mean (SD) for continuous variables with normal distribution, as median (IQR) for continuous variables with non-normal distributions, ordinal variables, and age, and as frequencies (percentage) for categorical variables.

Results

Twenty volunteers were included after written and oral informed consent (Fig 1). One of the included subjects did not show up on the second experimental day (study-unrelated reason). Both intervention A and B were completed per protocol in 19 volunteers.

Characteristics

Median (range) age of the 19 subjects who were included in both groups was 22 (21 to 28) yr, mean weight was 80.1 (8.0) kg, mean height was 186 (6.5) cm, and mean BMI was 25.1 (2.8) kg m^{-2}.

Median (range) age of the 20 subjects who were included in the Shamrock group was 22.5 (21 to 30) yr, mean weight was 80.1 (7.8) kg, mean height was 185 (6.9) cm, and mean BMI was 25.3 (2.9) kg m^{-2}.

Outcomes

The procedure-related outcomes are displayed in Table 1. Due to registration errors, value for block procedure time is missing for one subject in the LUT group and values for minimal electrical nerve stimulation and response are missing for one subject in the Shamrock group.

Fig 2 illustrates the spread of injectate on MRI in one subject. The MRI analysis showed no difference in perineural injectate spread to the anterior ramus of L1 (Shamrock, 7/20 [35%]; LUT, 7/19 [37%]; *P*=1.00), L2 (Shamrock, 19/20 [95%]; LUT, 15/19 [79%]; *P*=0.38), L3 (Shamrock, 18/20 [90%]; LUT, 16/19 [84%]; *P*=1.00), L4 (Shamrock, 15/20 [75%]; LUT, 12/19 [63%]; *P*=0.63), and L5 (Shamrock, 3/20 [15%]; LUT, 6/19 [32%]; *P*=1.22), the femoral (Shamrock, 18/20 [90%]; LUT, 15/19 [79%]; *P*=0.69), obturator (Shamrock, 14/20 [70%]; LUT, 14/19 [74%]; *P*=1.00), and lateral femoral cutaneous (Shamrock, 16/20 [80%]; LUT, 15/19 [79%]; *P*=1.00) nerves, as well as the lumbosacral trunk (Shamrock, 3/20 [15%]; LUT, 6/19 [32%]; *P*=0.22).

Epidural spread of the injectate was confirmed in 0/20 (0%) subjects after Shamrock and in 1/19 (5%) subjects after LUT (*P*=1.00). The sensory effect of the epidural spread was observed in the dermatomes L5 and S1 of the one subject.

Values for baseline and post-block muscle strength are displayed in Table 2.

Table 3 displays the number of subjects with sensory blockade at T_{45}.
There was no difference in block success (Shamrock, 7/20 [35%]; LUT, 7/19 [37%]; *P*=1.00). An exploratory analysis showed no difference in motor block success of the femoral (Shamrock, 14/20 [70%]; LUT, 15/19 [79%]; *P*=0.73), obturator (Shamrock, 12/20 [60%]; LUT, 14/19 [74%]; *P*=0.55), superior gluteal (Shamrock, 3/20 [15%]; LUT, 5/19 [26%]; *P*=0.69), and sciatic (Shamrock, 9/20 [45%]; LUT, 10/19 [53%]; *P*=0.73) nerves, or in motor block success of the femoral and obturator nerves combined (Shamrock, 12/20 [60%]; LUT, 14/19 [74%]; *P*=0.55).
The mean C_{max}, median T_{omc}, and the p-lidocaine concentration-time area under the curve were similar for the techniques and showed no statistically significant differences (Fig 3).
The mean marginal cost per LPB was 2 GBP, corresponding to the shorter mean block procedure time for Shamrock (98 s) and estimating the total cost per hour for an anaesthesiologist and an assistant nurse to be 81 GBP. Both techniques were related to the same marginal costs for disposals and equipment.

Safety

No harm or unintended effects were observed during the trial.

Discussion

In this first randomised controlled crossover trial investigating the Shamrock technique, we found that Shamrock was faster to perform, required fewer needle insertions, and was more comfortable in healthy normal-weighted volunteers compared with the LUT technique. The techniques were apparently equally effective for anaesthesia.

The shorter Shamrock procedure time can be considered a proxy marker of an improved visualisation of the target lumbar plexus, the paravertebral topography, and the block needle compared to LUT. The better visualisation may also explain that fewer needle insertions were required with Shamrock. The target plexus is often not directly visualised with LUT,[15] which is also the case with several other previously described techniques.[12 16-19]

The shorter procedure time and fewer needle insertions probably explain why Shamrock was a more comfortable procedure than LUT. The fewer needle insertions with the Shamrock technique can also be speculated to reduce the risk of tissue injury and complications such as nerve injury, muscular or vascular lesions, and haematomas. As direct visualisation of the target lumbar plexus often is inadequate with LUT, it can be speculated to induce a higher risk of epidural spread of local anaesthetics compared to the Shamrock technique in some patients.[21] However, the study was not powered to detect such differences.

The lumbosacral sonoanatomy has been compared to MRI previously[29] although only a few studies have explored the spread of local anaesthetic after LPB with MRI.[21 30] The sensorimotor mapping demonstrated a primary effect on the muscles and dermatomes innervated by the femoral, obturator, and lateral femoral cutaneous nerves – the terminal nerves of the anterior rami of the spinal nerves of L2 to L4. The terminal nerves can be anaesthetised by spread of local anaesthetic either around the anterior rami of spinal nerves L2 to L4, or around the lumbar plexus branches between the two layers of the psoas major muscle, or around the terminal nerves after they have emerged from the psoas major muscle. The sensorimotor results are in accordance with the MRI analysis of injectate spread, which demonstrated primary perineural spread around the anterior rami L2 to L4 as well as the terminal nerves. This accordance was also found in previous studies.[21 30]

Both Shamrock and LUT aim to inject local anaesthetic into the fascial plane between the anterior and posterior lamina of the psoas major muscle. The MRI scans display how the local anaesthetic is contained inside this fascial plane implicating that significant blockade of the lumbosacral trunk as well as the superior gluteal nerve cannot be expected.

The success rate in the present study is only relevant as a measure of comparison of the effectiveness of the techniques – it is inapplicable as an estimate of the success rate in a clinical setting. In a recent dose-finding study with 30 patients scheduled for lower limb surgery, it was found that the minimum effective anaesthetic volume of ropivacaine 0.5% to achieve block success in 50% of the patients (ED_{50}) with the Shamrock technique was 20.4 ml (95% CI 13.9 to 30.0), and that ED_{95} was 36.0 ml (95% CI 19.7 to 52.2).[25] We used a relatively low volume of 20 ml lidocaine because the volunteers were discharged on the day of the intervention. The aim of the present study was not to obtain maximum LPB success, but to validate and compare two LPB techniques. Consequently, we chose lidocaine as local anaesthetic and a dose that we expected to be approximately the ED_{50} dose.

Furthermore, defining block success in healthy volunteers is complex; the standard criteria for clinically successful blockade in patients, i.e. no need for rescue blocks, conversion to general or spinal anaesthesia, or analgesic drugs, are inapplicable. In the present study, motor blockade (of the femoral and obturator nerves) was used as a proxy marker of sensory blockade, because sensory testing based on dermatomal mapping of the lower limb is unpredictable due to anatomical variation of segmental and terminal nerve innervation and overlapping of adjacent segmental and terminal nerve cutaneous territories.[31] In our study, a successful motor blockade was defined as at least 50% decrease in baseline muscle strength in order to avoid overestimation due to dual nerve innervation. However, this is an arbitrary cut-off and the success rate should be considered merely a measure of comparison between the two techniques.

The uncertainty related to dermatomal sensory mapping should be taken into account when interpreting the results of sensory blockade. While motor and sensory blockade is variable and depends on the trial subject, blinded analysis of the perineural injectate spread on MRI is an objective measure. We therefore recommend inclusion of analysis of perineural injectate spread on MRI in healthy volunteers as part of the validation of new

block techniques.

The lidocaine pharmacokinetics results were similar for the two techniques and p-lidocaine did not exceed toxic dose.[32] The time interval from injection of lidocaine-adrenaline to maximum concentration of p-lidocaine was approximately 1 h, which complies with previous pharmacokinetic studies about the plasma concentration of local anaesthetics in regional anaesthesia.[21 33] Since we used approximately the ED_{50} of lidocaine-adrenaline for the Shamrock technique,[25] an injection of a larger and more clinical relevant volume may affect the p-lidocaine differently.

The present study has a number of limitations. The lumbar paravertebral anatomy may change with age[34 35] and the results of this study may therefore be different in older hip surgery patients compared to healthy normal-weighted young men. The lumbar plexus can be more difficult to visualise in the many over-weighted hip surgery patients and the skin to target needle depth varies proportional to BMI.[13 36] This may limit the external validity. By using an endpoint for nerve stimulation in the range 0.3 to 0.5 mA – whenever the target lumbar plexus was not ultrasonographically visible – appropriate needle-nerve proximity could be assumed.[37] However, current settings >0.5 mA have sometimes been advocated to prevent unintentional needle-to-nerve contacts and improve safety during peripheral nerve block procedures.[38] All observers were blinded and we strived towards blinding all subjects with identical trial setup. However, the anaesthesiologist who performed all interventions could not be blinded to group allocation. To minimise this source of bias, the operator adhered to a strict double-controlled protocol procedure, although the risk of performance bias cannot be ruled out, as is the case with all procedure related studies. Future clinical studies should include the clinical applicability of the Shamrock technique combined with a sacral plexus block for hip surgical anaesthesia in old and fragile patients.

Conclusion

The Shamrock technique was faster to perform, required fewer needle insertions, was more comfortable, and was equally effective compared to the Lumbar Ultrasound Trident technique.

Authors' contributions

J.M.C.S.: Designed the study protocol, recruited all study subjects, conducted the clinical trial, collected and analysed the data, and authored the initial manuscript.

A.R.S.: Designed the study protocol and conducted the clinical trial.

K.U.: Conducted the clinical trial and collected data.

M.N.A.: Conducted the clinical trial and collected and analysed the lidocaine pharmacokinetics data.

M.D.: Conducted the clinical trial and collected data.

M.A.F.B.: Conducted the clinical trial and collected data.

E.M.P: Designed the study protocol.

J.B.: Designed the study protocol, conducted the clinical trial, and collected data.

T.F.B.: Designed the study protocol, conducted the clinical trial, and analysed the anonymised MRI data.

All authors read and revised the manuscript and approved the final version.

Declaration of interests

A.R.S. has received payment for consulting from B. Braun and Philips and has received speaker fees by Siemens. J.B. has received grants to cover congress participation and payment for consulting from Secma (Sonosite Denmark). T.F.B. has received payment for consulting from BK Medical. All other authors have no interests to declare.

Funding

The A.P. Møller and Chastine Mc-Kinney Møller Foundation for General Purposes, Copenhagen, Denmark and the Department of Anaesthesiology, Oslo University Hospital Rikshospitalet, Oslo, Norway supported this work. The content is solely the responsibility of the authors.

Table of References

1. de Visme V, Picart F, Le Jouan R, Legrand A, Savry C, Morin V. Combined lumbar and sacral plexus block compared with plain bupivacaine spinal anesthesia for hip fractures in the elderly. *Reg Anesth Pain Med* 2000; **25**: 158-62

2. Bendtsen TF, Haskins S, Kølsen Petersen JA, Børglum J. Do ultrasound-guided regional blocks signify a new paradigm in high-risk patients? *Best Pract Res Clin Anaesthesiol* 2016; **30**: 191-200

3. Gottschalk A, Van Aken H, Zenz M, Standl T. Is anesthesia dangerous? *Dtsch Arztebl Int* 2011; **108**: 469-74

4. Memtsoudis SG, Rasul R, Suzuki S*, et al*. Does the impact of the type of anesthesia on outcomes differ by patient age and comorbidity burden? *Reg Anesth Pain Med* 2014; **39**: 112-9

5. Whiting PS, Molina CS, Greenberg SE, Thakore RV, Obremskey WT, Sethi MK. Regional anaesthesia for hip fracture surgery is associated with significantly more peri-operative complications compared with general anaesthesia. *Int Orthop* 2015; **39**: 1321-7

6. Chelly JE, Casati A, Al-Samsam T, Coupe K, Criswell A, Tucker J. Continuous lumbar plexus block for acute postoperative pain management after open reduction and internal fixation of acetabular fractures. *J Orthop Trauma* 2003; **17**: 362-7

7. Bono JV, Robbins CE, Mehio AK, Aghazadeh M, Talmo CT. Pharmacologic pain management before and after total joint replacement of the hip and knee. *Clin Geriatr Med* 2012; **28**: 459-70

8. Birnbaum K, Prescher A, Hessler S, Heller KD. The sensory innervation of the hip joint – an anatomical study. *Surg Radiol Anat* 1997; **19**: 371-5

9. Kampa RJ, Prasthofer A, Lawrence-Watt DJ, Pattison RM. The internervous safe zone for incision of the capsule of the hip. A cadaver study. *J Bone Joint Surg Br* 2007; **89**: 971-6

10. Sauter A, Ullensvang K, Bendtsen T, Børglum J. The "Shamrock Method" - a new and promising technique for ultrasound guided lumbar plexus blocks. *Br J Anaesth* E-letter published on February 26, 2013. Available from: http://bja.oxfordjournals.org/forum/topic/brjana_el%3B9814 (accessed 16 September 2016)

11. Bendtsen TF, Lönnqvist PA, Jepsen KV, Petersen M, Knudsen L, Børglum J. Preliminary results of a new ultrasound-guided approach to block the sacral plexus: the parasacral parallel shift. *Br J Anaesth* 2011; **107**: 278-80
12. Kirchmair L, Entner T, Kapral S, Mitterschiffthaler G. Ultrasound guidance for the psoas compartment block: an imaging study. *Anesth Analg* 2002; **94**: 706-10; table of contents
13. Kirchmair L, Enna B, Mitterschiffthaler G*, et al*. Lumbar plexus in children. A sonographic study and its relevance to pediatric regional anesthesia. *Anesthesiology* 2004; **101**: 445-50
14. Morimoto M, Kim JT, Popovic J, Jain S, Bekker A. Ultrasound-guided lumbar plexus block for open reduction and internal fixation of hip fracture. *Pain Pract* 2006; **6**: 124-6
15. Karmakar MK, Ho AM, Li X, Kwok WH, Tsang K, Ngan Kee WD. Ultrasound-guided lumbar plexus block through the acoustic window of the lumbar ultrasound trident. *Br J Anaesth* 2008; **100**: 533-537
16. Doi K, Sakura S, Hara K. A modified posterior approach to lumbar plexus block using a transverse ultrasound image and an approach from the lateral border of the transducer. *Anaesth Intensive Care* 2010; **38**: 213-4
17. Ilfeld BM, Loland VJ, Mariano ER. Prepuncture ultrasound imaging to predict transverse process and lumbar plexus depth for psoas compartment block and perineural catheter insertion: a prospective, observational study. *Anesth Analg* 2010; **110**: 1725-8
18. Madison SJ, Ilfeld BM, Loland VJ, Mariano ER. Posterior lumbar plexus perineural catheter insertion by ultrasound guidance alone. *Acta Anaesthesiol Scand* 2011; **55**: 1031-2
19. Karmakar MK, Li JW, Kwok WH, Hadzic A. Ultrasound-guided lumbar plexus block using a transverse scan through the lumbar intertransverse space: a prospective case series. *Reg Anesth Pain Med* 2015; **40**: 75-81
20. Cappelleri G, Ghisi D, Ceravola E*, et al*. A randomised controlled comparison between stimulating and standard catheters for lumbar plexus block. *Anaesthesia* 2015; **70**: 948-55
21. Bendtsen TF, Pedersen EM, Haroutounian S*, et al*. The suprasacral parallel shift vs lumbar plexus blockade with ultrasound guidance in healthy volunteers – a randomised controlled trial. *Anaesthesia* 2014 Nov; **69**: 1227-40

22. de Luise C, Brimacombe M, Pedersen L, Sørensen HT. Comorbidity and mortality following hip fracture: a population-based cohort study. *Aging Clin Exp Res* 2008; **20**: 412-8

23. Chidambaram R, Cobb AG. Change in the age distribution of patients undergoing primary hip and knee replacements over 13 years – an increase in the number of younger men having hip surgery. *Orthopaedic Proceedings* 2009; **91-B**: 152. Available from http://www.bjjprocs.boneandjoint.org.uk/content/91-B/SUPP_I/152.1 (accessed 16 September 2016)

24. Centers for Disease Control and Prevention National Hospital Discharge Survey, 2010. Number of all-listed procedures for discharges from short-stay hospitals, by procedure category and age: United States, 2010. Available from http://www.cdc.gov/nchs/data/nhds/4procedures/2010pro4_numberprocedureage.pdf (accessed 16 September 2016)

25. Sauter AR, Ullensvang K, Niemi G*, et al*. The Shamrock lumbar plexus block: A dose-finding study. *Eur J Anaesthesiol* 2015; **32**: 764-70

26. Capdevila X, Macaire P, Dadure C*, et al*. Continuous psoas compartment block for postoperative analgesia after total hip arthroplasty: new landmarks, technical guidelines, and clinical evaluation. *Anesth Analg* 2002 Jun; **94**: 1606-13, table of contents

27. Sørensen LK, Hasselstrøm JB. A high-throughput multi-class liquid chromatography tandem mass spectrometry method for quantitative determination of licit and illicit drugs in whole blood. *Anal Methods* 2013; **5**: 3185-93

28. Ehlers L, Jensen JM, Bendtsen TF. Cost-effectiveness of ultrasound vs nerve stimulation guidance for continuous sciatic nerve block. *Br J Anaesth* 2012; **109**: 804-8

29. Karmakar MK, Li JW, Kwok WH, Soh E, Hadzic A. Sonoanatomy relevant for lumbar plexus block in volunteers correlated with cross-sectional anatomic and magnetic resonance images. *Reg Anesth Pain Med* 2013; **38**: 391-7

30. Mannion S, Barrett J, Kelly D, Murphy DB, Shorten GD. A description of the spread of injectate after psoas compartment block using magnetic resonance imaging. *Reg Anesth Pain Med* 2005; **30**: 567-71

31. Downs MB, Laporte C. Conflicting dermatome maps: educational and clinical implications. *J Orthop Sports Phys Ther* 2011; **41**: 427-34

32. Danish Health and Medicines Authority. *[Summary of product characteristics for lidocaine-adrenaline SAD, injection, solution]*. Copenhagen, July 7, 2015
33. Børglum J, Jensen K, Christensen AF*, et al*. Distribution patterns, dermatomal anesthesia, and ropivacaine serum concentrations after bilateral dual transversus abdominis plane block. *Reg Anesth Pain Med* 2012; **37**: 294-301
34. Amonoo-Kuofi HS. Changes in the lumbosacral angle, sacral inclination and the curvature of the lumbar spine during aging. *Acta Anat (Basel)* 1992; **145**: 373-7
35. Sevinc O, Barut C, Is M, Eryoruk N, Safak AA. Influence of age and sex on lumbar vertebral morphometry determined using sagittal magnetic resonance imaging. *Ann Anat* 2008; **190**: 277-83
36. Kirchmair L, Entner T, Wissel J, Moriggl B, Kapral S, Mitterschiffthaler G. A study of the paravertebral anatomy for ultrasound-guided posterior lumbar plexus block. *Anesth Analg* 2001; **93**: 477-81, 4th contents page
37. De Andres J, Alonso-Inigo JM, Sala-Blanch X, Reina MA. Nerve stimulation in regional anesthesia: theory and practice. *Best Pract Res Clin Anaesthesiol* 2005; **19**: 153-74
38. Vassiliou T, Muller HH, Limberg S, De Andres J, Steinfeldt T, Wiesmann T. Risk evaluation for needle-nerve contact related to electrical nerve stimulation in a porcine model. *Acta Anaesthesiol Scand* 2016; **60**: 400-6

Tables

Table 1 Procedure-related outcomes for the Shamrock vs. the Lumbar Ultrasound Trident (LUT) technique. Values are displayed as mean (SD), median (IQR), or frequency (%). MAP, mean arterial pressure; NRS, numeric rating scale (0=no discomfort, 10=worst possible discomfort).

	Shamrock (*n*=20)	**LUT (*n*=19)**	***P* value**
Block procedure time (s)	238 (74)	334 (156) (*n*=18)	0.009
Number of needle insertions	2 (1–3)	6 (2–12)	0.003
Needle insertion point from midline (cm)	3.0 (3.0–3.0)	5.0 (5.0–6.0)	<0.001
Needle depth (cm)	8.0 (7.0–8.5)	7.0 (6.5–7.0)	0.001
Minimal nerve stimulation (mA)	0.50 (0.32–0.70) (*n*=19)	0.36 (0.32–0.46)	0.07
Response on nerve stimulation			0.57
Quadriceps femoris	17 (89%)	13 (68%)	0.45
Sartorius	1 (5%)	3 (16%)	0.63
Other motor	0 (0%)	0 (0%)	1.00
Paresthesia	0 (0%)	1 (5%)	1.00
None	1 (5%)	2 (11%)	1.00
Procedural discomfort (NRS units)	3 (2–4)	4 (3–6)	0.03
ΔMAP (mmHg)	1.1 (9.4)	÷2.7 (11.3)	0.47

Table 2 Baseline and post-block muscle strength for the Shamrock vs. the Lumbar Ultrasound Trident (LUT) technique. Values are displayed as median (IQR).

	Shamrock (*n*=20)	**LUT (*n*=19)**	***P* value**
Knee extension (femoral nerve)			
Baseline muscle strength	264 (242–313)	275 (261–310)	
Post-block muscle strength	0 (0–156)	0 (0–46)	0.44
P value	<0.001	<0.001	
Hip adduction (obturator nerve)			
Baseline muscle strength	160 (136–189)	156 (138–171)	
Post-block muscle strength	31 (0–121)	0 (0–77)	0.36
P value	<0.001	<0.001	
Hip abduction (superior gluteal nerve)			
Baseline muscle strength	147 (137–162)	149 (140–166)	
Post-block muscle strength	110 (82–147)	110 (79–147)	0.83
P value	<0.001	0.006	
Knee flexion (sciatic nerve)			
Baseline muscle strength	259 (239–294)	248 (215–286)	
Post-block muscle strength	154 (75–207)	121 (63–187)	0.61
P value	<0.001	<0.001	

Table 3 Block of somatosensation tested in the dermatomes Th8 to S3 and in the skin area innervated by the lateral femoral cutaneus nerve (LFCN) 45 minutes after the Shamrock (*n*=20) vs. the Lumbar Ultrasound trident (LUT) technique (*n*=19). Values are presented as frequency (%).

	Cold			**Warmth**			**Touch**			**Pain**		
	Shamrock	**LUT**	***P* value**	**Shamrock**	**LUT**	***P* value**	**Shamrock**	**LUT**	***P* value**	**Shamrock**	**LUT**	***P* value**
Th8	0 (0)	0 (0)	1.00	0 (0)	0 (0)	1.00	0 (0)	0 (0)	1.00	0 (0)	0 (0)	1.00
Th9	0 (0)	0 (0)	1.00	0 (0)	0 (0)	1.00	0 (0)	0 (0)	1.00	0 (0)	0 (0)	1.00
Th10	0 (0)	0 (0)	1.00	0 (0)	0 (0)	1.00	0 (0)	0 (0)	1.00	0 (0)	0 (0)	1.00
Th11	0 (0)	0 (0)	1.00	0 (0)	0 (0)	1.00	0 (0)	0 (0)	1.00	0 (0)	0 (0)	1.00
Th2	0 (0)	0 (0)	1.00	0 (0)	0 (0)	1.00	0 (0)	0 (0)	1.00	0 (0)	0 (0)	1.00
L1	2 (10)	0 (0	1.00	4 (20)	1 (5)	0.63	4 (20)	0 (0)	0.25	4 (20)	0 (0)	0.25
L2	12 (60)	9 (47)	0.45	12 (60)	8 (42)	0.34	11 (55)	6 (32)	0.18	13 (65)	8 (42)	0.18
L3	16 (80)	15 (79)	1.00	15 (75)	15 (79)	1.00	7 (35)	10 (53)	0.58	12 (60)	15 (79)	0.34
L4	11 (55)	15 (79)	0.23	11 (55)	15 (79)	0.34	9 (45)	12 (63)	0.58	9 (45)	13 (68)	0.39
L5	5 (25)	6 (32)	1.00	2 (10)	3 (16)	1.00	0 (0)	0 (0	1.00	0 (0	2 (11)	0.50
S1	14 (70)	14 (74)	1.00	10 (50)	9 (47)	1.00	0 (0	0 (0	1.00	2 (10)	3 (16)	1.00
S2	0 (0)	1 (5)	1.00	0 (0)	1 (5)	1.00	0 (0	0 (0	1.00	0 (0)	2 (11)	0.50
S3	0 (0)	1 (5)	1.00	0 (0)	1 (5)	1.00	0 (0	1 (5)	1.00	1 (5)	2 (11)	1.00
LFCN	14 (70)	9 (47)	0.13	15 (75)	10 (53)	0.29	16 (80)	8 (42)	0.02	13 (65)	9 (47)	0.22

Figures and Legends

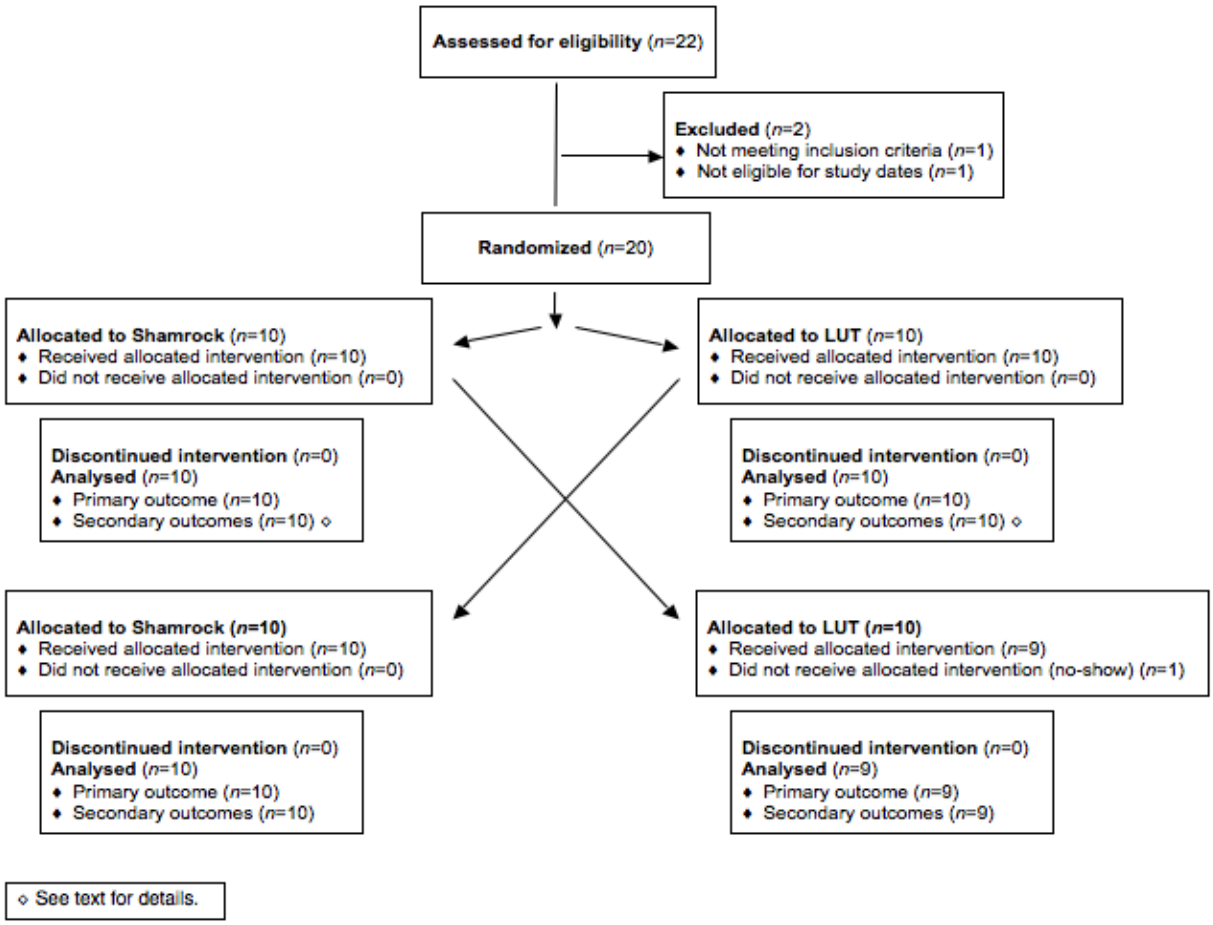

Fig 1 Modified CONSORT 2010 flow diagram of the study subjects. LUT, Lumbar Ultrasound Trident.

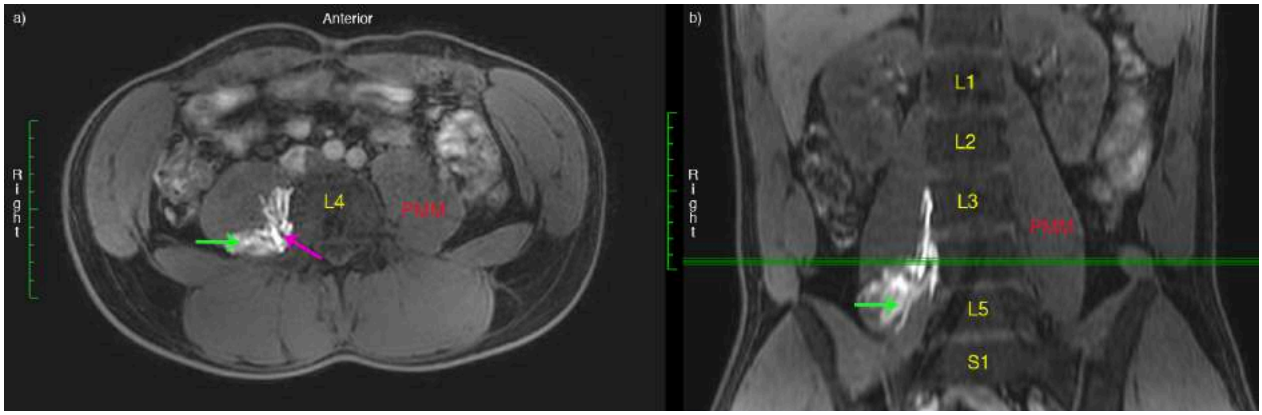

Fig 2 Spread of injectate (lidocaine-adrenaline with added contrast agent) in one subject visualised on a T1-weighted mDixon all in-phase sequence with fat suppression. The injectate (green arrow) is visualised as the bright area between the anterolateral large layer and the posteromedial small layer of the major psoas muscle (PMM), surrounding the lumbar plexus (grey-black structures within the local anaesthetic) including the femoral nerve root from spinal nerve L3 (magenta arrow). a) Axial plane b) Frontal plane: The green lines indicate the level of the axial plane. L1-S1, vertebral bodies of L1 to S1.

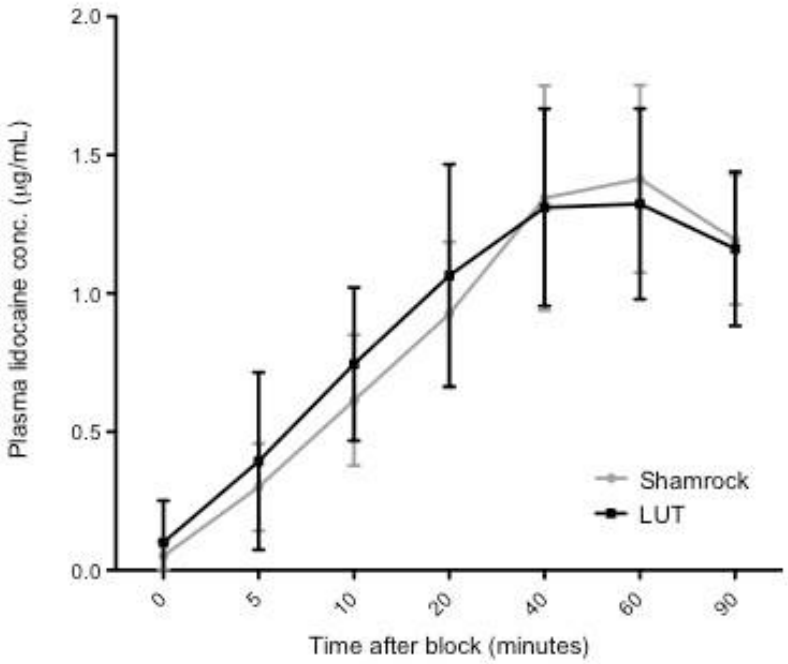

Fig 3 Plasma concentration of lidocaine 0 to 90 minutes after injection with the Shamrock vs. the Lumbar Ultrasound Trident (LUT) technique. Values are presented as mean (SD)**.**

Study II

Thomas Fichtner Bendtsen, M.D., Ph.D.
Department of Anaesthesiology and Intensive Care, Aarhus University Hospital
Nørrebrogade 44, DK-8000 Aarhus C, Denmark
Phone: +4551542997, E-mail: tfb@dadlnet.dk

Real-time Ultrasound/MRI Fusion for Suprasacral Parallel Shift Approach to Lumbosacral Plexus Blockade and Injectate Spread - an Exploratory Randomised Controlled Trial*

J. M. C. Strid,[1] E. M. Pedersen,[2] S. N. H. Al-Karradi,[3] M. A. F. Bendtsen,[4] S. Bjørn,[1,4] M. Dam,[5] M. Daugaard,[1] M. S. Hansen,[4] K. D. Linnet,[6] J. Børglum,[5] K. Søballe[7] and T. F. Bendtsen[1]

1 Department of Anaesthesiology and Intensive Care, Aarhus University Hospital, Aarhus, Denmark
2 Department of Radiology, Aarhus University Hospital, Aarhus, Denmark
3 Department of Biomedicine, Faculty of Health, Aarhus University, Aarhus, Denmark
4 Medical Science, Faculty of Health, Aarhus University, Aarhus, Denmark
5 Department of Anaesthesiology and Intensive Care Medicine, Zealand University Hospital, University of Copenhagen, Denmark
6 Department of Anaesthesiology and Intensive Care Medicine, Slagelse Hospital, Denmark
7 Department of Orthopaedic Surgery, Aarhus University Hospital, Aarhus, Denmark

Correspondence to: Dr. Thomas F. Bendtsen, Department of Anaesthesiology and Intensive Care, Aarhus University Hospital, Nørrebrogade 44, DK-8000 Aarhus, Denmark. Phone +4551542997, E-mail: tfb@dadlnet.dk

*A preliminary protocol of the study was presented at the 33rd Annual European Society of Regional Anaesthesia (ESRA) Congress 2014 in Seville, Spain, on 3-6 September 2014.

Short title: Real-time US/MRI fusion guidance of lumbosacral plexus block

Keywords (3-5): Femoral nerve block: anatomy; Nerve block landmarks; Ultrasound structures: echogenicity

Author contributions: J.M.C.S., E.M.P., and T.F.B. designed the study protocol. J.M.C.S. recruited all study subjects. J.M.C.S., S.N.H.A-K., M.A.F.B., S.B., M.D., M.D., M.S.H., K.D.L., and T.F.B. conducted the clinical trial. T.F.B. made the blinded MRI analysis. J.M.C.S. analysed all data. J.M.C.S. and T.F.B. authored the manuscript. All co-authors read and revised the manuscript and approved the final version.

Summary

Fusion of real-time ultrasound and magnetic resonance imaging (MRI) is successfully used to improve the accuracy of advanced image guided procedures especially in interventional radiology. However, its use for advanced needle guidance in regional anaesthesia is practically non-existent. The aim of this randomised controlled crossover trial is to 1) investigate efficacy and safety of real-time ultrasound/MRI fusion vs. ultrasound guidance alone applied on the Suprasacral Parallel Shift (SSPS) technique for lumbosacral plexus blockade, and 2) explore patterns of injectate spread with real-time ultrasound/MRI fusion guidance of the SSPS technique. Twenty-six healthy subjects aged 21–36 years received two SSPS blocks (20 ml 2% lidocaine-adrenaline added 1 ml diluted contrast) guided by ultrasound/MRI fusion vs. ultrasound alone. Primary outcome was block success of the femoral and obturator nerves and the lumbosacral trunk defined as a decrement in muscle force compared to baseline. Secondary outcomes were procedure-related, MRI analysed injectate spread, sensory blockade, and lidocaine pharmacokinetics. Block success was similar (ultrasound/MRI, 88%; ultrasound, 88%; $p = 1.00$). Median (IQR [range]) preparation and procedure times (s) were longer for the ultrasound/MRI fusion guided technique (686 [552–1023 (393–2501)] vs. 196 [167–228 (105–351)], $p < 0.001$ and 333 [254–439 (201–1421)] vs. 216 [176–294 (117–458)], $p = 0.001$). Both techniques produced perineural spread and corresponding sensory analgesia from L2 to S1. Epidural spread (ultrasound/MRI, 12%; ultrasound, 19%; $p = 0.73$) and lidocaine pharmacokinetics were similar. The ultrasound/MRI fusion guided SSPS technique was equally effective and safe compared to the ultrasound guided technique, but had prolonged preparation and procedure time. We identified three characteristic compartmentalised patterns of injectate spread. Based on these specific patterns we suggest a possible new anterior approach employing the desirable properties of real-time image fusion of ultrasound and MRI.

Introduction

A safe, effective and easy-to-perform peripheral nerve block technique for surgical anaesthesia of the hip and concurrent postoperative analgesia would be advantageous because many of the patients admitted for hip surgery are elderly, fragile and sometimes impaired by severe cardiovascular comorbidity. [1-3] Compared to general and spinal anaesthesia, more stable haemodynamics, fewer complications and superior postoperative pain relief are achieved with peripheral regional anaesthesia with a minimal use of opioids. [4-8]

The femoral and obturator nerves are the terminal nerves of the lumbar plexus that innervate the hip joint together with the lumbosacral trunk of the sacral plexus. All these nerves can be anaesthetised with a single injection paravertebrally between the transverse process of the fifth lumbar (L5) vertebra and the cranial margin of the sacral ala. [9-11] However, the accuracy of targeting the nerves with an ultrasound guided injection may be impaired due to the deep location of the target nerves as well as the lumbosacral bony structures generating acoustic shadows that impede the visualisation of the needle trajectory [12] – especially in old, fragile, comorbid or obese patients. [13-16] The impaired visualisation and accuracy due to the depth and bony structures near by the neuraxis may undesirably affect efficiency of the blockade and safety with epidural spread of the injectate, as well as vascular, neural, or muscular injury. [12]

The accuracy of image guided procedures may be improved by fusing real-time ultrasound with magnetic resonance imaging (MRI) thus defeating the limitations of ultrasonography as a stand alone technique. [17, 18] Furthermore, the image fusion technology includes electromagnetic needle tip tracking, which allows the operator to continuously assess the best needle insertion point, the needle trajectory, and the target of the injection.

In all practicality, a MRI dataset of the region of interest is uploaded to the ultrasound system with image fusion software. An electromagnetic field generator is placed to cover the region of interest. In the electromagnetic field, the fusion system records the three-dimensional (3D) position and orientation of sensors mounted on the ultrasound probe and the block needle in reference to a patient tracker affixed to the patient. [17, 18] The MRI dataset is spatially co-registered with real-time ultrasound using synchronisation of an internal plane and/or external or internal landmarks. The MRI is hereafter reformatted to fit

the ultrasonographic matrix and any movement of the probe results in synchronised movements of both image modalities displayed side-by-side or overlaid. [18] Any misalignment of the datasets can be manually adjusted by system built-in means of rotation and shifting. [19] When the block needle is within the electromagnetic field, a projection of its position, present and anticipated needle trajectory and the anticipated intersection between the needle and the plane of the ultrasound beam are displayed on both image modalities on the monitor.

Image fusion of real-time computer tomography (CT) or MRI has been used successfully especially in interventional radiology. [17, 18] An application of fused ultrasonography and CT or MR images of the lumbar spine for neuraxial needle guidance has been briefly described in a phantom and in volunteers, respectively, but no injections were performed. [19] In chronic pain therapy, only a few cadaver and case reports have assessed the benefit of ultrasound/CT or MRI fusion guided injections primarily of the sacroiliac joint, hand, and wrist. [20-24]

In this randomised controlled crossover trial, we aim to investigate real-time ultrasound/MRI fusion vs. ultrasound needle guidance applied on the Suprasacral Parallel Shift (SSPS) technique for lumbosacral plexus blockade. Primary outcome is block success of the femoral and obturator nerves as well as the lumbosacral trunk. Secondary outcomes are procedure-related, injectate spread analysed with MRI, sensory blockade, lidocaine pharmacokinetics, and cost-effectiveness. In addition, we aim to explore the patterns of injectate spread with the ultrasound/MRI fusion guided SSPS technique.

Methods

Ethics

The Regional Research Ethics Committee (MJ: 1-10-72-179-13), the Danish Medicines Agency (2013-004013-13), and the Danish Data Protection Agency (1-16-02-160-14) approved this randomised controlled crossover trial. The study was registered in EudraCT (2013-004013-41) and in ClinicalTrials.gov (NCT02593370), monitored by the Good Clinical Practice unit at Aalborg and Aarhus University Hospitals, and complied with the Declaration of Helsinki II. Written informed consent was obtained from all study subjects.

Recruitment

Study subjects aged ≥18 years with an ASA physical status of I were recruited through a Danish website for research volunteers. Subjects who were non-Danish speakers, unable to cooperate, had a history of allergy to local anaesthetics or MRI contrast agents, daily consumption of analgesics, abuse of medicine or alcohol, contraindication to MRI including pregnancy, infection or prior surgery of the paravertebral lumbosacral region, and/or who were legally incompetent were excluded.

The study was conducted at the Department of Radiology, Aarhus University Hospital, in Denmark during two three-day sessions with a one-week interim period in October to November 2015. The volunteers received payment for participation.

MRI for fusion with ultrasound

An experienced radiographer recorded supine MRI scans of all subjects with a 1.5T Philips Ingenia MRI scanner (Koninklijke Philips Electronics N.V., Eindhoven, Netherlands) upon arrival on the first session. The subjects were scanned with a pillow under their knees to minimise lumbar lordosis and a dS flex coverage anterior coil for signal reception. The recordings of the lumbar spine were coronal 3D T2-TSE sequences (VISTA) with an isotropic scanning resolution of 1.2x1.2x1.2 mm^3 (overlapping 2.4 mm slices, 1.2 spacing), TE 60 ms, and TR 1200 ms. A feet-head phase encoding was applied to minimise artefacts due to respiration and peristalsis. All sequences were converted to axial orientation using OsiriX v6.5.2 64-bit (Pixmeo SARL, Bernex, Switzerland) prior to upload to the ultrasound system with image fusion software (Epiq 7 1.4; Koninklijke Philips

Electronics N.V., Eindhoven, Netherlands), because the system only accepts axially orientated datasets for fusion.

Lumbosacral plexus block procedure

The subjects were monitored with three-lead ECG, non-invasive blood pressure measurement, and pulse oximetry. A peripheral intravenous access was established for blood sampling and safety.

All blocks were performed with the Epiq 7 1.4 ultrasound system. The regional anaesthetist (T.F.B.) who performed all block procedures has extensive clinical experience with ultrasound and electrical nerve stimulation guided nerve blocks and experimental experience with real-time image fusion guided lumbosacral procedures.

While performing all block procedures the field generator (Koninklijke Philips Electronics N.V., Eindhoven, Netherlands) was positioned over the lumbosacral region to generate the electromagnetic field or strengthen blinding of the subjects. After pre-scanning and any co-registration of ultrasound and MRI, the skin was swapped with chlorhexidine in isopropyl alcohol and covered with a sterile fenestrated drape. The curved array ultrasound probe (C5-1; Koninklijke Philips Electronics N.V., Eindhoven, Netherlands) with the attached sensor was draped with a sterile cover. The skin and the subcutaneous tissue were infiltrated with 2 mL 2% lidocaine prior to insertion of a 22 Gauge, 100 mm nerve block needle (Stimuplex Ultra; B. Braun, Melsungen, Germany).

The injectate of each nerve block was 20 ml 2% lidocaine-adrenaline added 1 ml diluted MRI contrast (0.13 ml 27.9% gadoterate meglumine [Dotarem®; Guerbet, Roissy CdG Cedex, France] and 0.87 ml 0.9% isotonic saline).

Ultrasound/MRI fusion guided SSPS: The patient tracker was affixed to the iliac crest with adhesive tape on the side to be anaesthetised. The initial co-registration was conducted with the subject supine. The probe was oriented axially on the abdomen. The axial plane immediately caudad to the aortic bifurcation and an identical reference point in the plane at the bifurcation of the common iliac arteries were selected for co-registration of the real-time ultrasound and the MRI dataset. The overlaid ultrasound and MR images were aligned using the iliac arteries, the aortic bifurcation, and the anterior margin of the lumbar vertebral body at the same level. Subsequently, the subject was turned to the lateral

decubitus position with the side to be anaesthetised facing upwards. The alignment of the ultrasound and MR images was fine adjusted as good as possible for the position change using the borders of the L5 transverse process and vertebral body as well as the positions of the psoas major, quadratus lumborum, and erector spinae muscles. Hereafter, the ultrasound and MRI were displayed side-by-side. The probe was placed in the sagittal plane on the iliac crest and parallel shifted medially until the interspace (osteofibrotic tunnel) between the transverse process of L5 and the cranial margin of the sacral ala was visualised on both images. Based on ultrasound/MR visualisation of the intertransverse ligament (posteriorly) and the lumbosacral ligament (anteriorly) – marking out the osteofibrotic tunnel – the tip of the block needle with mounted sensor was placed in the anticipated position for needle insertion caudad to the intercristal line. Using needle navigation, the position and angle of insertion were adjusted until the anticipated intersection of the needle tip and the ultrasound beam coincided with the target psoas compartment (i.e. the subcompartment posterior to the psoas major muscle at the level of the osteofibrotic tunnel [9]) displayed on the MRI image (Fig. 1). Guided by real-time ultrasound/MRI fusion and needle navigation, the needle was advanced until a “loss of resistance” confirmed the visualised penetration through the lumbosacral ligament and the needle tip positioned anterior to the ligament inside the retro-psoas subcompartment on MRI.

Ultrasound guided SSPS: This technique has been described in detail previously. [12] The endpoint of injection was “loss of resistance” confirming the needle penetration of the lumbosacral ligament (sonographically visualised if possible).

An electrical nerve stimulator (0.1 ms, 2 Hz, 0.2 mA) was connected to the block needle during both procedures as a safety device in order to decrease the risk of intraneural injection of local anaesthetics. Prior to injection, any response to electrical nerve stimulation with 0.3 to 0.5 mA was registered, [25] but was not used for target nerve location. The local anaesthetic with contrast was injected with intermittent aspiration. Time zero (T_0) min was the time of withdrawal of the block needle from the skin after completed injection. All subjects were followed up until T_{90} for data sampling and were observed for adverse effects until the sensorimotor blockade had worn off.

Outcomes and assessment

The primary outcome was success of motor blockade of the femoral and obturator nerves and the lumbosacral trunk defined as a reduction of baseline muscle force (N) of the knee extensors, hip adductors, and hip abductors, respectively, at T_{40}. Muscle force was estimated in the supine position with a dynamometer (Commander Muscle Testing; JTECH Medical, Midvale, USA) maintained immobile by a steady grip of an observer. The observer instructed the subject to exert maximal pressure against the dynamometer during knee extension (with 90° flexion of the hip and knee joints), hip adduction (with the lower limb extended and 45° abducted), and hip abduction (with extended lower limb). The highest value of three tests with 20 s intermittent intervals was recorded for each motion. As exploratory analysis, the values for muscle force and motor blockade of the separate nerves are reported.

The secondary outcomes were: a) preparation time (s) from positioning of the subject on the bed until end of pre-scanning and co-registration, if any; b) block procedure time (s) from placement of the probe on the skin until withdrawal of the block needle after completed injection; c) number of needle insertions defined as each withdrawal of the needle followed by an advancement regardless the number of skin penetrations; d) needle insertion point defined as the horizontal distance (cm) from the sagittal midline to the skin penetration; e) depth of needle tip gauged by reading the distance (cm) marked on the needle shaft at the endpoint of the injection; f) minimal electrical nerve stimulation (mA) required to trigger any sensorimotor response immediately prior to injection; g) type of response to electrical nerve stimulation (“Quadriceps”, “Adductor”, “Other motor”, “Paraesthesia”, “None”); h) maximum procedural discomfort assessed by the subject with NRS score 0-10 (0 = ”no discomfort”, 10 = ”worst possible discomfort”) at T_0; i) change in mean arterial blood pressure (ΔMAP) from baseline to T_5; j) perineural spread of injectate; k) compartmental spread of injectate; l) epidural spread of injectate; m) sensory blockade; n) maximum p-lidocaine (C_{max}); o) time to C_{max} (T_{omc}); p) p-lidocaine concentration-time area under the curve; and q) cost-effectiveness.

Injectate spread was analysed on axial 3D T1-weighted MRI sequences (mDixonAll generating in-phase, out-of-phase, water, fat, and diffusion weighted images) sampled with a Philips Achieva 3.0T dstream scanner (Koninklijke Philips Electronics, Eindhoven,

Netherlands) at T_{15}. Perineural spread was assessed for the anterior rami of spinal nerves L2 to S1 and for the femoral, obturator, and lateral femoral cutaneous nerves, and the lumbosacral trunk in their intra- or extra psoas major trajectories. Perineural spread was considered “present” when direct contact was visualised between the injectate and the target nerve. The MRI scans were also analysed for patterns of confinement of injectate inside fascial compartments and associated spread of injectate around compartment-specific nerves. Epidural spread was considered “present” when there was circumferential epidural distribution of the injectate on any axial MRI level and concomitant bilateral blockade of cold in at least one pair of dermatomes.

Sensory blockade of cold, warmth, touch, and pain of the dermatomes Th12-S3 [26] and the skin innervated by the lateral femoral cutaneous nerve was tested with standardised stimuli (40° and 25° thermo test [Rolltemp II; Somedic, Hörby, Sweden], brush [SENSELab^{TM} Brush-05; Somedic AB, Hörby, Sweden], and punctuated pin prick [PinPrick 512 mN; MRC Systems GmbH, Heidelberg, Germany]) at T_{50}. Sensation for each stimulus was assessed as “present” or “reduced/absent” where “reduced/absent” was considered a successful blockade. The dermatomes Th12, L1, S2, and S3 were included in order to assess the effect of any epidural spread.

For the analysis of p-lidocaine, blood samples were collected at $T_{0,\ 5,\ 10,\ 20,\ 40,\ 60,\ \text{and}\ 90}$ and centrifuged at 1,800 G for 9 min. The plasma was transferred to 1.5 mL cryotubes and stored at -80°C until analysis with liquid chromatography tandem mass spectrometry. [27]

The difference in mean marginal cost of the interventions was calculated as a measure of cost-effectiveness (extra price per patient). [28] Unit costs were collected in Danish Kroner (DKK) in July 2016 and converted into GBP (euros/US dollars) in October 2016 (100 DKK = £12.08 [€13.44/$14.86]). Average annual total wages were used to calculate unit costs for medical staff corresponding to the difference in preparation and block procedure time used by an anaesthesiologist and an assistant nurse and in time used by the radiographer for preparations and sampling of the MRI VISTA scan for the fusion guided procedure (20 min). Because of the complexity of calculating the expense for the 1.5 T MRI scanner use, this cost is given as a time unit.

Randomisation and blinding

J.M.C.S. enrolled all subjects. Two study-independent assistants randomly assigned 26 consecutive subject identification numbers to sequences of interventions (Ultrasound/MRI fusion guided SSPS on day one and ultrasound guided SSPS on day two or vice versa) and side (right on day one and left on day two or vice versa). Twenty-six sheets with the sequences pre-printed were put in 26 identical opaque and sealed envelopes marked 1 to 26. T.F.B. and S.B. double-checked the intervention assignment immediately prior to each procedure without revealing the allocation to others. The sheet was re-enveloped and resealed. The procedure was repeated prior to the second intervention.

All sampling and analyses of data were blinded to the intervention. All interventions were performed with identical trial setup and equipment in order to blind the subjects. The MRI records of injectate spread were anonymised by a radiographer and analysed in a random order by T.F.B.

Statistics

The primary outcome was block success of the femoral and obturator nerves and the lumbosacral trunk. We hypothesised an increase in block success from 75% with ultrasound guidance to 100% with ultrasound/MRI fusion guidance. Detection of a 25% increase with 80% power ($1-\beta$) and $\alpha=0.05$ would require a sample size of 24 subjects in a two-sided crossover analysis. [29] To avoid decreased power due to dropouts, we included 26 subjects.

Statistics were analysed with Stata IC 14 (StataCorp LP, College Station, USA). Normality of distribution was assessed visually with the normal Q-Q-plot. Normally distributed differences between paired continuous variables were analysed with one-sample Student t-test. Non-normally distributed differences between paired continuous variables and differences between paired ordinal variables were analysed with Wilcoxon matched-pairs signed rank test. Differences between paired categorical variables were analysed with McNemar's test. The level of significance was 0.05. Data are presented as mean (SD) for continuous variables with normal distribution, as median (IQR [range]) for continuous variables with non-normal distribution and ordinal variables, and as number (proportion) for categorical variables.

Results

Twenty-six subjects (14/26 [54%] males) were enrolled during October 3 to 24, 2015 (Fig. 2). Twenty-five subjects completed both interventions and follow-up per protocol. One ultrasound guided SSPS intervention was aborted due to aspiration of blood, but the subject completed the follow-up and contributed with his data per protocol.

The median (IQR [range]) age for all 26 subjects was 22.0 (22.0–24.0 [21.0–36.0]) years, mean (SD) weight was 73.2 (11.7) kg, mean (SD) height was 178 (8.1) cm, and mean (SD) BMI was 23.4 (2.7) $kg.m^{-2}$.

Appendix 1 displays values for block success and motor blockade of the separate nerves. Appendix 2 displays values for base line and post-block muscle force. Appendix 3 displays values for the procedure-related outcomes. There was no evidence for any difference between the techniques except for median (IQR [range]) preparation time (ultrasound/MRI, 686 [552–1023 (393–2501)] s; ultrasound, 196 [167–228 (105–351)] s; $p < 0.001$) and block procedure time (ultrasound/MRI, 333 [254–439 (201–1421)] s; ultrasound, 216 [176–294 (117–458)] s; $p = 0.001$).

Three characteristic patterns of injectate spread were identified in the study subjects. Fig. 3, 4, and 5 are of three different subjects illustrating these patterns.

Appendix 4 displays values for perineural spread. Appendix 5 displays values for sensory blockade. There was no evidence for any difference between the techniques.

Epidural spread was recorded in 3/26 (12%) and 5/26 (19%) of subjects subjected to ultrasound/MRI fusion and ultrasound guided SSPS block ($p = 0.73$), respectively. The sensory effect was observed in the dermatomes L1 to S3 with individual variation.

Appendix 6 illustrates the mean (SD) C_{max} of p-lidocaine. There was no evidence for any difference in mean (SD) C_{max}, median (IQR [range]) T_{omc}, or mean (SD) concentration-time area under the curve (Appendix 6). [30] One subject in the ultrasound group was excluded from the analysis due to insufficient blood sampling.

The mean marginal cost of a SSPS block was Δ£22.91 (€23.60/$28.19) and 6 min and 34 s in the 1.5 T MRI scanner for the ultrasound/MRI fusion guided procedure compared to the ultrasound guided.

Safety and harm

No serious adverse events were observed.

One subject experienced a transitory hot flush starting prior to the intervention due to vasovagal needle phobia. Four subjects had two incidents of vasovagal syncope and three incidents of dizziness; two were related to reinsertion of an intravenous catheter or blood sampling during the follow-up and one was related to previously diagnosed orthostatic hypotension.

Discussion

This is the first randomised controlled trial investigating ultrasound/MRI fusion guided lumbosacral plexus blockade. We found that the ultrasound/MRI fusion guided technique was equally effective and safe, but required longer preparation and block procedure time compared to the ultrasound guided technique.

The initial hypothesis of higher block success with ultrasound/MRI fusion guidance compared to ultrasound was falsified. This may be explained by the demographics of the study subjects; i.e. the target clinical group would be elderly and fragile patients in whom the ultrasonoanatomical image quality may be impaired. In such patients, it can be speculated that the additional visualisation and needle navigation with ultrasound/MRI fusion might improve the efficiency of needle guidance. In young volunteers, however, adequate ultrasonographic quality is achieved with a higher frequency thus making the MRI scan, real-time image fusion and needle navigation redundant. Nonetheless, we chose to assess the fusion guided technique in healthy volunteers instead of a clinical patient trial because only lumbar ultrasound/MRI fusion – without fusion guided lumbar needle insertions – has been explored in phantoms and volunteers previously. [19] Furthermore, the subjects were positioned supine during the MRI sampling because this is technically and clinically most optimal, but the real-time fusion guided procedure was performed in the lateral decubitus position. Dissimilar positioning, movement, respiration as well as peristalsis during the sampling, co-registration and alignment of MRI and ultrasound may deform the topography and dimensional stability of the anatomical structures under study, which in turn may affect the accuracy of the ultrasound/MRI fusion guided injection. [18, 21] Although any misalignment can be manually adjusted and a pilot study revealed no evidence that the target nerves – situated paravertebral to the rigid lumbar spine – moved significantly during change from supine to lateral decubitus position, we cannot entirely rule out such an effect.

The prolonged total procedure time for the ultrasound/MRI fusion guided technique is in keeping with previous studies concerning real-time fusion, and is explained by the extra time used on co-registration and alignment of the datasets and on needle navigation. [17] The lower mean marginal cost for the ultrasound guided technique reflects this time difference as well as the cost of the MRI system and its operation by authorised personnel.

Notably, both success rate and procedure time of a new technique follow a learning curve and technical perfection requires practice. [17]

Few previous studies have compared ultrasonography and MRI of the lumbosacral anatomy [31] and analysed injectate spread with MRI. [12, 32] The sensory mapping demonstrated segmental anaesthesia from L2 to S1 in accordance with the perineural spread analysed on MRI. A cadaver study on lumbosacral plexus blockade guided by anatomical landmarks showed weak staining of spinal nerve S1 in only 3/20 (15%) cadavers. [10] Our study demonstrates that an injection – guided by ultrasound/MRI fusion or ultrasound – at the neuraxial level of L5/S1 may indeed block the cranial part (the lumbosacral trunk from anterior rami of spinal nerves L4 and L5) of the sacral plexus. However, the sensory mapping of dermatomes should be interpreted with caution as it may be unreliable due to anatomical variation and overlapping of innervation of adjacent cutaneous segments and terminal nerves territories. [33] We used motor blockade as a proxy marker of sensory blockade, but the definition of motor blockade does not take account for bi- and triple nerve innervation of specific muscle groups or measurement error of the method to estimate muscle force. However, knowledge concerning the correlation between reduced muscle force in healthy volunteers and sufficient motor blockade in clinical patients is lacking, indicating that any definition of successful motor blockade in healthy volunteers is arbitrary. The values of block success should therefore be considered as a measure of comparison of the techniques – not as a clinically applicable measure. Due to the uncertainty of sensorimotor mapping and assessment of block success in healthy subjects, where the clinical criteria for a successful blockade does not apply and the interpretation of the blockade is subjective, we recommend inclusion of an objective analysis such as MRI of injectate spread when validating techniques in healthy subjects.

No dose-finding studies have been conducted for the SSPS technique, but the minimal effective anaesthetic volume of 0.5% ropivacaine to accomplish a successful lumbar plexus blockade with the Shamrock technique in 95% of patients (ED_{95}) is 36.0 ml (95% CI 19.7 to 52.2). [34] Since the aim of the current study was to compare two techniques in a standardised setting and the subjects were discharged on the day of the intervention, we chose a comparatively low dose of 20 ml 2% lidocaine-adrenaline, corresponding

approximately to the ED_{50} of 0.5% ropivacaine [34] and allowing fast discharge of the volunteers. The mean C_{max} was similar for the techniques and showed a peak C_{max} approximately one hour after injection, which is in accordance with previous studies investigating plasma concentration of local anaesthetics in regional anaesthesia. [12, 35] However, injection of more clinical relevant local anaesthetic volumes in excess of 20 ml lidocaine-adrenaline would result in an increased C_{max}. Also, pharmacokinetics of local anaesthetic changes with age, and the results might therefore not be directly applicable in elderly patients. [36]

Apart from the external limitations discussed above, the expert anaesthesiologist performing all blocks could not be blinded – as is the case with all procedure related studies. We endeavoured to limit this source of bias by adhering to a strict double-controlled protocol.

The additional aim of this study was to explore the patterns of injectate spread because inclusion of high-resolution MRI for fusion with ultrasound and analysis of injectate spread offers the potential of improved understanding of the (ultrasonographic) anatomy without limitations due to acoustic artefacts and depth. [24] This additional knowledge can be applied to revise existing and to develop new ultrasound guided regional anaesthetic techniques. Fig. 3, 4 and 5 show three characteristic patterns of injectate spread in three different fascial compartments observed in this study.

The first compartment is medial to the psoas major muscle (Fig. 3). It extends from the level of the neural foramen of vertebra L4 cranially to the neural foramen of S1 caudally and contains the anterior rami of spinal nerves L4 and L5, the lumbosacral trunk and the obturator nerve. We call it the *para-psoas (PPC) compartment*, since it is medial to the iliopsoas compartment. The iliopsoas compartment is the space posterior to the retroperitoneal space that contains the iliacus, psoas major and psoas minor muscles as well as the lumbar plexus. [37] The iliopsoas compartment is bounded by the iliopsoas fascia from the medial arcuate ligament to the minor trochanter. Cranial to the transverse process of vertebra L5 and the iliolumbar ligament the iliopsoas compartment is bounded medially by the lateral sides of the lumbar vertebral bodies and the intervertebral discs; posteriorly it is bounded by the lumbar transverse processes, the intertransversaria ligaments and muscles as well as the most medial part of the quadratus lumborum muscle.

The psoas major muscle is tightly adherent to the posteromedial wall cranial to the transverse process of vertebra L5. The iliopsoas fascia is continuous with the transversalis fascia laterally, where it is tied down to the lumbar transverse processes by a connective tissue band that separates the iliopsoas compartment from the quadratus lumborum compartment. Caudal to the transverse process of vertebra L5, the psoas major muscle deviates anterolaterally away from the neuraxis and become fused with the iliacus muscle as the iliopsoas muscle. At this level, the iliopsoas compartment is bounded medially by the iliopsoas fascia that is tied down to the sacral ala and separates the iliopsoas compartment from the PPC (Fig. 3).

The second compartment is a triangular groove between the psoas major and iliacus muscles (Fig. 4). It extends from the transverse process of vertebra L5 and the iliolumbar ligament cranially, and caudally between the psoas major and iliac muscles until they become fused as the iliopsoas muscle. Medially the compartment is bounded by the iliopsoas fascia, which separates it from the PPC. Laterally the compartment is also bounded by the iliopsoas fascia, where it covers the groove between the psoas major and iliacus muscles. This compartment was called the *Psoas compartment* by Chayen et al. in the original description of the psoas compartment block in 1976.[9] However, as it is a subcompartment of the iliopsoas compartment, it may be more accurate to call it the *retro-psoas subcompartment (RPSC).* The RPSC contains the femoral and lateral femoral cutaneous nerves, as they emerge from the postero-lateral border of the psoas major muscle caudal to the level of the iliac crest.

The third compartment is lateral to the iliopsoas compartment (Fig. 5). It is the retroperitoneal fat-pad compartment between the peritoneum and the transversalis fascia. This compartment contains none of the major terminal lumbar plexus nerves. The transversalis fascia is tightly adherent to the iliac crest.

The observed patterns of spread imply that local anaesthetic has to be injected into the PPC as well as the RPSC for sufficient spread to all target nerves relevant for anesthesia of the hip joint with a high success rate. However, the ultrasonographic visualisation of the PPC and RPSC is impeded by bony structures when the SSPS technique is employed. Sampling the MRI and real-time ultrasound in different positions (supine and lateral decubitus) may also reduce the accuracy of the ultrasound/MRI fusion guided technique.

Co-registration and alignment of ultrasound and MRI in two positions is also relatively time-consuming. Additionally, gravity may facilitate medial spread of the local anaesthetic through the osteofibrotic tunnel to the epidural space in the lateral decubitus position with the side to be anaesthetised facing upwards. [38] A supine position might decrease this risk. The ideal technique would therefore provide good visualisation of the PPC and RPSC in the supine position with real-time ultrasound/MRI fusion as well as ultrasound alone. Ideally, it should be based on a safe, efficient and easy needle path from skin surface to the target nerves inside the PPC as well as the RPSC compartment. Fig. 6 illustrates a theoretical anterior needle trajectory to the lumbosacral plexus in the supine position devised based on our analysis of the MRI scans in this trial. This speculative needle trajectory is probably ideal for real-time ultrasound/MRI fusion needle guidance. Fig. 7 illustrates the suggested approach guided by ultrasound/MRI fusion in a future experimental trial.

Fusion of real-time ultrasound and MRI for needle guidance in the lumbar region is an evolving technique and is proven to be neither more inaccurate nor unsafe compared to the ultrasound guided technique. Future studies of real-time ultrasound/MRI needle guidance may include automatic co-registration based on image recognition or external fiducials compatible with MRI, or techniques that minimise the effect of position change thereby improving the accuracy, time-efficiency and ease-of-performance of real-time fusion. Further research is needed to clarify which regional anaesthetic technique is best for hip anaesthesia and analgesia.

In summary, the ultrasound/MRI fusion guided SSPS technique required longer preparation and block procedure time and was neither more effective nor safer compared to the ultrasound guided SSPS technique. Ultrasound/MRI fusion may have the potential of improving ultrasound guided regional anaesthesia and analgesia. Our exploratory study identified that the retro-psoas subcompartment (RPSC) is exclusively inside the iliopsoas compartment and contains only the terminal femoral and lateral femoral cutaneous nerves. The iliopsoas fascia separates the RPSC from the para-psoas compartment (PPC) as well as from the retroperitoneal space. The PPC contains the obturator nerve, the anterior rami of the L4, L5 and S1 spinal nerves as well as the lumbosacral trunk. Based on our findings

we have suggested a new theoretical anterior approach in the supine patient to block the lumbosacral nerves innervating the hip joint.

Acknowledgements

The A.P. Møller and Chastine Mc-Kinney Møller Foundation for General Purposes supported this study. The content is solely the responsibility of the authors. The study was registered in EudraCT (2013-004013-41) and in ClinicalTrials.gov (NCT02593370).

Competing Interests

No competing interests to declare.

Appendices

Appendix 1 Success of motor blockade of the femoral and obturator nerves, the lumbosacral trunk, and combinations hereof for ultrasound/MR fusion guided vs. ultrasound guided lumbosacral plexus blockade with the Suprasacral Parallel Shift technique. Values are presented as number (proportion).

	US/MRI* ***(n=26)***	**US†** ***(n=26)***	**p**
Femoral nerve	25 (96%)	24 (92%)	1.00
Obturator nerve	25 (96%)	24 (92%)	1.00
Lumbosacral trunk	24 (92%)	24 (92%)	1.00
Combinations			
Femoral + obturator	24 (92%)	23 (88%)	1.00
Femoral + obturator + lumbosacral trunk	23 (88%)	23 (88%)	1.00

* MRI; magnetic resonance imaging

† US; ultrasound

Appendix 2 Baseline and post-block muscle force of the femoral, obturator, and the lumbosacral trunk for ultrasound/MRI fusion guided vs. ultrasound guided lumbosacral plexus blockade with the Suprasacral Parallel Shift technique. Values are displayed as median (IQR [range]) or mean (SD).

	US/MRI* ***(n=26)***	**US†** ***(n=26)***	**p**
Femoral nerve (knee extension)			
Baseline muscle force; N	244 (204–266 [176–343])	229 (215–253 [136–374])	
Post-block muscle force; N	75 (0–121 [0–244])	72 (0–134 [0–255])	0.73
Difference; N	-151 (78)	-141 (81)	
p	< 0.001	< 0.001	
Muscle force in % of baseline; %	29 (0–48 [0–100)	35 (0–57 [0–113)	
Obturator nerve (hip adduction)			
Baseline muscle force; N	138 (114–176 [105–255])	134 (114–176 [101–237])	
Post-block muscle force; N	0 (0–70 [0–149])	0 (0–31 [0–209])	0.43
Difference; N	-110 (56)	-119 (63)	
p	< 0.001	< 0.001	
Muscle force in % of baseline; %	0 (0–45 [0–100])	0 (0–19 [0–187])	
Lumbosacral trunk (hip abduction)			
Baseline muscle force; N	147 (114–160 [79–204])	144 (114–167 [79–233])	
Post-block muscle force; N	79 (35–105 [0–173])	54 (41–79 [0–169])	0.27
Difference; N	-65 (47)	-81 (55)	
p	< 0.001	< 0.001	
Muscle force in % of baseline; %	58 (30–78 [0–101]	47 (24–60 [0–139])	

***** MRI; magnetic resonance imaging

† US; ultrasound

Appendix 3 Procedure-related outcomes for ultrasound/MRI fusion guided vs. ultrasound guided lumbosacral plexus blockade with the Suprasacral Parallel Shift technique. Values are displayed as median (IQR [range]) or number (proportion).

	US*/MRI† ***(n=26)***	**US** ***(n=26)***	**p**
Preparation time; s	686 (552–1023 [393–2501)	196 (167–228 [105–351])	< 0.001
Block procedure time; s	333 (254–439 [201–1421])	216 (176–294 [117–458])	0.001
Number of needle insertions	4.5 (3.0–7.0 [2.0–24.0])	5.0 (3.0–7.0 [2.0–15.0])	0.87
Needle insertion point from midline; cm	4.0 (4.0–5.0 [2.0–6.0])	6.0 (5.0–6.0 [4.0–8.0])	< 0.001
Needle depth; cm	8.0 (7.0–9.0 [5.0–10.0])	8.0 (7.0–8.5 [4.0–10.0])	0.37
Minimal nerve stimulation; mA	0.50 (0.50–0.50 [0.20–0.60])	0.50 (0.40–0.50 [0.30–0.50])	0.075
Electrical nerve stimulation response			0.37
1 Quadriceps femoris	4 (15%)	4 (15%)	1.00
2 Adductor	0 (0%)	1 (4%)	1.00
3 Other motor	0 (0%)	0 (0%)	1.00
4 Paresthesia	2 (8%)	0 (0%)	0.50
0 None	20 (77%)	21 (81%)	1.00
Procedural discomfort; NRS 0-10‡	2 (1–3 [0–7])	3 (2–4 [0–5])	0.036
ΔMAP; mmHg§	0.23 (12.77)	-4.50 (10.44)	0.070

***** US; ultrasound

† MRI; magnetic resonance imaging

‡ NRS, numeric rating scale

§ ΔMAP; change in mean arterial pressure from baseline to 5 min after completed injection of local anaesthetic

Appendix 4 Injectate spread to the anterior rami of spinal nerves L2 to S1, the femoral, obturator, and lateral femoral cutaneous nerves, and the lumbosacral trunk for ultrasound/MRI fusion vs. ultrasound guided lumbosacral plexus blockade with the Suprasacral Parallel Shift technique. Values are presented as number (proportion).

	US†/MRI* ***(n=26)***	**US** ***(n=26)***	**p**
Anterior ramus of spinal nerve L2	14/26 (54%)	11/26 (42%)	0.58
Anterior ramus of spinal nerve L3	21/26 (81%)	21/26 (81%)	1.00
Anterior ramus of spinal nerve L4	22/26 (85%)	25/26 (96%)	0.38
Anterior ramus of spinal nerve L5	10/26 (38%)	18/26 (69%)	0.057
Anterior ramus of spinal nerve S1	5/26 (19%)	8/26 (31%)	0.55
Femoral nerve	16/26 (62%)	13/26 (50%)	0.61
Obturator nerve	14/26 (73%)	11/26 (85%)	0.58
Lateral femoral cutaneous nerve	16/26 (62%)	11/26 (42%)	0.58
Lumbosacral trunk	10/26 (38%)	15/26 (58%)	0.58

***** US; ultrasound

† MRI; magnetic resonance imaging

Appendix 5 Block of somatosensation of the dermatomes Th12-S3 and of the skin area innervated by the lateral femoral cutaneus nerve after ultrasound/MRI fusion guided (*n=26*) vs. ultrasound guided (*n=26*) lumbosacral plexus blockade with the Suprasacral Parallel Shift technique. Values are presented as number (proportion).

	Cold			Warmth			Touch			Pain		
	US*/MRI†	**US**	**p**	**US/MRI**	**US**	**p**	**US/MRI**	**US**	**p**	**US/MRI**	**US**	**p**
Th12	2 (8%)	0 (0%)	0.50	1 (4%)	1 (4%)	1.00	4 (15%)	1 (4%)	0.38	7 (8%)	2 (8%)	1.00
L1	4 (15%)	3 (12%)	1.00	2 (12%)	4 (15%)	1.00	9 (35%)	6 (23%)	0.55	7 (27%)	4 (15%)	0.51
L2	8 (31%)	10 (38%)	0.79	9 (35%)	10 (38%)	1.00	9 (35%)	11 (42%)	0.80	12 (46%)	11 (42%)	1.00
L3	18 (69%)	16 (62%)	0.75	13 (50%)	16 (42%)	0.58	7 (27%)	9 (35%)	0.75	15 (58%)	9 (35%)	0.18
L4	18 (69%)	15 (58%)	0.61	17 (65%)	14 (54%)	0.61	13 (50%)	13 (50%)	1.00	13 (50%)	14 (54%)	1.00
L5	10 (38%)	11 (42%)	1.00	9 (35%)	12 (46%)	0.55	8 (31%)	10 (38%)	0.75	8 (31%)	10 (38%)	0.75
S1	16 (62%)	14 (54%)	0.63	16 (52%)	18 (69%)	0.69	3 (12%)	10 (38%)	0.016	8 (31%)	12 (46%)	0.39
S2	5 (19%)	7 (27%)	0.75	7 (27%)	10 (38%)	0.55	8 (31%)	7 (27%)	1.00	7 (27%)	6 (23%)	1.00
S3	5 (19%)	8 (27%)	0.75	5 (19%)	7 (27%)	0.75	7 (27%)	9 (25%)	0.77	7 (27%)	8 (31%)	1.00
LFCN‡	13 (50%)	9 (35%)	0.39	14 (54%)	10 (38%)	0.34	16 (62%)	10 (38%)	0.18	17 (65%)	10 (38%)	0.092

***** US; ultrasound

† MRI; magnetic resonance imaging

‡ LFCN, lateral femoral cutaneous nerve

Appendix 6 Plasma concentration of lidocaine 0 to 90 min after injection with the ultrasound/MRI fusion guided (US/MRI) vs. the ultrasound guided (US) Suprasacral Parallel Shift technique for lumbosacral plexus blockade (*n=25*). Values are presented as mean (SD).

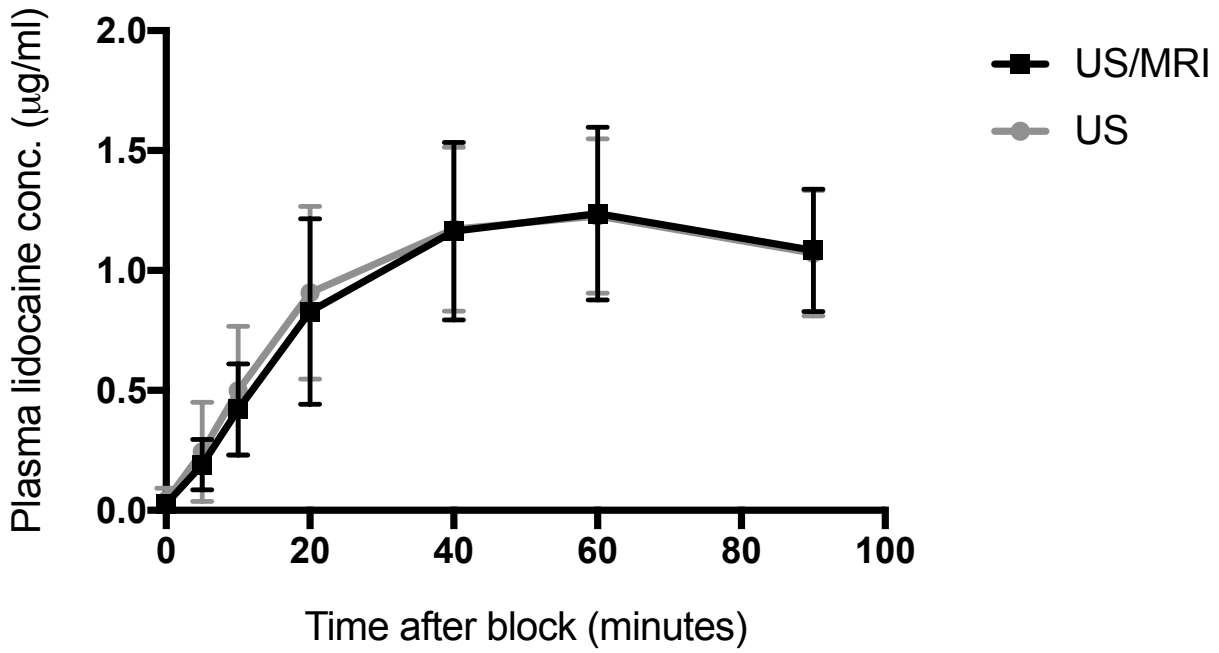

References

1. CDS/NCHS National Hospital Discharge Survey, 2010. Number of all-listed procedures for discharge from short-term hospitals, by procedure category and age: United States, 2010. www.cdc.gov/nchs/data/nhds/4procedures/2010pro4_numberprocedureage.pdf. (accessed 21/10/2016).

2. de Luise C, Brimacombe M, Pedersen L, Sørensen HT. Comorbidity and mortality following hip fracture: A population-based cohort study. *Aging Clinical Experimental Research* 2008; **20**: 412-8.

3. Chidambaram R, Cobb AG. Change in the age distribution of patients undergoing primary hip and knee replacements over 13 years – an increase in the number of younger men having hip surgery. *Orthopaedic Proceedings* 2009; **91-B**: 152.

4. de Visme V, Picart F, Le Jouan R, Legrand A, Savry C, Morin V. Combined lumbar and sacral plexus block compared with plain bupivacaine spinal anesthesia for hip fractures in the elderly. *Regional Anesthesia and Pain Medicine* 2000; **25**: 158-62.

5. Bendtsen TF, Haskins S, Kølsen Petersen JA, Børglum J. Do ultrasound-guided regional blocks signify a new paradigm in high-risk patients? *Best Practice & Research. Clinical Anaesthesiology* 2016; **30**: 191-200.

6. Gottschalk A, Van Aken H, Zenz M, Standl T. Is anesthesia dangerous? *Deutsches Ärzteblatt International* 2011; **108**: 469-74.

7. Memtsoudis SG, Rasul R, Suzuki S, et al. Does the impact of the type of anesthesia on outcomes differ by patient age and comorbidity burden? *Regional Anesthesia and Pain Medicine* 2014; **39**: 112-9.

8. Whiting PS, Molina CS, Greenberg SE, Thakore RV, Obremskey WT, Sethi MK. Regional anaesthesia for hip fracture surgery is associated with significantly more peri-operative complications compared with general anaesthesia. *International Orthopaedics* 2015; **39**: 1321-7.

9. Chayen D, Nathan H, Chayen M. The psoas compartment block. *Anesthesiology* 1976; **45**: 95-9.

10. Huntoon MA, Yeasting A. Analysis of contrast spread of a modified posterior approach to lumbosacral plexus blockade in a cadaver model. *Regional Anesthesia and Pain*

Medicine 1998; **23**: 16.
11. Bendtsen TF, Søballe K, Petersen EM, et al. Ultrasound guided single injection lumbosacral plexus blockade for hip surgery anaesthesia. *British Journal of Anaesthesia* E-letter published 15/04/2013. bja.oxfordjournals.org/forum/topic/brjana_el%3b9982 (accessed 21/10/2016).
12. Bendtsen TF, Pedersen EM, Haroutounian S, et al. The suprasacral parallel shift vs lumbar plexus blockade with ultrasound guidance in healthy volunteers – a randomised controlled trial. *Anaesthesia* 2014; **69**: 1227-40.
13. Amonoo-Kuofi HS. Changes in the lumbosacral angle, sacral inclination and the curvature of the lumbar spine during aging. *Acta Anatomica* 1992; **145**: 373-7.
14. Shao Z, Rompe G, Schiltenwolf M. Radiographic changes in the lumbar intervertebral discs and lumbar vertebrae with age. *Spine* 2002; **27**: 263-8.
15. Sevinc O, Barut C, Is M, Eryoruk N, Safak AA. Influence of age and sex on lumbar vertebral morphometry determined using sagittal magnetic resonance imaging. *Annals of Anatomy* 2008; **190**: 277-83.
16. Kirchmair L, Entner T, Wissel J, Moriggl B, Kapral S, Mitterschiffthaler G. A study of the paravertebral anatomy for ultrasound-guided posterior lumbar plexus block. *Anesthesia and Analgesia* 2001; **93**: 477-81, 4th contents page.
17. Zacchino M, Calliada F. Ultrasound image fusion: a new strategy to reduce x-ray exposure during image guided pain therapies. In: Nenoi M, ed. *Current topics in ionizing radiation research.* Rijeka: InTech, 2012: 395-406.
18. Ewertsen C, Săftoiu A, Gruionu LG, Karstrup S, Nielsen MB. Real-time image fusion involving diagnostic ultrasound. *American Journal of Roentgenology* 2013; **200**: W249-55.
19. Kwok WH, Karmakar MK. Fusion imaging: Ultrasound and CT or ultrasound and MRI image fusion for spinal sonography - preliminary experience. In: Karmakar MK, ed. *Musculoskeletal ultrasound for regional anaesthesia and pain medicine.* Hong Kong: Department of Anaesthesia and Intensive Care, The Chinese University of Hong Kong; 2016: 503-8.
20. Klauser AS, De Zordo T, Feuchtner GM, et al. Fusion of real-time US with CT images to guide sacroiliac joint injection in vitro and in vivo. *Radiology* 2010; **256**: 547-53.
21. Zacchino M, Almolla J, Canepari E, Merico V, Calliada F. Use of ultrasound-magnetic

resonance image fusion to guide sacroiliac joint injections: a preliminary assessment. *Journal of Ultrasound* 2013; **16**: 111-8.
22. Iagnocco A, Perella C, D'Agostino MA, Sabatini E, Valesini G, Conaghan PG. Magnetic resonance and ultrasonography real-time fusion imaging of the hand and wrist in osteoarthritis and rheumatoid arthritis. *Rheumatology* 2011; **50**: 1409-13.
23. Zacchino M, Allegri M, Canepari M, et al. Feasibility of pudendal nerve anesthetic block using fusion imaging technique in chronic pelvic pain. *European Journal of Pain Supplements* 2010; **4**: 329-33.
24. Galiano K, Obwegeser AA, Bale R, et al. Ultrasound-guided and CT-navigation-assisted periradicular and facet joint injections in the lumbar and cervical spine: A new teaching tool to recognize the sonoanatomic pattern. *Regional Anesthesia and Pain Medicine* 2007; **32**: 254-57.
25. De Andres J, Alonso-Inigo JM, Sala-Blanch X, Reina MA. Nerve stimulation in regional anesthesia: Theory and practice. *Best Practice & Research. Clinical Anaesthesiology* 2005; **19**: 153-74.
26. Lee MW, McPhee RW, Stringer MD. An evidence-based approach to human dermatomes. *Clinical Anatomy* 2008; 21: 363-73.
27. Sørensen LK, Hasselstrøm JB. A high-throughput multi-class liquid chromatography tandem mass spectrometry method for quantitative determination of licit and illicit drugs in whole blood. *Analytical Methods* 2013; **5**: 3185-93.
28. Ehlers L, Jensen JM, Bendtsen TF. Cost-effectiveness of ultrasound vs nerve stimulation guidance for continuous sciatic nerve block. *British Journal of Anaesthesia* 2012; **109**: 804-8.
29. Sealed Envelope Ltd. Power calculator for binary outcome superiority trial, 2012. www.sealedenvelope.com/power/binary-superiority (accessed 21/10/2016).
30. Danish Health and Medicines Authority. [Summary of product characteristics for lidocaine-adrenaline SAD, injection, solution], 2015. http://www.produktresume.dk/docushare/dsweb/GetRendition/Document-15496/html (accessed 21/10/2016).

31. Karmakar MK, Li JW, Kwok WH, Soh E, Hadzic A. Sonoanatomy relevant for lumbar plexus block in volunteers correlated with cross-sectional anatomic and magnetic resonance images. *Regional Anesthesia and Pain Medicine* 2013; **38**: 391-7.
32. Mannion S, Barrett J, Kelly D, Murphy DB, Shorten GD. A description of the spread of injectate after psoas compartment block using magnetic resonance imaging. *Regional Anesthesia and Pain Medicine* 2005; **30**: 567-71.
33. Downs MB, Laporte C. Conflicting dermatome maps: Educational and clinical implications. *The Journal of Orthopaedic and Sports Physical Therapy* 2011; **41**: 427-34.
34. Sauter AR, Ullensvang K, Niemi G, et al. The Shamrock lumbar plexus block: a dose-finding study. *European Journal of Anaesthesiology* 2015; **32**: 764-70.
35. Børglum J, Jensen K, Christensen AF, et al. Distribution patterns, dermatomal anesthesia, and ropivacaine serum concentrations after bilateral dual transversus abdominis plane block. *Regional Anesthesia and Pain Medicine* 2012; **37**: 294-301.
36. Sadean MR, Glass PS. Pharmacokinetics in the elderly. *Best Practice & Research. Clinical Anaesthesiology* 2003; **17**: 191-205.
37. Van Dyke JA, Holley HC, Anderson SD. Review of iliopsoas anatomy and pathology. *Radiographics* 1987; **7**: 53-84.
38. Di Benedetto P, Pinto G, Arcioni R, et al. Anatomy and imaging of lumbar plexus. *Minerva Anestesiologica* 2005; 71: 549-54.

Figures and Captions

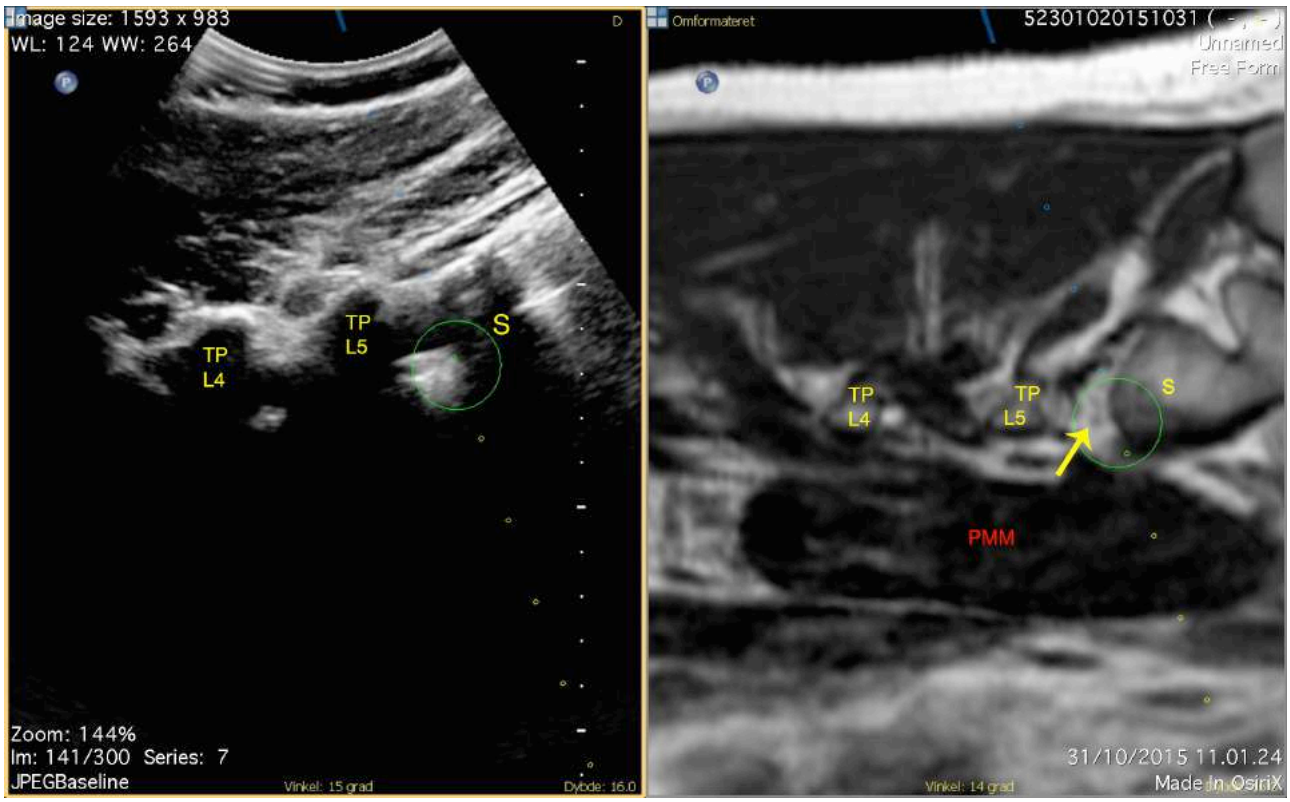

Fig. 1. The ultrasonographic (left) and MR (right) images are fused and displayed side-by-side. The blue line in the top is the projection of the block needle and the large green circle marks the anticipated intersection of the block needle tip and the ultrasound beam, here coinciding with the rami of spinal nerve L5 (yellow arrow) displayed on the MR image. The line of small blue and yellow circles marks the anticipated trajectory of the block needle prior to and after the intersection with the ultrasound beam, respectively. PMM; major psoas muscle; S, sacral ala; TP L4-5; transverse processes of L4 and L5.

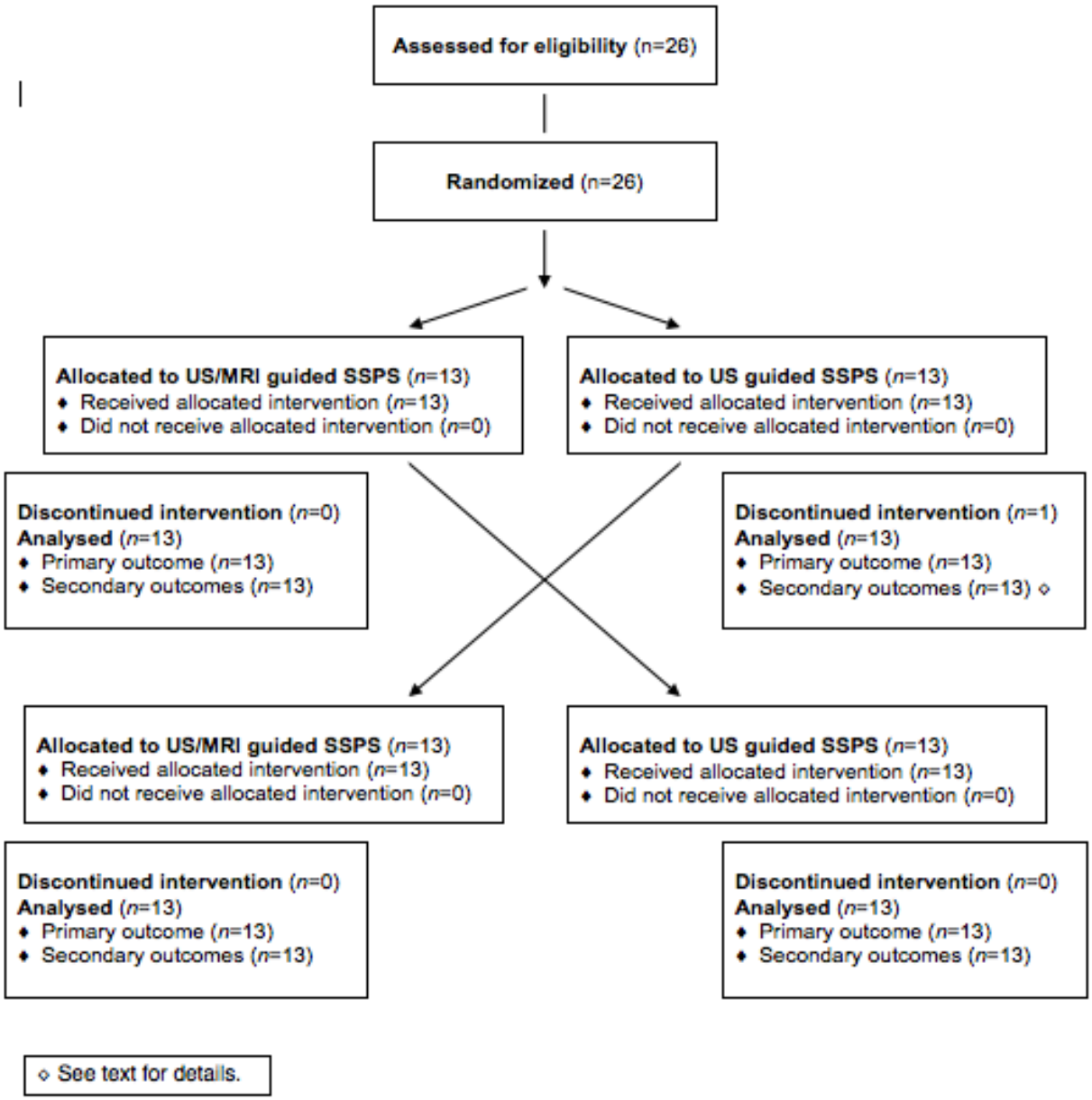

Fig. 2. Modified CONSORT 2010 flow diagram of the study subjects receiving ultrasound (US)/magnetic resonance imaging (MRI) fusion vs. US guided lumbosacral plexus blockade with the Suprasacral Parallel Shift (SSPS) technique

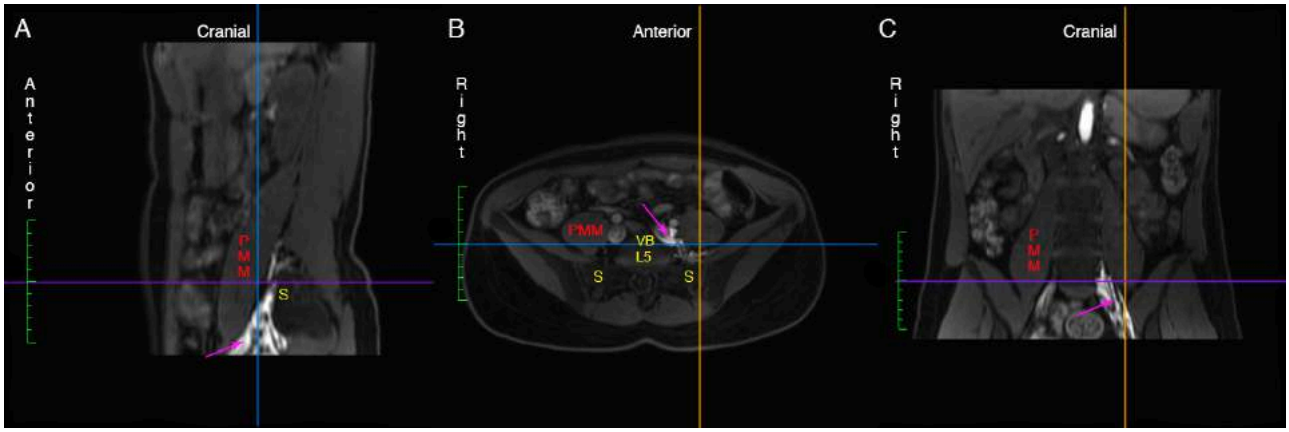

Fig. 3. MRI of one subject visualising spread of lidocaine-adrenaline added diluted contrast (magenta arrow) primarily medial to the psoas major muscle (PMM) – i.e. in the *para-psoas compartment (PPC)* – but not between the anterior and posterior lamina of the muscle and with minimal spread to the *retro-psoas subcompartment*. A) Sagittal plane. B) Axial plane. C) Frontal plane. Line (blue), position of frontal plane; Line (orange), position of sagittal plane; Line (purple), position of axial plane; S, sacral ala; VB L5, fifth vertebral body.

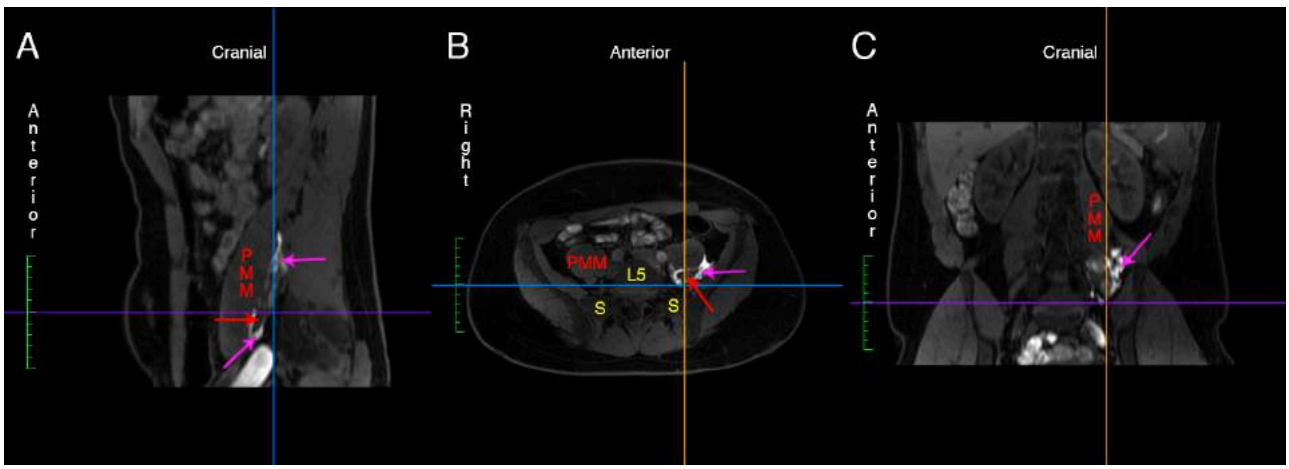

Fig. 4. MRI of one subject visualising spread of lidocaine-adrenaline added diluted contrast (magenta arrow) primarily posterior to the psoas major muscle – i.e. into the *retro-psoas subcompartment* – with minor seeping into the fascial plane between the anterior and posterior (red arrow) lamina of the psoas major muscle (PPM) that contains the lumbar

plexus. A) Sagittal plane. B) Axial plane. C) Frontal plane. L5, fifth lumbar vertebral body; Line (blue), position of frontal plane; Line (orange), position of sagittal plane; Line (purple), position of axial plane; S, sacral ala.

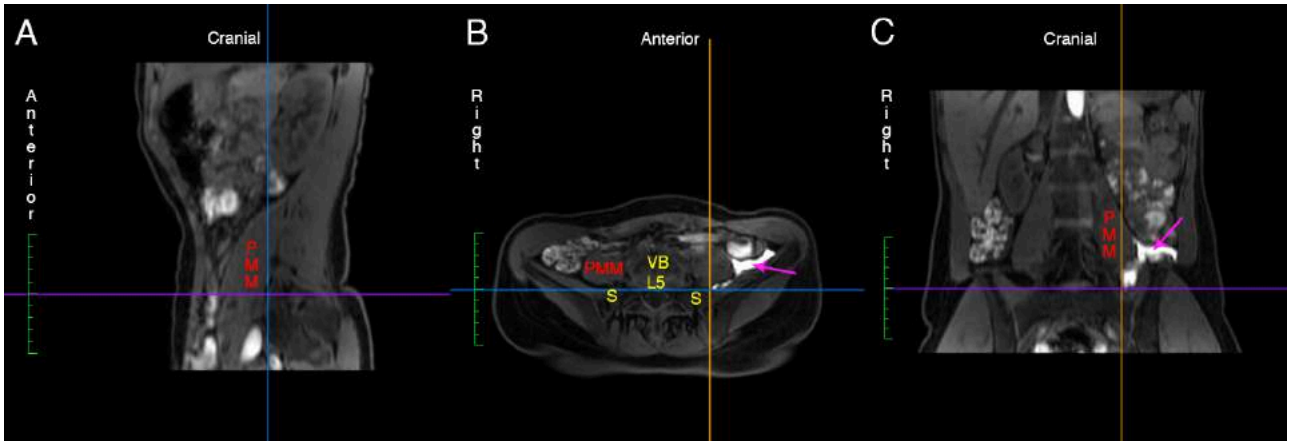

Fig. 5. MRI of one subject visualising spread of lidocaine-adrenaline added diluted contrast (magenta arrow) primarily lateral to the psoas major muscle (PMM) – i.e. into the *retroperitoneal compartment* – with minor seeping into the retro-psoas subcompartment; but not between the anterior and posterior lamina of the psoas major muscle. A) Sagittal plane. B) Axial plane. C) Frontal plane. Line (blue), position of frontal plane; Line (orange), position of sagittal plane; Line (purple), position of axial plane; S, sacral ala; VB L5, fifth lumbar vertebral body.

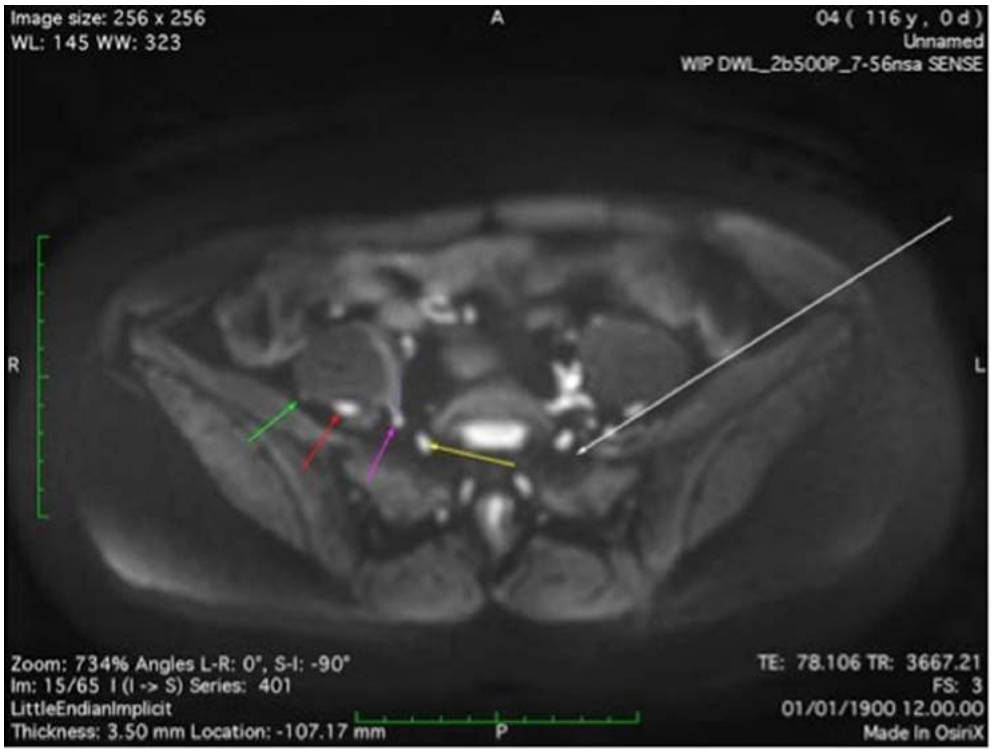

Fig. 6. Axial diffusion weighted MRI at the level of the cranial margin of the sacral ala, demonstrating a possible anterior approach to the lumbosacral plexus in the supine position. A needle (white arrow) can be inserted close to the anterior superior iliac spine and advanced between the psoas major and iliacus muscles. A first injection of local anaesthetic into the *retro-psoas subcompartment* will spread to the femoral nerve (red arrow) and the lateral femoral cutaneous nerve (green arrow). A second injection of local anaesthetic into the *para-psoas compartment* will spread to the anterior rami of spinal nerves L4, L5 and the lumbosacral trunk (yellow arrow), and the obturator nerve (pink arrow).

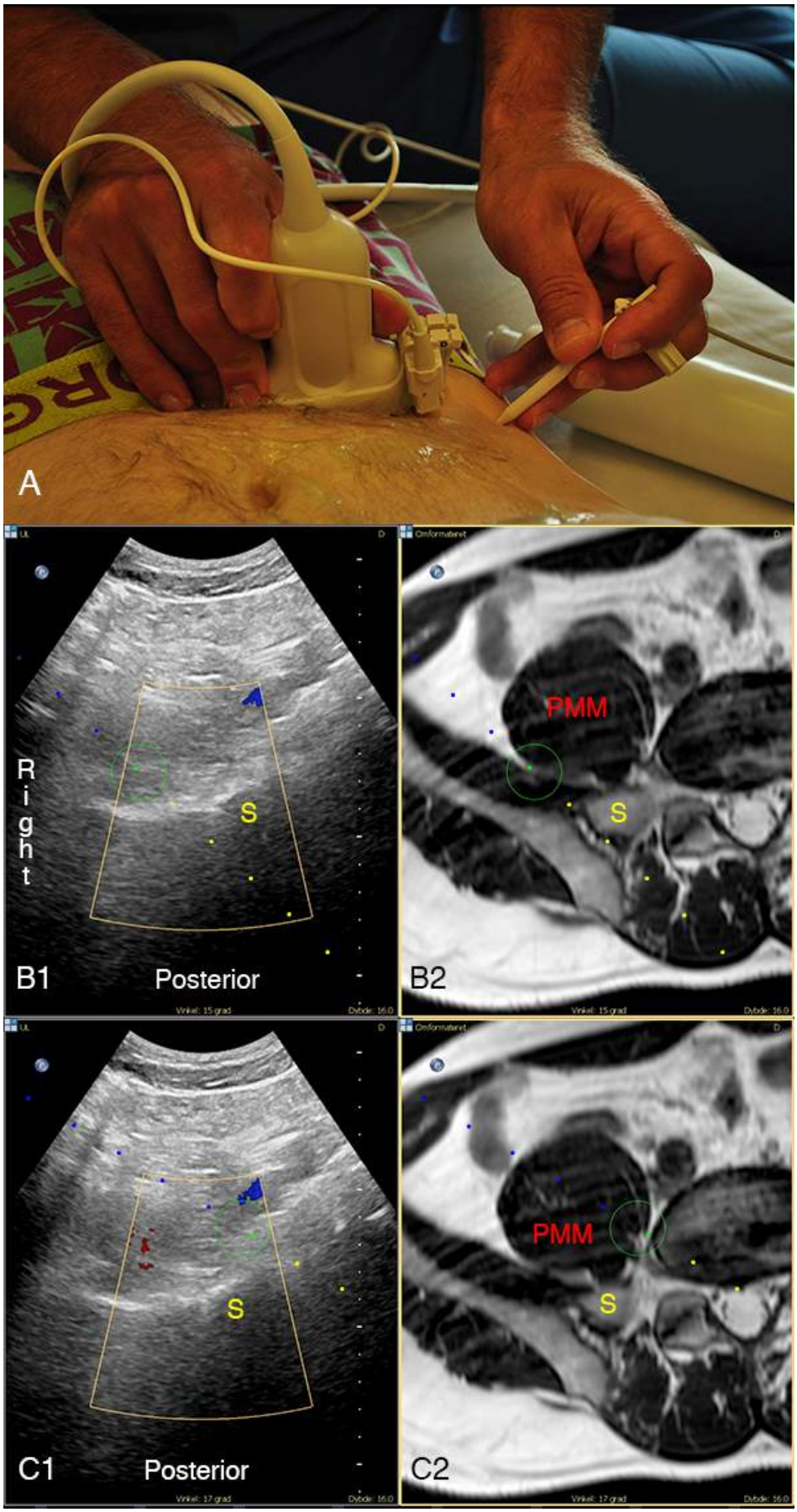
A
Right
S
B1
Posterior
PMM
S
B2
S
C1
Posterior
PMM
S
C2

Fig. 7. The anterior lumbosacral plexus approach guided by real-time ultrasound/MRI fusion in an anticipated experimental setting. A) The probe is axially orientated, slightly rotated clock-wise, and medial to the anterior superior iliac spine where the phantom needle is oriented in-plane with the US/MR image planes. B) Fused real-time ultrasound (B1) and MRI (B2) depicting the needle trajectory into the posterior psoas compartment. C) Fused real-time ultrasound (C1) and MRI (C2) depicting the needle trajectory through the psoas major muscle (PMM) into the paravertebral compartment. Guided by real-time ultrasound/MRI fusion and needle navigation, the “insertion point” and angulation of the phantom needle is adjusted until the anticipated intersection between the needle tip and the image plane (green circle) coincides with the target lumbosacral plexus nerves in the retro-psoas compartment (B) and in the para-psoas subcompartment (C) anterior to the border of the sacral ala (S). The small blue, green, and yellow dots illustrate the anticipated needle trajectory. Green dots mark in-plane needle trajectory, and blue and yellow dots mark out-of-plane trajectory.

Study III

Thomas Fichtner Bendtsen
Department of Anaesthesiology and Intensive Care, Aarhus University Hospital
Nørrebrogade 44, DK-8000 Aarhus C, Denmark
Phone: +4551542997, E-mail: tfb@dadlnet.dk

Real-time Ultrasound/MRI Fusion for Shamrock Lumbar Plexus Blockade and Analysis of Injectate Spread - an Exploratory Randomised Controlled Trial*

J. M. C. Strid,[1] E. M. Pedersen,[2] M. A. F. Bendtsen,[3] S. Bjørn,[1,3] M. Dam,[4] M. Daugaard,[1] M. S. Hansen,[3] O. Vendelbo,[2] J. Børglum,[4] K. Søballe[5] and T. F. Bendtsen[1]

1 Department of Anaesthesiology and Intensive Care, Aarhus University Hospital, Aarhus, Denmark
2 Department of Radiology, Aarhus University Hospital, Aarhus, Denmark
3 Medical Science, Faculty of Health, Aarhus University, Aarhus, Denmark
4 Department of Anaesthesiology and Intensive Care Medicine, Zealand University Hospital, University of Copenhagen, Denmark
5 Department of Orthopaedic Surgery, Aarhus University Hospital, Aarhus, Denmark

Correspondence to: Dr. Thomas F. Bendtsen, Department of Anaesthesiology and Intensive Care, Aarhus University Hospital, Nørrebrogade 44, DK-8000 Aarhus, Denmark. Phone: +4551542997, E-mail: tfb@dadlnet.dk

* Preliminary results on motor blockade of the femoral and obturator nerves, sensory blockade of the lateral femoral cutaneous nerve, and procedural discomfort were presented to the 35th Annual European Society of Regional Anaesthesia (ESRA) Congress 2016 in Maastricht, the Netherlands, on 7-10 September 2016

Short title: Real-time US/MRI fusion guided Shamrock lumbar plexus block

Keywords: Femoral nerve block: anatomy; Nerve block landmarks; Ultrasound structures: echogenicity

Author contributions: J.M.C.S., E.M.P., and T.F.B. designed the study protocol. J.M.C.S. recruited all study subjects. J.M.C.S., M.A.F.B., S.B., M.D., M.D., M.S.H., O.V., and T.F.B. conducted the clinical trial. J.M.C.S., M.A.F.B., M.D., M.D., M.S.H., O.V. recorded all data. T.F.B. conducted the blinded analysis of injectate spread on MRI. J.M.C.S. performed the statistical analysis. J.M.C.S. authored the initial manuscript. All authors read and revised the manuscript and approved the final version.

Summary

Applications of fusion of real-time ultrasonography and magnetic resonance imaging (MRI) for increased accuracy of peripheral regional anaesthesia is practically non-existent in the literature. In this randomised controlled trial, we aim to compare effectiveness and safety of real-time ultrasound/MRI fusion vs. ultrasound guided Shamrock lumbar plexus block, and to investigate patterns of spread of injectate with ultrasound/MRI fusion and high-resolution MRI. We enrolled 22 ASA I subjects ≥18 years. All subjects received one ultrasound/MRI fusion and one ultrasound guided Shamrock lumbar plexus block (20 ml 2% lidocaine-adrenaline added 1 ml diluted contrast). Primary outcome was number of participants with blockade of the femoral, obturator, and lateral femoral cutaneous nerves (block success). Secondary outcomes were procedure-associated, injectate spread analysed on MRI, and sensory blockade. Block success (ultrasound/MRI, 16/22; ultrasound, 18/22; $p = 0.69$) and performance time (ultrasound/MRI, 438 [272-567 (164-903)] s; ultrasound, 396 [296-524 (197-1044)] s; $p = 0.42$) were similar, but the ultrasound/MRI fusion guided technique had a longer preparation time (ultrasound/MRI, 868 [661-947 (506-1634)] s; ultrasound, 471 [369-631 (165-1090)] s; $p < 0.001$). Perineural injectate spread and sensory mapping of both techniques showed similar primary effect on the anterior rami of spinal nerves L2-L4 and the lateral femoral cutaneous nerve. The injectate of both techniques was visualised primarily inside the *intra-psoas subcompartment*, which is the interfascial plane between the anterior and posterior lamina of the psoas major muscle that contains the lumbar plexus. No spread was observed into the *retro-psoas subcompartment* or the *para-psoas compartment.* Epidural spread was similar (ultrasound/MRI, 1/22 subjects; ultrasound, 2/22 subjects; $p = 1.00$). Effectiveness, safety, and performance time of the ultrasound/MRI fusion guided and the ultrasound guided Shamrock technique were similar, but the ultrasound/MRI fusion guided technique required longer preparation time.

Introduction

Patients admitted for surgery of the hip are primarily older than 65 years and may be afflicted by comorbidity and/or obesity, increasing the risk of perioperative complications. [1-3] In these patients, an effective and safe technique for peripheral regional anaesthesia would be desirable, because it is associated with fewer complications, improved haemodynamics and effective postoperative analgesia with reduced use of opioids compared to general and spinal anaesthesia. [3-7]

A lumbar plexus block (LPB) anaesthetises the femoral, obturator, and lateral femoral cutaneous nerves. A LPB combined with a sacral plexus block and an iliohypogastric nerve block provides efficacious surgical anaesthesia of the hip. A single lumbar plexus block provides efficacious analgesia after hip surgery. [8-10]

The Shamrock technique for lumbar plexus blockade employs ultrasound scanning in the axial plane from the flank of the patient. It provides good ultrasonographic visualisation of the paravertebral lumbar anatomy (including the target lumbar plexus and ultrasonographic landmarks), the block needle tip, and perineural spread of the injectate. [10-14] In an yet unpublished randomised controlled trial, the Shamrock technique was faster to perform, required fewer needle insertions, was more comfortable, and was equally effective and safe compared with the Lumbar Ultrasound Trident technique – a well-established posterior approach for lumbar plexus blockade. [15] However, due to the distance between probe and needle with the Shamrock technique, it may be difficult to pinpoint the most optimal needle skin insertion point in the paravertebral lumbar region and inclination of the needle. Further, the target lumbar plexus is situated deeply, why only poor visualisation of the lumbar plexus is feasible in some patients. [13] Insufficient ultrasonographic visualisation of the target lumbar plexus, surrounding landmarks, and the block needle tip and trajectory may reduce the precision – and thereby the effectiveness and safety – of the procedure.

Image fusion of real-time ultrasound and computed tomography imaging (CT) or magnetic resonance imaging (MRI), without the inherent limitations of ultrasound alone, are used to enhance the precision of image guided procedures primarily in interventional radiology, [16, 17] but also to better existing ultrasound guided needle procedures. [18] In addition, the fusion system allows needle navigation, which may be applied to track and optimise

the needle insertion point, the (actual and anticipated) needle trajectory, and the interventional target. In regional anaesthesia, a protocol of fused ultrasound and CT or MRI for neuraxial sonography without needle insertion in a phantom and in volunteers has been described. [19] In chronic pain therapy, fusion of ultrasound and CT or MRI has shown to be feasible and effective for guidance of injections of primarily the sacroiliac joint in cadavers and patients. [20-23]

In this blinded randomised controlled crossover trial, we aim to compare ultrasound/MRI fusion vs. ultrasound for guidance of lumbar plexus blockade using the Shamrock approach. The primary outcome is the proportion of study subjects with motor blockade of the femoral and obturator nerves as well as sensory blockade of the lateral femoral cutaneous nerve. The secondary outcomes are block procedure-associated, perineural spread of the injectate analysed on MRI, epidural injectate spread, sensory mapping, and cost-effectiveness. In addition, we aim to analyse patterns of injectate spread on MRI.

Methods

Ethical Considerations

The Research Ethics Committee of the Central Denmark Region (MJ: 1-10-72-368-15), the Danish Medicines Agency (2015-005544-33), and the Danish Data Protection Agency approved this blinded randomised controlled study with crossover design. The study was prospectively registered in EudraCT (2015-005544-33) and ClinicalTrials.gov (NCT02255591). All study subjects were included after written informed consent. The Good Clinical Practice Unit at Aalborg and Aarhus University Hospitals monitored the study, which complied with the Helsinki II Declaration.

Study Subjects

ASA I subjects ≥ 18 years with a body mass index (BMI) $18.5 \leq BMI \leq 30$ kg.m^{-2} were recruited through a Danish website for research volunteers. Subjects who were unable to communicate or cooperate in Danish, were allergic to local anaesthetics or contrast agents, had daily use of analgesics, abuse of medicine or alcohol, infection or prior surgery in the lumbar paravertebral region or the flank, contraindications for MRI, and/or were legally incompetent, were excluded. The subjects received payment for their participation.

The study was conducted during two three-day sessions one week apart at the Department of Radiology, Aarhus University Hospital, Denmark, in April 2016.

MRI for fusion with ultrasound

Upon arrival on the first session, the subjects were placed in the supine position with a pillow under the knees to minimise lumbar lordosis on the 70 cm bore of a 1.5T Philips Ingenia MRI scanner (Koninklijke Philips Electronics N.V., Eindhoven, the Netherlands). A dS flex coverage anterior coil was used for signal reception while an experienced radiographer sampled coronal 3D T2-TSE VISTA sequences ($1.2 \times 1.2 \times 1.2$ m^3 isotropic scanning resolution [super-imposed 2.4 mm slices, 1.2 mm spacing], TE 60 ms, and TR 1,200 ms) of the lumbar spine. Feet-head phase encoding was used to minimise respiratory and peristaltic artefacts. J.M.C.S used OsiriX v6.5.2 64-bit (Pixmeo SARL, Bernex, Switzerland) to convert the orientation to axial prior to upload in the ultrasound

system with fusion software (Epiq 7 1.4; Koninklijke Philips Electronics N.V., Eindhoven, the Netherlands), because the system can only import axially oriented sequences for fusion.

Block Procedures

All subjects received one single injection ultrasound/MRI fusion guided and one ultrasound guided Shamrock lumbar plexus block with a one-week interim period. All injections were 20 ml 2% lidocaine-adrenaline added 1 ml diluted MRI contrast agent (0.13 ml 27.9% gadoterate meglumine [Dotarem®; Guerbet, Roissy CdG Cedex, France] diluted in 0.87 ml 0.9% isotonic saline). All subjects were equipped with peripheral I.V. access and monitored with three-lead ECG, non-invasive blood pressure measurement, and pulse oximetry.

The same anaesthesiologist (T.F.B.) with extensive experience of ultrasound and electrical nerve stimulation guided blocks and experimental experience of real-time ultrasound/MRI fusion guided blocks performed all interventions. All interventions were performed with an Epiq 7 1.4 (Koninklijke Philips Electronics N.V., Eindhoven, Netherlands) and a C5-1 MHz convex probe with a mounted sensor. After co-registration of the previously sampled MRI dataset and real-time ultrasound, pre-scanning, and marking of the anticipated needle insertion point, the skin was swabbed with chlorhexidine in isopropyl alcohol and draped with a sterile fenestrated sheet. The probe with the mounted sensor was draped with a sterile cover. Two ml 2% lidocaine was injected in the skin and subcutaneous tissue prior to insertion of a 22 Gauge 100 mm nerve block needle (Stimuplex Ultra, B. Braun, Melsungen, Germany).

Ultrasound/MRI fusion guided Shamrock: For the co-registration, the subject was placed supine equalling the position during initial MRI sampling. The patient tracker (i.e. the patient sensor) was attached to the iliac crest on the side of the subject not to be anaesthetised. The probe – with the mounted probe sensor – was placed on the abdomen and aligned in the axial plane that intersected the bifurcation of aorta. This plane was identified on both MRI and real-time ultrasound (Fig. 1A). The image datasets were co-registered using the jointing point of the common iliac arteries as a common reference point in the selected axial plane. Any misalignment of the aorta, common iliac arteries,

inferior vena cava, and/or the anterior border of the vertebral body was adjusted by using the system built-in functions of rotation and shifting (Fig. 1B). The subject was turned to the lateral decubitus position with the side to be anaesthetised non-dependent and a rolled-up blanket supporting the flank in order to decrease lumbar scoliosis. The probe was aligned in the axial plane in the axillary midline just cranial to the iliac crest. The Shamrock "three-leaf clover sign" of the psoas major, quadratus lumborum, and the erector spinae muscles and the transverse process of vertebra L4 was visualised by sliding the probe posteriorly. Any ultrasound/MRI misalignment of the lateral border of vertebra L5, the transverse process of vertebra L4, and/or the neural foramina was adjusted. The screen display was changed to side-by-side presentation of the fused ultrasonographic and MR images. The tail of the probe was tilted cranially until the transverse process of L4 no longer intersected the image plane. The lumbar plexus was identified inside the intra-psoas subcompartment between the anterior and posterior lamina of the psoas major muscle on MRI and, if possible, also on the ultrasonographic image. The block needle with mounted sensor was placed in the best needle position (typically 3 to 4 cm lateral to the lumbar median) with the anticipated needle trajectory intersecting the image plane exactly at the lateral border of the target lumbar plexus. The anticipated needle trajectory was displayed on the monitor as a real-time overlay on both the ultrasound and the MR image (needle navigation). Guided by ultrasound/MRI fusion and needle navigation, the needle tip was advanced in a postero-anterior direction until it was visualised adjacent to the target lumbar plexus on MRI and – if possible – on ultrasound (Fig. 2).

Ultrasound guided Shamrock: This technique has been described in-depth previously. [10, 13]

For safety, an electrical nerve stimulator (0.1 ms, 2.0 Hz, 0.2 mA) was connected to the block needle during both procedures to warn about intraneural location of the needle tip. The endpoint of injection was visualisation of the needle tip immediately at the lateral margin of the ultrasonographically visible lumbar plexus or – if the plexus was not visualised – an appropriate motor response from the quadratus femoris and/or the hip adductors to electrical nerve stimulation (0.3 to 0.5 mA). In both cases, the current required to trigger a motor or paraesthesia response and the type of response was recorded. The injection was in incremental doses with intermittent aspiration. The

intervention was completed (Time 0 [T_0]) at withdrawal of the block needle from the skin. Subsequently, the subjects were followed-up for 90 min (T_{90}) and observed until the sensorimotor effects of the blockade had disappeared.

Outcomes and Assessment

The primary outcome was number of subjects with blockade of the femoral, obturator, and lateral femoral cutaneous nerves (block success). Successful blockade was defined as a decrease in muscle force (N) during knee extension (femoral nerve) and hip adduction (obturator nerve) at T_{60} compared to baseline and decreased and/or absent sensation for cold and/or pain in the skin innervated by the lateral femoral cutaneous nerve compared to the contralateral side at T_{70}.

The secondary outcomes were: a) preparation time defined as the time (s) from placement of the subject on the bed until end of pre-scanning and co-registration of ultrasound and MRI; b) procedure time defined as the time (s) from placement of the probe on the skin after completed preparations to withdrawal of the block needle after completed intervention; c) electrical nerve stimulation (mA) required to trigger response prior to injection; d) type of response to electrical nerve stimulation (knee extension/quadriceps femoris/femoral nerve; hip adduction/obturator nerve; other motor response; paraesthesia; none; e) number of block needle insertions defined as a withdrawal of the needle followed by a repeat needle introduction regardless of the number of skin penetrations; f) location of the needle skin insertion point assessed as the horizontal distance (cm) between the median and the skin insertion point; g) distance (cm) from the needle skin insertion point to the needle tip at the endpoint of injection assessed by the markings on the needle shaft; h) procedural discomfort assessed by the subject on a numeric rating scale (“0” = no discomfort, “10” = worst possible discomfort) at T_0; i) Δ mean arterial pressure (MAP, mmHg) from baseline to T_5; j) proportion of subjects with spread of injectate to the anterior rami of spinal nerves L1 to S1, femoral, obturator, and lateral femoral cutaneous nerves, and lumbosacral trunk assessed on MRI at T_{15}; k) compartmental patterns of injectate spread assessed on MRI at T_{15} into the intra-psoas and retro-psoas subcompartments (IPSC and RPSC) of the iliopsoas compartment as well as the para-psoas compartment (PPC); [24] l) proportion of subjects with visually confirmed circumferential epidural

injectate spread assessed on MRI at T_{15} and decreased/absent sensation for cold in at least one pair of bilateral dermatomes at T_{70}; m) proportion of subjects with motor blockade of femoral and obturator nerves, respectively, defined as a decrease in muscle force (N) during knee extension (femoral nerve) and hip adduction (obturator nerve) at T_{60} compared to baseline; n) number of subjects with sensory blockade of cold, warmth, touch, and pain in the dermatomes T8 to S3, [25] respectively, assessed at T_{70}; o) cost-effectiveness.

Maximum muscle force for each joint movement was defined as the peak force of three tests with a handheld dynamometer with 20 s intermittent intervals. The subjects were positioned supine with their knee joints flexed 90° and the lower leg hanging freely from the bedside. They exerted maximum active force against the dynamometer, held stable by an observer, during knee extension and hip adduction (with 45° abducted lower limb). Baseline muscle force was assessed during the first session before the intervention.

Injectate spread was assessed on axial 3D T1 MRI sequences (mDixon generating in-phase, out-of-phase, water, and fat images) and diffusion weighted images sampled by two experienced radiographers following a strict protocol and using a 3T Philips Achieva dstream scanner (Koninklijke Philips Electronics, Eindhoven, the Netherlands).

The *intra-psoas subcompartment* (IPSC) is the interfascial plane between the anterior and posterior lamina of the psoas major muscle that contains the lumbar plexus. [24] The *retro-psoas subcompartment* (RPSC) is the space posterior to the psoas major muscle and that contains the femoral and lateral femoral cutaneous nerves after they emerge from the psoas major muscle. [24] The cranial limit of the RPSC is typically the transverse process (TP) of vertebra L5, sometimes the TP of vertebra L4 or even L3. The caudal limit of RPSC is the fusion of psoas major and iliacus muscles. The *para-psoas compartment* (PPC) is the space medial to the iliopsoas compartment caudal to the transverse process of vertebra L5. The PPC contains the obturator nerve after it emerges from the psoas major muscle as well as the anterior rami of spinal nerves L4, L5 and S1 and the lumbosacral trunk. [24]

Sensory blockade was tested with standardised stimuli for cold and warmth (25° and 40° Rolltemp II thermo test; Somedic, Hörby, Sweden), touch (SENSELab^{TM} Brush-05; Somedic AB, Hörby, Sweden), and pain (PinPrick 512 mN; MRC Systems GmbH,

Heidelberg, Germany). Sensory blockade was assessed as “present” or “decreased/absent” compared to the contralateral hip and lower limb – or the arm in case of epidural spread. The dermatomes Th8-Th12, S2 and S3 were included to observe the effect of any epidural spread.
Cost effectiveness or “extra price per patient” was calculated as the difference in mean marginal cost of the techniques. [26] The average annual total wages for medical staff were used to calculate unit costs for the time spent by the radiographer on preparing and sampling the MRI scan for fusion and for the difference in time spent by the operating anaesthesiologist and an assistant nurse on preparing and performing the intervention. The unit cost for use of the 1.5T MRI scanner is given as a time unit due to the complexity of calculating the monetary cost. All costs were collected in Danish Kroner (DKK) in July 2016 and converted into GBP in October 2016 (100 DKK = £12.08 [€13.44/$14.86]).
All data were recorded using the "research electronic data capture" (REDCap) system. [27]

Randomisation and Blinding

J.M.C.S. enrolled and allocated consecutive identification numbers to the 22 included subjects. Two study-independent assistants computer-generated a randomisation list with random allocation of interventions (“1st session Ultrasound/MRI + 2nd session Ultrasound” or *vice versa*) and side (“1st session right + 2nd session left” or *vice versa*) to the 22 study identification numbers. The randomisation list was uploaded to a protected REDCap server, only accessible for the assistant who double-controlled the interventions. Prior to each intervention, the double-controlling assistant and the operator performing all interventions checked the allocated intervention and side in REDCap without revealing it to others.
All observers and analysts of data were blinded. The image fusion field generator was included in all set-ups in order to blind the subjects and none of the subjects were able to see the ultrasound monitor.

Statistical Analysis

We hypothesised that ultrasound/MRI fusion guidance would increase the proportion of subjects with blockade of the femoral, obturator, and lateral femoral cutaneous nerves

from 40% to 70% compared with ultrasound guidance. A sample size of 20 subjects would be required to detect a 30% increase in a two-sided crossover analysis with 80% power (1-β) and α=0.05. [28] We enrolled 22 subjects in order to avoid decreased power due to dropouts.

Stata IC 14.1 (StataCorp LP, College Station, USA) was used to compute all statistical analyses. We assessed normality of distribution with normal Q-Q plot and analysed differences of continuous variables with normal distribution with the Student t-test. Differences of continuous variables with non-normal distribution and ordinal variables were analysed with Wilcoxon matched-pairs signed rank test. Differences between paired categorical variables were analysed with McNemar's test. Level of significance was 0.05. The values of continuous variables with normal distribution are presented as mean (SD), continuous variables with non-normal distribution and ordinal variables as median (IQR [range]), and categorical variables as numbers.

Results

Twenty-two subjects were enrolled during March 8 to 31, 2016. All subjects received the intended interventions and were followed-up and analysed for the primary outcome during April 2 to 10, 2016 (Fig. 3).

The median (IQR [range]) age of the 22 subjects was 22.5 (22.0-24.0 [18.0-60.0]) years. The mean (SD) weight was 73.0 (8.8) kg. The mean (SD) height was 177 (9.6) cm. The mean (SD) BMI was 23.2 (2.0) $kg.m^{-2}$.

There was no evidence for any difference in the proportion of subjects who had blockade of the femoral, obturator, and lateral femoral cutaneous nerves (Appendix 1). The underlying data on muscle force and sensory mapping are presented in Appendix 2 and 3. The procedure-associated outcomes (a-i) are displayed in Appendix 4. The median (IQR [range]) preparation time was longer for the ultrasound/MRI fusion guided technique (868 [661-947 (506-1634) s) compared with the ultrasound guided (471 [369-631 (165-1090)] s; p value < 0.001). The median (IQR [range]) minimal electrical nerve stimulation required to trigger a response was lower for the ultrasound/MRI fusion guided technique (0.26 [0.24-0.28 (0.22-0.28) mA) compared with the ultrasound guided (0.28 [0.26-0.28 (0.22-0.40)] mA; p value = 0.012). There was no evidence for any difference between the groups concerning the other procedure-associated outcomes.

There was no evidence for any difference between the two groups in the injectate spread to the anterior rami of spinal nerves L1-S1, the femoral, obturator, and lateral femoral cutaneous nerves, and the lumbosacral trunk assessed on MRI (Appendix 5). The injectate did spread consistently around the lumbar plexus inside the *intra-psoas subcompartment* (IPSC) from the neural foramina of vertebrae L2 and L3 cranio-medially and deviating antero-lateral caudally (Fig. 4). No injectate spread was observed outside the iliopsoas compartment. No spread was observed cranial to the neural foramen of vertebra L2. The anterior ramus of spinal nerve L1 was never contained between the two lamina of the psoas major muscle and was not reached by injectate in any subject. No spread was observed caudal to the transverse process of L5. There was minimal or no spread to the anterior rami of spinal nerves L4, L5 and S1 or the lumbosacral trunk (Appendix 5) inside the *para-psoas compartment* (PPC), medial to the iliopsoas compartment caudal to the transverse process of vertebra L5. In some subjects the

anterior ramus of spinal nerve L4 entered the intra-psoas subcompartment, where it was reached by injectate (see Appendix 5).

The injectate did not spread to the terminal femoral and lateral femoral cutaneous nerves inside the *retro-psoas subcompartment (RPSC)*, posterior to the psoas major muscle inside the iliopsoas compartment and caudal to the transverse process of vertebra L5 (Fig 5).

There was no evidence for any difference in the number (proportion) of subjects with epidural spread (ultrasound/MRI, 1/22 subjects; ultrasound, 2/22 subjects; p = 1.00). With individual variation, the effect of the epidural spread was observed in the dermatomes Th11-S3 and in the skin innervated by the lateral femoral cutaneous nerve.

Appendix 1 and 3 display the number of participants with motor blockade of the femoral, obturator, superior gluteal, and sciatic nerves, respectively, and with sensory blockade of the dermatomes T8 to S3 and the lateral femoral cutaneous nerve, respectively. There was no difference between the groups concerning neither of the outcomes. The underlying data on muscle force are displayed in Appendix 2.

The mean marginal cost (“price per patient”) of a Shamrock block was Δ£17.64 (€18.17/$21.70) and 6 min and 34 s in the 1.5T MRI scanner in favour of ultrasound alone compared to real-time ultrasound/MR image fusion.

Safety and Harm

One subject experienced transitory tachycardia and a rash during the injection of local anaesthetic and the follow-up period, respectively. One subject experienced transitory dizziness during the injection of local anaesthetic. None of the subjects had other symptoms of local anaesthetic systemic toxicity or neurological symptoms. Four subjects experienced two incidents of headache, one incident of vasovagal syncope, and one incident of transitory hot flush during the follow-up period. The vasovagal syncope was related to hyperventilation during the motor test and the subject has a history of both. One subject experienced a muscular haematoma at the site of injection after the study was ended.

Discussion

The present study is the first randomised controlled trial exploring real-time ultrasound/MRI fusion guided lumbar plexus blockade. The ultrasound/MRI fusion and ultrasound guided Shamrock techniques were equally effective and safe and required the same performance time, but the ultrasound/MRI fusion guided technique required prolonged preparation time. An equal proportion of study subjects in the two groups had blockade of the femoral, obturator, and lateral femoral cutaneous nerves, falsifying the hypothesis that ultrasound/MRI fusion guidance would increase block success compared with ultrasound guidance only. Ultrasound/MRI fusion offers more detailed and improved visualisation of the target lumbar plexus and surrounding anatomical structures compared to ultrasonographical visualisation, which often is impaired by low-resolution imaging of the deeply situated target lumbar plexus and acoustic shadows generated by the adjacent bony structures. The target clinical group of a lumbar plexus blockade in elective or emergency hip surgery is elderly, fragile, comorbid and/or obese patients. In these patients, the benefit of ultrasound/MRI fusion may be more obvious than in healthy, young normal weight study subjects, in whom sufficient ultrasonographic visualisation of the target lumbar plexus was achieved with a high frequency. However, initially we chose to assess the ultrasound/MRI fusion guided Shamrock technique in healthy subjects because the fusion technique has not been applied for needle guidance in regional anaesthesia previously.

The accuracy of the fusion of the ultrasound and MRI datasets depends on the congruence of the 3D topography of the two datasets and dimensional stability despite change of body position from supine to lateral decubitus during image sampling. Any differences in the positioning or movement of the subject, respiration, and peristalsis during image sampling affect the topography of the anatomical structures and hence affect the accuracy of the co-registration and needle navigation. MRI is technically and clinically most optimal to perform in the supine position, but the Shamrock lumbar plexus block is performed in the lateral decubitus position. Therefore, the present fusion technique included a shift in position. Although a pilot study demonstrated only minor displacement of the anterior rami of spinal nerves L3 and L4 on MRI sampled in the supine and in the lateral decubitus position, and misalignment of the fused datasets can be adjusted for, we

cannot exclude that the position shift did affect the accuracy of the fused datasets and hence the results. In addition, the success rate of a new technique follows a learning curve. [16]

We used motor blockade as a surrogate marker for sensory blockade, because dermatomal sensory mapping may be an unreliable marker of anaesthesia of a specific terminal nerve due to overlapping of contiguous terminal nerve territories as well as wide individual anatomical variation of location – and even existence – of such territories. [29] However, the measurement of muscle force is associated with measurement error and any threshold value defining a "successful blockade" is arbitrary. Furthermore, the external validity of successful blockade in healthy study subjects for clinical patients can only be speculated. Because the aim of this study was to compare two techniques in a standard setting, motor blockade was defined as decrease in muscle force compared to baseline. The measurement estimates should therefore be considered as measures of comparison between the two techniques – not as clinically applicable proxy markers of successful anaesthesia.

Moreover, we injected a volume of lidocaine-adrenaline corresponding approximately to the minimum effective anaesthetic volume of 0.5% ropivacaine that produces a successful Shamrock lumbar plexus block in 50% of patients undergoing orthopaedic surgery of the lower extremity. [13] We chose a volume of 20 ml because the aim of the study was to compare two techniques – not to achieve maximum block success. We chose lidocaine-adrenaline in order to obtain a short post-block observation period and fast discharge of the subjects.

Due to the time spent on co-registration, the preparation time was extended for the ultrasound/MRI fusion guided technique compared to the ultrasound guided technique. The difference is in keeping with previous studies on fusion guided procedures [16] and explains the higher cost per Shamrock block guided by ultrasound/MRI fusion.

The ultrasonoanatomy of the lumbar region has been compared with MRI in a previous study. [30] Only few studies have investigated perineural injectate spread in the lumbar region with MRI. [31, 32] Because of the questionable internal validity of assessing a successful blockade in healthy subjects based on sensorimotor mapping, we also assessed perineural spread of injectate visualised on MRI. Furthermore, inclusion of a

high-resolution and anatomically detailed image modality, without the inherent limitations of ultrasound, such as 3D T1 and diffusion weighted MRI made it possible to carry out in-depth exploration of injectate spread into different relevant anatomical subcompartments. During our studies of injectate spread on MRI, we observed a consistent spread inside the intra-psoas subcompartment (IPSC), between the anterior and posterior lamina of the psoas major muscle after injection with both image guidance techniques. The spread extended cranio-medially to the neural foramina of vertebrae L2 and L3 and deviated antero-laterally to the caudal end of the IPSC, which varies between the level of the transverse process of vertebra L5 and the level of the upper margin of the ala sacrum. The IPSC contains the subset of the lumbar plexus from the anterior rami of L2 and L3 and sometimes L4. The most cranial part of the lumbar plexus from the anterior ramus of L1 is not contained inside the IPSC.

There was minimal or no spread observed inside the para-psoas compartment (PCC). The PCC is medial to the iliopsoas compartment and caudal to the transverse process of vertebra L5. [24] It contains the lumbosacral trunk from anterior rami of spinal nerves L4 and L5 as well as the obturator nerve after its emergence from the IPSC.

In addition, there was no or minor spread into the retro-psoas subcompartment (RPSC). The RPSC is the compartment posterior to the psoas major muscle caudal to the transverse process of vertebra L5. [24] Occasionally it extends cranially to the transverses process of vertebra L4 - sometimes even L3. It extends caudally to the fusion of the psoas major and iliacus muscles. It contains the femoral and lateral femoral cutaneous nerves after their emergence from the IPSC.

We observed that only the anterior rami of spinal nerves L2 and L3 consistently entered the IPCC between the two lamina of the psoas major muscle. The branches of the anterior rami of spinal nerve L4 that contributed to the femoral nerve also entered this compartment. However, the major subset of the anterior ramus of spinal nerve L4 descended caudally inside the PCC to join the anterior ramus of spinal nerve L5 in the formation of the lumbosacral trunk without entering the intra-psoas compartment. It was not possible to determine whether the L2/L3 subset of the obturator nerve emerged from the IPSC and joined the L4 subset of the obturator nerve inside the PCC or *vice versa*. The Shamrock technique anaesthetises the lumbar plexus branches of femoral and lateral

femoral cutaneous nerves as well as the L2/L3 subset of the obturator nerve. The anterior rami of spinal nerves L4 and L5 and the lumbosacral trunk are located inside the PCC [24] and were not anaesthetised with the Shamrock technique in this trial.

The frequency of epidural spread was similar for the two techniques and comparable to other studies on lumbar plexus blockade with systematic testing for epidural spread. [13, 32]

Further, the data sampling and data analysis were blinded and we strived to blind the study subjects with identical trial setup, but the operator performing the Shamrock techniques could not be blinded. Similar to all procedure-related studies, this is a potential source of bias that we endeavoured to reduce by meticulously following a double-controlled protocol.

Application of fusion of real-time ultrasound and MRI is still an emerging technique, which is not yet matured for clinical application in regional anaesthesia. Future studies involving this technique should include co-registration based on MRI compatible external landmarks for point registration or automatic image recognition, preferably with the subjects in only one position. Another potential option is fusion of two MRI datasets: one that visualises the perineural anatomical topography with high resolution, e.g. a 3D T2-TSE sequence, and one that visualises the target nerves, e.g. a diffusion weighted sequence.

In summary, the effectiveness and safety of ultrasound/MRI fusion and ultrasound guidance using the Shamrock technique were equivalent. However, the preparation time for the ultrasound/MRI fusion guided technique was prolonged. The analysis of injectate spread on MR revealed primarily spread inside the intra-psoas subcompartment (IPSC) of the iliopsoas compartment extending from the neural foramina of vertebrae L2 and L2 to the caudal end of the IPSC, which is typically at the level of the transverse process of vertebra L5. No or minor spread was observed inside the subcompartment posterior to the psoas major muscle (retro-psoas subcompartment, RPSC) or into the para-psoas compartment (PPC) medial to the iliopsoas compartment and caudal to the transverse process of vertebra L5.

Acknowledgements

A. P. Møller Chastine Mc-Kinney Møller Foundation for General Purposes funded the study. The content is solely the responsibility of the authors. The study was registered in EudraCT (2015-005544-33) and in ClinicalTrials.gov (NCT02255591).

Competing interests

No competing interests to declare.

Appendices

Appendix 1. Number of subjects with motor blockade of the femoral and obturator nerves and sensory blockade of the lateral femoral cutaneous nerve, respectively, and a combination hereof (primary outcome) for ultrasound/MRI fusion vs. US guided Shamrock technique. Values are presented as number (proportion).

	US*/MRI† ***n*=22**	**US** ***n*=22**	**p**
Motor blockade			
FN‡	19 (86%)	21 (95%)	0.50
ON§	17 (77%)	20 (91%)	0.38
Sensory blockade			
LFCN‖	20 (91%)	20 (91%)	1.00
Primary outcome			
FN+ON+LFCN	16 (73%)	18 (82%)	0.69

Motor blockade was defined as a decrease in post-block muscle force compared to baseline. Sensory blockade was defined as a reduced/ absent sensation for cold or pain.

* US; ultrasound

† MRI; magnetic resonance imaging

‡ FN; femoral nerve

§ ON; obturator nerve

‖ LFCN; lateral femoral cutaneous nerve

Appendix 2. Baseline and post-block muscle force during knee extension, hip adduction, hip extension, and knee flexion for ultrasound/MRI fusion vs. ultrasound guided Shamrock lumbar plexus block. Values are presented as median (IQR [range]) and mean (SD).

	US*/MRI† ***n* = 22**	**US** ***n* = 22**	**p**
Knee extension (FN‡)			
Pre-block muscle force; N	360.0 (261.0-408.0 [134.0-510.0])	358.5 (297.0-404.0 [182.0-590.0])	
Post-block muscle force; N	149.0 (79.0-301.0 [0.0-501.0])	136.0 (0.0–270.0 [0.0–325.0])	0.21
Difference	-150.4 (131.0)	-202.8 (122.3)	
p value	< 0.001	< 0.001	
Hip adduction (ON§)			
Pre-block muscle force; N	180.0 (140.0-206.0 [102.0-325.0)	188.5 (149.0–206.0 [103.0–330.0)	
Post-block muscle force; N	74.5 (0.0-171.0 [0.0-286.0])	74.5 (0.0–132.0 [0.0–211.0])	0.53
Difference	-84.9 (84.1)	-108.1 (64.2)	
p value	< 0.001	< 0.001	

* US; ultrasound

† MRI; magnetic resonance imaging

‡ FN; femoral nerve

§ ON; obturator nerve

Appendix 3. Number of subjects with sensory blockade of cold, warmth, touch and pain in the dermatomes Th8 to S3 and of the lateral femoral cutaneous nerve after ultrasound/MR fusion (*n=22*) vs. ultrasound guided Shamrock lumbar plexus block (*n=22*). Values are presented as number (proportion).

	Cold			Warmth			Touch			Pain		
	US*/MRI†	**US**	**p**	**US/MRI**	**US**	**p**	**US/MRI**	**US**	**p**	**US/MRI**	**US**	**p**
Th8	0 (0%)	0 (0%)	1.00	0 (0%)	1 (5%)	1.00	0 (0%)	1 (5%)	1.00	0 (0%)	1 (5%)	1.00
Th9	0 (0%)	0 (0%)	1.00	0 (0%)	1 (5%)	1.00	0 (0%)	0 (0%)	1.00	0 (0%)	0 (0%)	1.00
Th10	0 (0%)	0 (0%)	1.00	1 (5%)	0 (5%)	1.00	1 (5%)	0 (5%)	1.00	0 (0%)	0 (0%)	1.00
Th11	0 (0%)	1 (5%)	1.00	0 (0%)	1 (5%)	1.00	0 (0%)	0 (0%)	1.00	0 (0%)	0 (0%)	1.00
Th12	4 (18%)	3 (14%)	1.00	3 (14%)	3 (14%)	1.00	3 (14%)	5 (23%)	0.63	3 (14%)	5 (23%)	0.73
L1	5 (23%)	12 (55%)	0.119	12 (55%)	10 (45%)	0.73	8 (36%)	10 (45%)	0.69	9 (41%)	11 (50%)	0.73
L2	17 (77%)	19 (86%)	0.69	16 (73%)	21 (95%)	0.125	14 (64%)	16 (73%)	0.75	15 (68%)	16 (86%)	0.29
L3	12 (55%)	16 (73%)	0.39	13 (59%)	16 (73%)	0.55	10 (45%)	12 (55%)	0.77	12 (55%)	14 (64%)	0.77
L4	12 (55%)	16 (73%)	0.39	14 (64%)	18 (82%)	0.29	10 (45%)	14 (65%)	0.42	10 (45%)	11 (50%)	1.00
L5	5 (23%)	12 (55%)	0.0923	7 (32%)	11 (50%)	0.34	0 (0%)	0 (0%)	1.00	0 (0%)	2 (9%)	0.50
S1	18 (82%)	18 (82%)	1.00	13 (59%)	15 (68%)	0.69	3 (14%)	1 (5%)	0.63	7 (32%)	4 (18%)	0.45
S2	2 (9%)	4 (18%)	0.62	3 (14%)	7 (32%)	0.34	3 (14%)	4 (18%)	1.00	2 (9%)	2 (9%)	1.00
S3	2 (9%)	3 (14%)	1.00	3 (14%)	7 (32%)	0.29	3 (14%)	5 (23%)	0.69	2 (9%)	6 (27%)	0.22
LFCN‡	19 (86%)	18 (82%)	1.00	17 (77%)	21 (95%)	0.22	16 (73%)	19 (86%)	0.38	16 (73%)	19 (86%)	0.38

Sensory blockade was defined as decreased/absent sensation.

* US; ultrasound

† MRI; magnetic resonance imaging

‡ LFCN; lateral femoral cutaneous nerve

Appendix 4 Procedure-associated outcomes of ultrasound/MRI fusion vs. ultrasound guided Shamrock lumbar plexus block. Values are displayed as mean (SD), median (IQR [range]), and number (proportion) subjects.

	US*/MRI† ***(n=22)***	**US** ***(n=22)***	**p**
Preparation time; s	868 (661-947 [506-1634])	471 (369-631 [165-1090])	< 0.001
Block procedure time; s	438 (272-567 [164-903])	396 (296-524 [197-1044])	0.42
Lumbar plexus ultrasonographically visualized	20 (91%)	20 (91%)	1.00
Minimal nerve stimulation; mA	0.26 (0.24-0.28 [0.22-0.28])	0.28 (0.26-0.28 [0.22-0.40])	0.012
Response on nerve stimulation			0.160
Quadriceps femoris	13 (59%)	16 (73%)	0.45
Adductor	9 (41%)	5 (23%)	0.73
Other motor	0 (0%)	0 (0%)	1.00
Paresthesia	0 (0%)	1 (5%)	1.00
None	0 (0%)	0 (0%)	1.00
Number of needle insertions	4.0 (2.0-5.0 [1.0-8.0])	4.5 (3.0-7.0 [1.0-18.0])	0.25
Needle insertion point from midline; cm	5.0 (4.0-6.0 [3.0-10.0])	5.0 (4.0-5.0 [3.0-9.0])	0.42
Needle depth; cm	8.0 (7.0-8.0 [6.0-9.0])	8.0 (8.0-8.0 [5.5-10.0])	0.0445
Procedural discomfort; NRS units‡	4 (3-7 [1-8])	4 (3-7 [1-8])	0.56
ΔMAP; mmHg§	-3 (-8-2 [-21-23])	-4 (-6-2 [-22-6])	0.53

* US; ultrasound

† MRI; magnetic resonance imaging

‡ NRS, numeric rating scale

§ ΔMAP, change in mean arterial pressure from baseline to 5 min after completed intervention

Appendix 5. Number of subjects with spread of lidocaine-adrenaline added MRI contrast to the anterior rami of L1-S1, the femoral, obturator, and lateral femoral cutaneous nerves and the lumbosacral trunk after ultrasound/MRI fusion vs. ultrasound guided Shamrock lumbar plexus block. Values are displayed as number (proportion).

	US†/MRI* ***(n=22)***	**US** ***(n=22)***	**p**
Anterior ramus of spinal nerve L1	0 (0%)	0 (0%)	1.00
Anterior ramus of spinal nerve L2	19 (86%)	21 (95%)	0.63
Anterior ramus of spinal nerve L3	17 (77%)	18 (82%)	1.00
Anterior ramus of spinal nerve L4	10 (45%)	9 (41%)	1.00
Anterior ramus of spinal nerve L5	1 (5%)	1 (5%)	1.00
Anterior ramus of spinal nerve S1	0 (0%)	0 (0%)	1.00
Femoral nerve	15 (68%)	14 (64%)	1.00
Obturator nerve	14 (64%)	15 (68%)	1.00
Lateral femoral cutaneous nerve	16 (73%)	15 (68%)	1.00
Lumbosacral trunk	2 (9%)	0 (2%)	0.50

***** US; ultrasound

† MRI; magnetic resonance imaging

References

1. CDS/NCHS National Hospital Discharge Survey, 2010.Number of all-listed procedures for discharge from short-term hospitals, by procedure category and age: United States, 2010. www.cdc.gov/nchs/data/nhds/4procedures/2010pro4_numberprocedureage.pdf (accessed 24/10/2016).
2. Chidambaram R, Cobb AG. Change in the age distribution of patients undergoing primary hip and knee replacements over 13 years – an increase in the number of younger men having hip surgery. *Orthopaedic Proceedings* 2009; **91-B**: 152.
3. Bono JV, Robbins CE, Mehio AK, Aghazadeh M, Talmo CT. Pharmacologic pain management before and after total joint replacement of the hip and knee. *Clinics in Geriatric Medicine* 2012; **28**: 459-70.
4. Gottschalk A, Van Aken H, Zenz M, Standl T. Is anesthesia dangerous? *Deutsches Ärzteblatt International* 2011; **108**: 469-74.
5. Memtsoudis SG, Rasul R, Suzuki S*,* et al. Does the impact of the type of anesthesia on outcomes differ by patient age and comorbidity burden? *Regional Anesthesia and Pain Medicine* 2014; **39**: 112-9.
6. Bendtsen TF, Haskins S, Kølsen Petersen JA, Børglum J. Do ultrasound-guided regional blocks signify a new paradigm in high-risk patients? *Best Practice & Research. Clinical Anaesthesiology* 2016; **30**: 191-200.
7. Chelly JE, Casati A, Al-Samsam T, Coupe K, Criswell A, Tucker J. Continuous lumbar plexus block for acute postoperative pain management after open reduction and internal fixation of acetabular fractures. *Journal of Orthopaedic Trauma* 2003; **17**: 362-7.
8. Capdevila X, Macaire P, Dadure C*,* et al. Continuous psoas compartment block for postoperative analgesia after total hip arthroplasty: new landmarks, technical guidelines, and clinical evaluation. *Anesthesia and Analgesia* 2002; **94**: 1606-13, table of contents.
9. Dadure C, Raux O, Gaudard P*,* et al. Continuous psoas compartment blocks after major orthopedic surgery in children: a prospective computed tomographic scan and clinical studies. *Anesthesia and Analgesia* 2004; **98**: 623-8, table of contents.
10. Sauter A, Ullensvang K, Bendtsen T, Børglum J. The "Shamrock Method" - a new and promising Technique for Ultrasound Guided Lumbar Plexus Blocks. *British Journal of*

Anaesthesia E-letter published 26/02/2013.
http://bja.oxfordjournals.org/forum/topic/brjana_el%3B9814 (accessed 24/10/2016).
11. Aksu,C, Gürkan,Y. Shamrock Method may prevent kidney injury. *British Journal of Anaesthesia* E-letter published 19/12/2013.
http://bja.oxfordjournals.org/forum/topic/brjana_el%3B9814 (accessed 24/10/2016).
12. Lin JA, Lu HT, Chen TL. Ultrasound standard for lumbar plexus block. *British Journal of Anaesthesia* 2014; **113**: 188-9.
13. Sauter AR, Ullensvang K, Niemi G, et al. The Shamrock lumbar plexus block: A dose-finding study. *European Journal of Anaesthesiology* 2015; **32**: 764-70.
14. Gürkan Y, Aksu C, Kus A, Toker K, Solak M. One operator's experience of ultrasound guided lumbar plexus block for paediatric hip surgery published as 'e-Pub ahead of print'. *Journal of Clinical Monitoring and Computing* 2016 March 31; doi: 10.1007/s10877-016-9869-x.
15. Strid JM, Sauter AR, Ullensvang K, et al. Shamrock vs. Lumbar Ultrasound Trident: ultrasound guided lumbar plexus blockade in volunteers - a randomised controlled trial. *British Journal of Anaesthesia* Accepted for publication.
16. Zacchino M, Calliada F. Ultrasound image fusion: a new strategy to reduce x-ray exposure during image guided pain therapies. In: Nenoi M, ed. *Current topics in ionizing radiation research*. Rijeka: InTech, 2012; 395-406.
17. Ewertsen C, Săftoiu A, Gruionu LG, Karstrup S, Nielsen MB. Real-time image fusion involving diagnostic ultrasound. *American Journal of Roentgenology* 2013; **200**: W249-55.
18. Galiano K, Obwegeser AA, Bale R, et al. Ultrasound-guided and CT-navigation-assisted periradicular and facet joint injections in the lumbar and cervical spine: a new teaching tool to recognize the sonoanatomic pattern. *Regional Anesthesia and Pain Medicine* 2007; **32**: 254-7.
19. Kwok WH, Karmakar MK. Fusion imaging: Ultrasound and CT or ultrasound and MRI image fusion for spinal sonography - preliminary experience. In: Karmakar MK, ed. *Musculoskeletal ultrasound for regional anaesthesia and pain medicine*. Hong Kong: Department of Anaesthesia and Intensive Care, The Chinese University of Hong Kong, 2016; 503-8.
20. Klauser AS, De Zordo T, Feuchtner GM, et al. Fusion of real-time US with CT images

to guide sacroiliac joint injection in vitro and in vivo. *Radiology* 2010; **256**: 547-53.
21. Zacchino M, Almolla J, Canepari E, Merico V, Calliada F. Use of ultrasound-magnetic resonance image fusion to guide sacroiliac joint injections: a preliminary assessment. *Journal of Ultrasound* 2013; **16**: 111-8.
22. Zacchino M, Allegri M, Canepari M*,* et al. Feasibility of pudendal nerve anesthetic block using fusion imaging technique in chronic pelvic pain. *European Journal of Pain Supplements* 2010; **4**: 329-33.
23. Iagnocco A, Perella C, D'Agostino MA, Sabatini E, Valesini G, Conaghan PG. Magnetic resonance and ultrasonography real-time fusion imaging of the hand and wrist in osteoarthritis and rheumatoid arthritis. *Rheumatology* 2011; **50**: 1409-13.
24. Strid JM, Pedersen EM, Al-Karradi SN*,* et al. Real-time ultrasound/MRI fusion for suprsacral parallel shift approach to lumbosacral plexus blockade and injectate spread - an exploratory randomised controlled trial. *Anaesthesia* Submitted.
25. Lee MW, McPhee RW, Stringer MD. An evidence-based approach to human dermatomes. *Clinical Anatomy* 2008; **21**: 363-73.
26. Ehlers L, Jensen JM, Bendtsen TF. Cost-effectiveness of ultrasound vs nerve stimulation guidance for continuous sciatic nerve block. *British Journal of Anaesthesia* 2012; **109**: 804-8.
27. Harris PA, Taylor R, Thielke R, Payne J, Gonzalez N, Conde JG. Research electronic data capture (REDCap)--a metadata-driven methodology and workflow process for providing translational research informatics support. *Journal of Biomedical Informatics* 2009; **42**: 377-81.
28. Sealed Envelope Ltd. Power calculator for binary outcome superiority trial, 2012. www.sealedenvelope.com/power/binary-superiority (accessed 24/10/2016).
29. Downs MB, Laporte C. Conflicting dermatome maps: educational and clinical implications. *The Journal of Orthopaedic and Sports Physical Therapy* 2011; **41**: 427-34.
30. Karmakar MK, Li JW, Kwok WH, Soh E, Hadzic A. Sonoanatomy relevant for lumbar plexus block in volunteers correlated with cross-sectional anatomic and magnetic resonance images. *Regional Anesthesia and Pain Medicine* 2013; **38**: 391-7.
31. Mannion S, Barrett J, Kelly D, Murphy DB, Shorten GD. A description of the spread of injectate after psoas compartment block using magnetic resonance imaging. *Regional*

Anesthesia and Pain Medicine 2005; **30**: 567-71.
32. Bendtsen TF, Pedersen EM, Haroutounian S*,* et al. The suprasacral parallel shift vs lumbar plexus blockade with ultrasound guidance in healthy volunteers--a randomised controlled trial. *Anaesthesia* 2014; **69**: 1227-40.

Figures and Captures

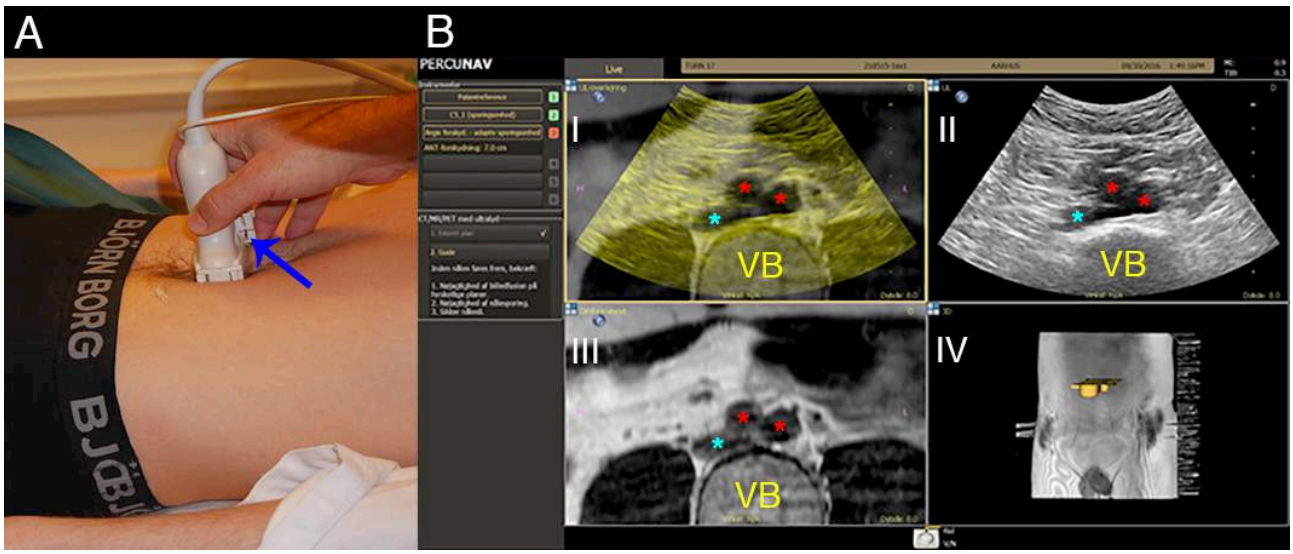

Fig. 1. Initial co-registration and alignment of the real-time ultrasound and the previously sampled magnetic resonance imaging (MRI) dataset. A) The subject is positioned supine and the ultrasound probe with the mounted sensor (blue arrow) is aligned in the axial plane on the abdomen. B) The monitor displays the matched ultrasound and MR images as overlay (I), separate (II and III), and as a 3D projection of the MRI dataset illustrating the position and orientation of the ultrasound probe and image plane (IV). Any misalignment of the common iliac arteries (red asterisks), inferior vena cava (turquoise asterisk), and/or the anterior border of the vertebral body (VB) was adjusted by using the system built-in functions of rotation and shifting.

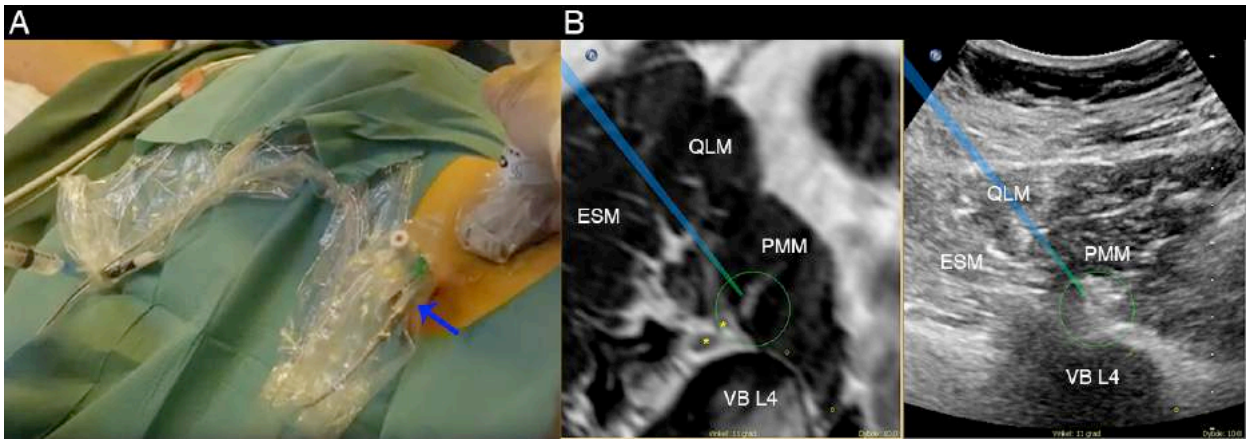

Fig. 2. Real-time ultrasound/magnetic resonance imaging (MRI) fusion guided Shamrock lumbar plexus block. A) The subject is placed in the lateral decubitus position, the ultrasound probe in the flank, and the block needle with mounted sensor (blue arrow) on the grip is inserted and advanced in-plane. B) The fused MRI and real-time ultrasound is displayed side-by-side. The needle (projected as the blue line) is inserted until the needle tip is visualised in the intra-psoas subcompartment between the anterior and posterior lamina of the psoas major muscle (PMM). Asterisks (yellow), anterior ramus of spinal nerve L4 and a branch hereof to the femoral nerve; Circle (green), anticipated intersection between the needle tip and the image plane; ESM, erector spina muscle; QLM, quadratus lumborum muscle; VB L4, vertebral body of L4.

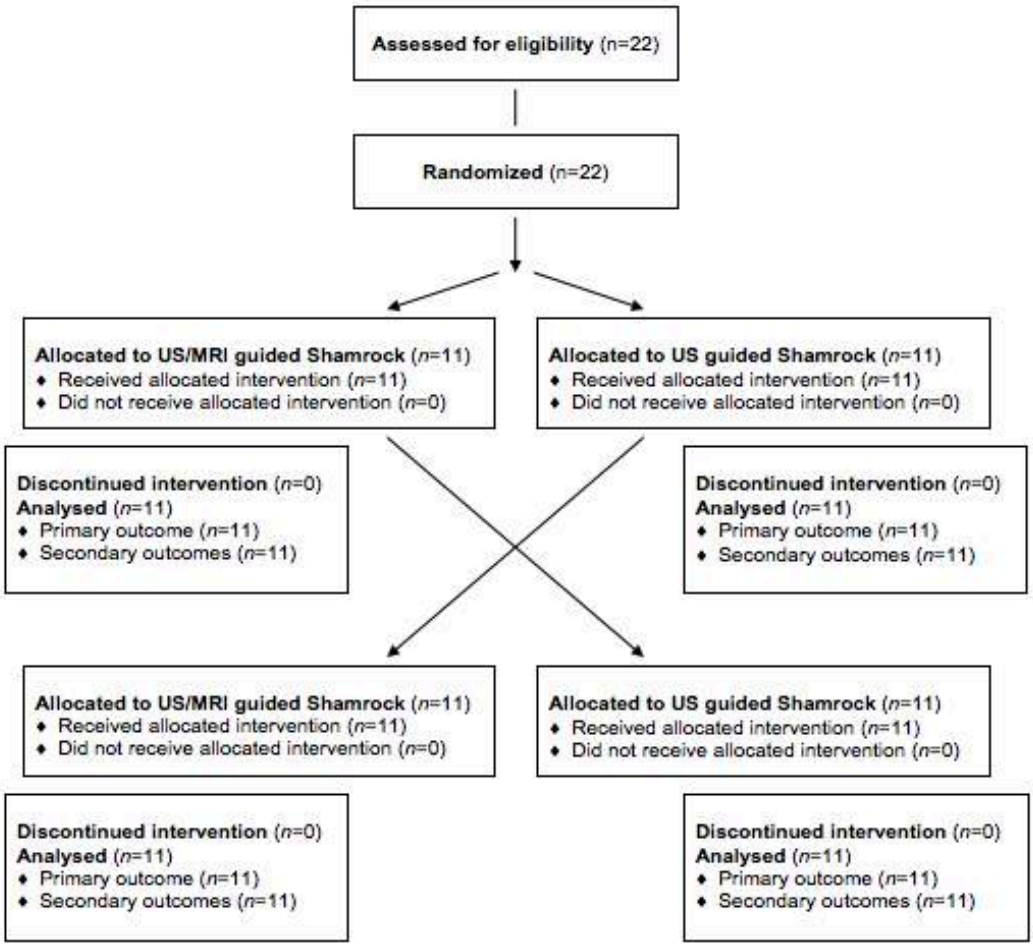

Fig. 3. Modified CONSORT 2010 flow diagram of the study subjects. MRI, magnetic resonance imaging; US, ultrasound.

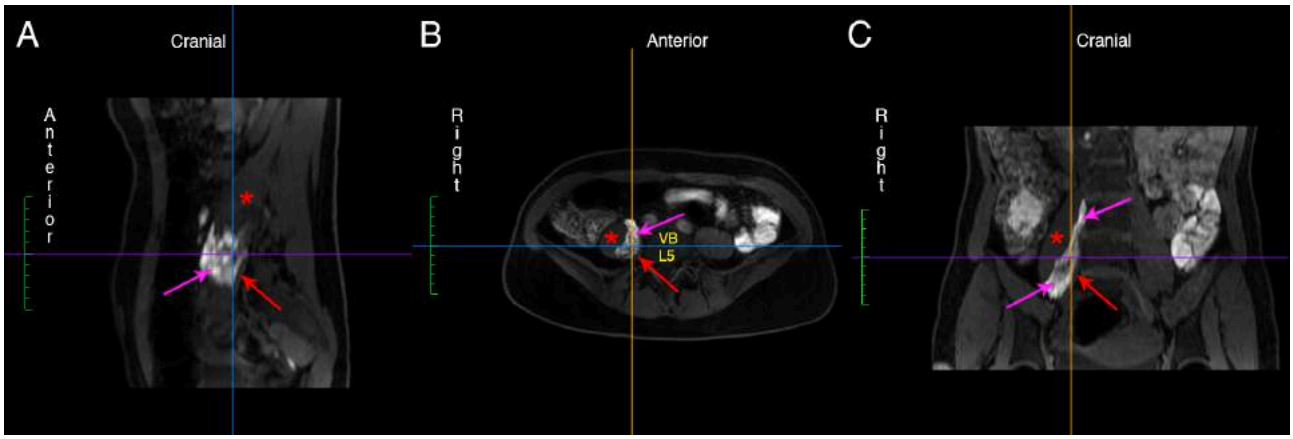

Fig. 4. Magnetic resonance (MR) image visualizing the spread of local anaesthetic added MRI contrast agent in one subject. A) Sagittal plane (orange line on B and C). B) Axial plane (purple line on A and C). C) Frontal plane (blue line on A and B). The injectate is visualized as the very bright and bright areas (magenta arrows) in the intra-psoas subcompartment, i.e. between the anterior and posterior (red arrow) lamina of the psoas major muscle (red asterisks), but not in the retro- psoas subcompartment, i.e. posterior to the psoas major muscle, or in the para-psoas subcompartment, i.e. medial to the iliopsoas compartment and the psoas major muscle caudal to the transverse process of vertebral body L5 (VB L5).

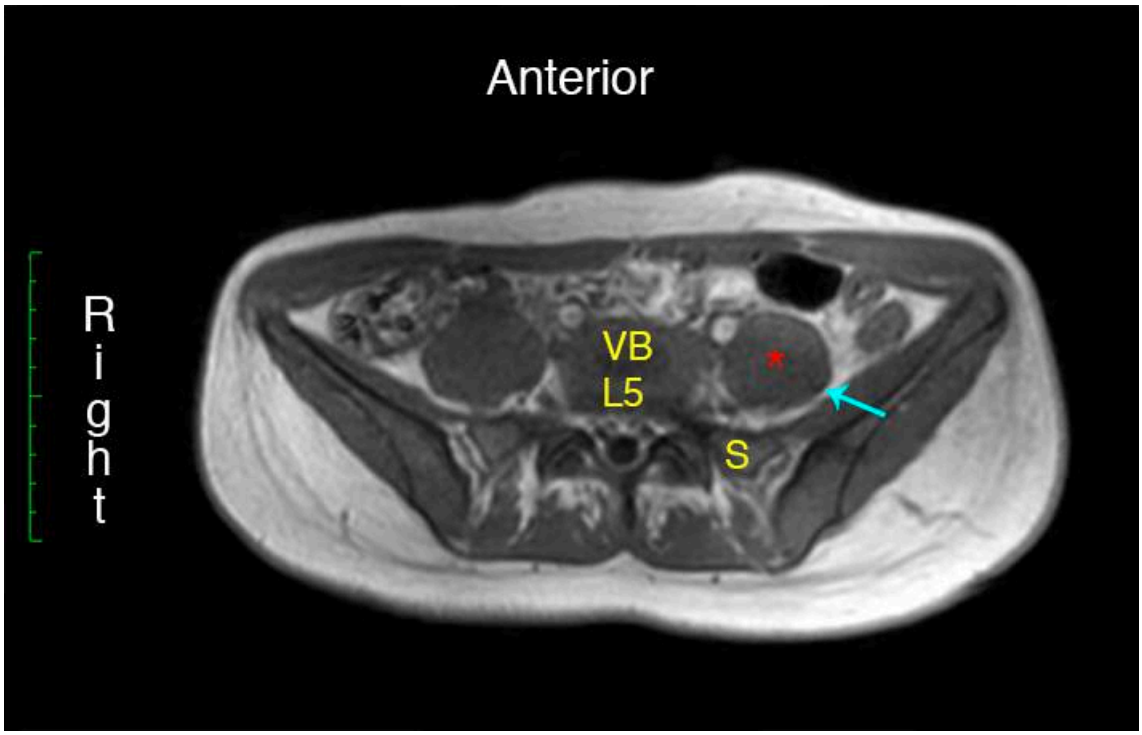

Fig. 5. Magnetic resonance (MR) image in the axial plane caudal to the transverse process of vertebra L5. There is no spread of local anaesthetic added MRI contrast in the retro-psoas subcompartment (RPSC) posterior to the psoas major muscle (red asterisk) where the femoral and lateral femoral cutaneous nerves (turquoise arrow) emerge at the lateral margin of the psoas major muscle. S, sacral ala; VB L5, vertebral

MS I

Methodological Study I

Results of the study of displacement of the anterior rami of spinal nerves L3 and L4 on MRI of 25 healthy volunteers in the supine and in the lateral decubitus position. The MRI datasets (3D T2-TSE sequences with an isotropic resolution of 1.2x1.2x1.2 mm^3 [overlapping 2.3 mm slices with 1.2 mm spacing], TE 60 ms, and TR 1,200 ms) were sampled twice in the coronal plane from vertebral body of L1 to S4 with the volunteers in the supine and in the lateral decubitus position, respectively, using a 1.5T Philips Ingenia MRI scanner (Koninklijke Philips Electronics N.V., Eindhoven, Netherlands) The corresponding datasets for each volunteer were co-registered (OsiriX v.6.5.2. 64 bit; Pixmeo SARL, 266 Rue de Bernex, CH1233 Bernex, Switzerland) using the axial planes through the transverse process of vertebrae L4 and L5, respectively. Two blinded observers (J.M.C.S. and N.D.N.) recorded the *x*- and *y*-coordinates of the anterior rami of spinal nerves L3 and L4) in both registration-planes (transverse processes of vertebrae L4 and L5) in both datasets (supine and lateral decubitus). Displacement of a nerve was calculated as the distance (mm) between the nerve in the supine position compared to the same nerve in the lateral decubitus position.

	Registration plane	
	TP* L4	**TP L5**
Displacement of L3; mm†	1.0 (0.6-1.4)	3.2 (1.6-4.2)
Displacement of L4; mm‡	4.1 (2.9)	1.8 (0.9-2.0)

Values are presented as median (IQR) or mean (SD).
***** TP; transverse process
† Anterior ramus of spinal nerve L3
‡ Anterior ramus of spinal nerve L4

We concluded from the results that the anterior rami of spinal nerves L3 and L4 were only marginally displaced due to the position change. We assessed that we could use supine MRI for fusion with real-time ultrasound in the lateral decubitus position, that we could adjust for any misalignment, and that any remaining inaccuracy was within the inherent registration error.

MS II

Methodological Study II

Results of the laboratory study on physical compatibility between relevant volumes of 2% lidocaine hydrochloride with 0.0005% adrenaline (Lidokain-adrenalin SAD; Amgros I/S, Copenhagen, Denmark) and 27.9% gadoterate meglumine (Dotarem®; Guerbet, Roissy CdG Cedex France) (Mixture 1 to 4) and between 2% lidocaine hydrochloride with 0.0005% adrenaline and 27.9% gadoterate meglumine (Dotarem®) diluted in isotonic saline (Mixture 5 to 8).

Blanding 1				
Drug 1	**Drug 2**	**Status**	**Information**	**Test Parameters**
Lidokain-adrenalin 20mg/mL-5µg/ml 20 ml SAD Anvendt volum: 20 ml	**Dotarem inj. 279,3 mg/mL** Guerbet Anvendt volum: **0,10 ml**	Kompatible	Fysisk kompatible. visuel udfældning, farve ændring, gas udvikling er ikke konstateret. - Ikke signifikant ændring for sub-visible partikler ift. værdier fra blandings komponenter. Overholder acceptgrænse for *Particulate contamination : sub-visible particles; Ph. Eur. 2.9.19; metode 1; test 1B* pH værdien er uændret ift. pH værdi for Lidokain/adrenalin 20 mg/ml-5 µg/ml opbevaring:Rum temperatur < 25 °C og beskyttes mod direkte sollys.	Reference: Bilag 1 og 2 undersøgelsesperiod: 2 timer. Method: - Visual observation -Sub-visible Partikler - pH måling. Container:Glas type 1, hætteglas
Blanding 2				
Drug 1	**Drug 2**	Status	Information	Test Parameters
Lidokain-adrenalin 20mg/mL-5µg/ml 20 ml SAD Anvendt volum: 20 ml	**Dotarem inj. 279,3 mg/mL** Guerbet Anvendt volum: **0,15 ml**	Kompatible	Fysisk kompatible. visuel udfældning, farve ændring, gas udvikling er ikke konstateret. - Ikke signifikant ændring for sub-visible partikler ift. værdier fra blandings komponenter. Overholder acceptgrænse for *Particulate contamination : sub-visible particles; Ph. Eur. 2.9.19; metode 1; test 1B*	Reference: Bilag 1 og 2 undersøgelsesperiod: 2 timer. Method: - Visual observation -Sub-visible Partikler - pH måling.
			pH værdien er uændret ift. pH værdi for Lidokain/adrenalin 20 mg/ml-5 µg/ml opbevaring:Rum temperatur < 25 °C og beskyttes mod direkte sollys.	
Blanding 3				
Drug 1	**Drug 2**	Status	Information	Test Parameters
Lidokain-adrenalin 20mg/mL-5µg/ml 20 ml SAD Anvendt volum: 20 ml	**Dotarem inj. 279,3 mg/mL** Guerbet Anvendt volum: **0,20 ml**	Kompatible	Fysisk kompatible. visuel udfældning, farve ændring, gas udvikling er ikke konstateret. - Ikke signifikant ændring for sub-visible partikler ift. værdier fra blandings komponenter. Overholder acceptgrænse for *Particulate contamination : sub-visible particles; Ph. Eur. 2.9.19; metode 1; test 1B* pH værdien er uændret ifht. pH værdi for Lidokain/adrenalin 20 mg/ml-5 µg/ml opbevaring:Rum temperatur < 25 °C og beskyttes mod direkte sollys.	Reference: Bilag 1 og 2 undersøgelsesperiod: 2 timer. Method: - Visual observation -Sub-visible Partikler - pH måling. Container:Glas type 1, hætteglas

Blanding 4				
Drug 1	**Drug 2**	Status	Information	Test Parameters
Lidokain-adrenalin 20mg/mL-5µg/ml 20 ml	**Dotarem inj. 279,3 mg/mL**	Kompatible	Fysisk kompatible. visuel udfældning, farve ændring, gas udvikling er ikke konstateret. - Ikke signifikant ændring for sub-visible partikler ift. værdier fra blandings	Reference: Bilag 1 og 2 undersøgelsesperiod: 2 timer.
SAD Anvendt volum: 20 ml	Guerbet Anvendt volum: **1,5 ml**		komponenter. Overholder acceptgrænse for *Particulate contamination : sub-visible particles; Ph. Eur. 2.9.19; metode 1; test 1B* pH værdien er steget fra 4.4 til 4.5, hvilket der forventes pH stigning, da Dotarem har en pH værdi på 7.1 opbevaring:Rum temperatur < 25 °C og beskyttes mod direkte sollys.	Method: - Visual observation -Sub-visible Partikler - pH måling. Container:Glas type 1, hætteglas
Blanding 5				
Drug 1	**Drug 2**	**Status**	**Information**	**Test Parameters**
Lidokain-adrenalin 20mg/mL-5µg/ml 20 ml SAD Anvendt volumen: 20 ml	**Dotarem opløsning.** 279,3 mg/mL i Isotonosk natriumklorid 9 mg/ml (blanding forhold **1 ml/10 ml)** Anvendt volum: 1 ml	Kompatible	Fysisk kompatible. visuel udfældning, farve ændring, gas udvikling er ikke konstateret. - Ikke signifikant ændring for sub-visible partikler ift. værdier fra blandings komponenter. Overholder acceptgrænse for *Particulate contamination : sub-visible particles; Ph. Eur. 2.9.19; metode 1; test 1B* pH værdien er uændret ift. pH værdi for Lidokain/adrenalin 20 mg/ml-5 µg/ml opbevaring: Rum temperatur < 25 °C og beskyttes mod direkte sollys.	Reference: Bilag 1 og 3 undersøgelsesperiod: 2 timer. Method: - Visual observation - Sub-visible Partikler - pH måling. Container:Glas type 1, hætteglas
Blanding 6				
Drug 1	**Drug 2**	Status	Information	Test Parameters
Lidokain-adrenalin 20mg/mL-5µg/ml 20 ml SAD Anvendt volumen: 20 ml	**Dotarem inj.** 279,3 mg/mL i Isotonosk natriumklorid 9 mg/ml (blanding forhold **1,5 ml/10 ml)** Anvendt volum:	Kompatible	Fysisk kompatible. visuel udfældning, farve ændring, gas udvikling er ikke konstateret. - Ikke signifikant ændring for sub-visible partikler ift. værdier fra blandings komponenter. Overholder acceptgrænse for *Particulate contamination : sub-visible particles; Ph. Eur. 2.9.19; metode 1; test 1B*	Reference: Bilag 1 og 3 undersøgelsesperiode: 2 timer. Method: - Visual observation - Sub-visible Partikler - pH måling. Container:Glas type 1, hætteglas
	1 ml		pH værdien er uændret ift. pH værdi for Lidokain/adrenalin 20 mg/ml-5 µg/ml opbevaring: Rum temperatur < 25 °C og beskyttes mod direkte sollys.	
Blanding 7				
Drug 1	**Drug 2**	Status	Information	Test Parameters
Lidokain-adrenalin 20mg/mL-5µg/ml 20 ml SAD Anvendt volumen: 20 ml	**Dotarem inj.** 279,3 mg/mL i Isotonosk natriumklorid 9 mg/ml (blanding forhold **2 ml/10 ml)** Anvendt volum: 1 ml	Kompatible	Fysisk kompatible. visuel udfældning, farve ændring, gas udvikling er ikke konstateret. - Ikke signifikant ændring for sub-visible partikler ift. værdier fra blandings komponenter. Overholder acceptgrænse for *Particulate contamination : sub-visible particles; Ph. Eur. 2.9.19; metode 1; test 1B* pH værdien er uændret ift. pH værdi for Lidokain/adrenalin 20 mg/ml-5 µg/ml opbevaring: Rum temperatur < 25 °C og beskyttes mod direkte sollys.	Reference: Bilag 1 og 3 undersøgelsesperiod: 2 timer. Method: - Visual observation -Sub-visible Partikler - pH måling. Container:Glas type 1, hætteglas

Blanding 8				
Drug 1	**Drug 2**	Status	Information	Test Parameters
Lidokain-adrenalin 20mg/mL-5µg/ml 20 ml	**Dotarem inj.** 279,3 mg/mL i Isotonosk natriumklorid 9 mg/ml	Kompatible	Fysisk kompatible. visuel udfældning, farve ændring, gas udvikling er ikke konstateret. - Ikke signifikant ændring for sub-visible partikler ift. værdier fra	Reference: Bilag 1 og 3 undersøgelsesperiod: 2 timer.
SAD Anvendt volum: 20 ml	(blanding forhold **10 ml/10 ml)** Anvendt volum: 1 ml		blandingskomponenter. Overholder acceptgrænse for *Particulate contamination : sub-visible particles; Ph. Eur. 2.9.19; metode 1; test 1B* pH værdien er steget fra 4.4 til 4.7, hvilket der forventes pH stigning, da Dotarem har en pH værdi på 7.1 og Natriumklorid på 5,7 opbevaring: Rum temperatur < 25 °C og beskyttes mod direkte sollys.	Method: - Visual observation -Sub-visible Partikler - pH måling. Container:Glas type 1, hætteglas

The tests were in accordance with the European Pharmacopeia for physical compatibility and were approved by Youssef Nejatbakhsh, MSc (pharm).

We concluded from the study that 2% lidocaine-adrenaline and diluted Dotarem® was physically compatible in the concentration ratio relevant for studies I to III, in concentration ratios with 10% lower and higher concentration of Dotarem®, respectively, as well as in concentrations ratios with ten times higher concentration of Dotarem®. Considering the results together with any available data on solutions of local anaesthetics with gadolinium based contrast agents as well as the very small volume (0.13 ml) of Dotarem® required to visualise 20 ml of 20 ml of 2% lidocaine-adrenaline, we assessed that the risk of toxic effects and harm associated with the injection in studies I to III was negligible.

AARHUS UNIVERSITY

Declaration of co-authorship

Full name of the PhD student: Jennie Maria Christin Strid

This declaration concerns the following article/manuscript:

Title:	Shamrock vs. Lumbar Ultrasound Trident: Ultrasound Guided Lumbar Plexus Blockade in Volunteers – a Randomised Controlled Trial
Authors:	Strid JMC, Sauter AR, Ullensvang K, Andersen MN, Daugaard M, Bendtsen MAF, Søballe K, Pedersen EM, Børglum J, Bendtsen TF

The article/manuscript is: Published ☐ Accepted ☒ Submitted ☐ In preparation ☐

If published, state full reference:

If accepted or submitted, state journal: British Journal of Anaesthesia

Has the article/manuscript previously been used in other PhD or doctoral dissertations?

No ☒ Yes ☐ If yes, give details:

The PhD student has contributed to the elements of this article/manuscript as follows:

A. No or little contribution
B. Has contributed (10-30 %)
C. Has contributed considerably (40-60 %)
D. Has done most of the work (70-90 %)
E. Has essentially done all the work

Element	Extent (A-E)
1. Formulation/identification of the scientific problem	B
2. Planning of the experiments and methodology design and development	D
3. Involvement in the experimental work/clinical studies/data collection	D
4. Interpretation of the results	D
5. Writing of the first draft of the manuscript	E
6. Finalization of the manuscript and submission	D

Signatures of the co-authors

Date	Name	Signature
17-10-2016	Axel Rudolf Sauter	A. Sauter Digitally signed by Axel R. Sauter DN: cn=Axel R. Sauter, o=Oslo University Hospital Rikshospitalet, ou=Department of Anaesthesiology, email=sauter@start.no, c=NO Date: 2016.10.17 11:14:29 +01'00'
19-10-2016	Kyrre Ullensvang	
17-10-2016	Morten Nørgaard Andersen	
18.10.2016	Morten Daugaard	

AARHUS
UNIVERSITY

17. oktober 2016	Mathias Alrøe Fichtner Bendtsen	
20.10.2016	Kjeld Søballe	
18.10.2016	Erik Morre Pedersen	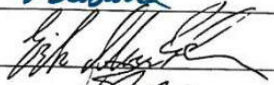
17.10.2016	Jens Børglum	
19.10.2016	Thomas Fichtner Bendtsen	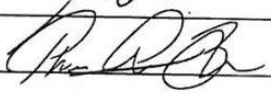

In case of further co-authors please attach appendix

Date: 20.10.2016

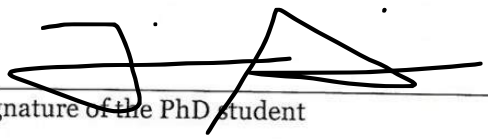

Signature of the PhD student

AARHUS UNIVERSITY

Declaration of co-authorship

Full name of the PhD student: Jennie Maria Christin Strid

This declaration concerns the following article/manuscript:

Title:	Real-time Ultrasound/MRI Fusion for Suprasacral Parallel Shift Approach to Lumbosacral Plexus Blockade and Injectate Spread – an Exploratory Randomised Controlled Trial
Authors:	Strid JMC, Pedersen EM, Al-Karradi SNH, Bendtsen MAF, Bjørn S, Dam M, Daugaard M, Hansen MS, Linnet KD, Børglum J, Søballe K, Bendtsen TF

The article/manuscript is: Published ☐ Accepted ☐ Submitted ☒ In preparation ☐

If published, state full reference:

If accepted or submitted, state journal: Anaesthesia

Has the article/manuscript previously been used in other PhD or doctoral dissertations?

No ☒ Yes ☐ If yes, give details:

The PhD student has contributed to the elements of this article/manuscript as follows:

A. No or little contribution
B. Has contributed (10-30 %)
C. Has contributed considerably (40-60 %)
D. Has done most of the work (70-90 %)
E. Has essentially done all the work

Element	Extent (A-E)
1. Formulation/identification of the scientific problem	C
2. Planning of the experiments and methodology design and development	D
3. Involvement in the experimental work/clinical studies/data collection	D
4. Interpretation of the results	D
5. Writing of the first draft of the manuscript	E
6. Finalization of the manuscript and submission	D

Signatures of the co-authors

Date	Name	Signature
18.10.2016	Erik Morre Pedersen	
23.10.16	Sinan Naseer Hussain Al-Karradi	
21. oktober 2016	Mathias Alrøe Fictner Bendtsen	

AARHUS
UNIVERSITY

23.10.16	Siska Bjørn	
21.10.2016	Mette Dam	
19.10.2016	Morten Daugaard	
22/09-2016	Martin Sejr Hansen	
23-10-16	Katrine Danker Linnet	
23.10.16	Jens Børglum	
20.10.2016	Kjeld Søballe	
19.10.2016	Thomas Fichtner Bendtsen	

In case of further co-authors please attach appendix

Date: 24.10.16

Signature of the PhD student

AARHUS
UNIVERSITY

Declaration of co-authorship

Full name of the PhD student: Jennie Maria Christin Strid

This declaration concerns the following article/manuscript:

Title:	Real-time Ultrasound/MRI Fusion for Shamrock Lumbar Plexus Blockade and Analysis of Injectate Spread – an Exploratory Randomised Controlled Trial
Authors:	Strid JMC, Pedersen EM, Bendtsen MAF, Bjørn S, Dam M, Daugaard M, Hansen MS, Vendelbo O, Borglum J, Søballe K, Bendtsen TF

The article/manuscript is: Published ☐ Accepted ☐ Submitted ☐ In preparation ☒

If published, state full reference:

If accepted or submitted, state journal:

Has the article/manuscript previously been used in other PhD or doctoral dissertations?

No ☒ Yes ☐ If yes, give details:

The PhD student has contributed to the elements of this article/manuscript as follows:

A. No or little contribution
B. Has contributed (10-30 %)
C. Has contributed considerably (40-60 %)
D. Has done most of the work (70-90 %)
E. Has essentially done all the work

Element	Extent (A-E)
1. Formulation/identification of the scientific problem	C
2. Planning of the experiments and methodology design and development	D
3. Involvement in the experimental work/clinical studies/data collection	D
4. Interpretation of the results	D
5. Writing of the first draft of the manuscript	E
6. Finalization of the manuscript and submission	D

Signatures of the co-authors

Date	Name	Signature
18.10.2016	Erik Morre Pedersen	
21. oktober 2016	Mathias Alroe Fictner Bendtsen	
23.10.2016	Siska Bjorn	
21.10.2016	Mette Dam	

AARHUS
UNIVERSITY

19.10.2016	Morten Daugaard	
22/10-216	Martin Sejr Hansen	
24.12.2016	Olga Vendelbo	
23.10.2016	Jens Børglum	
20.10.2016	Kjeld Søballe	
19.10.2016	Thomas Fichtner Bendtsen	

In case of further co-authors please attach appendix

Date: 24.10.2016

Signature of the PhD student